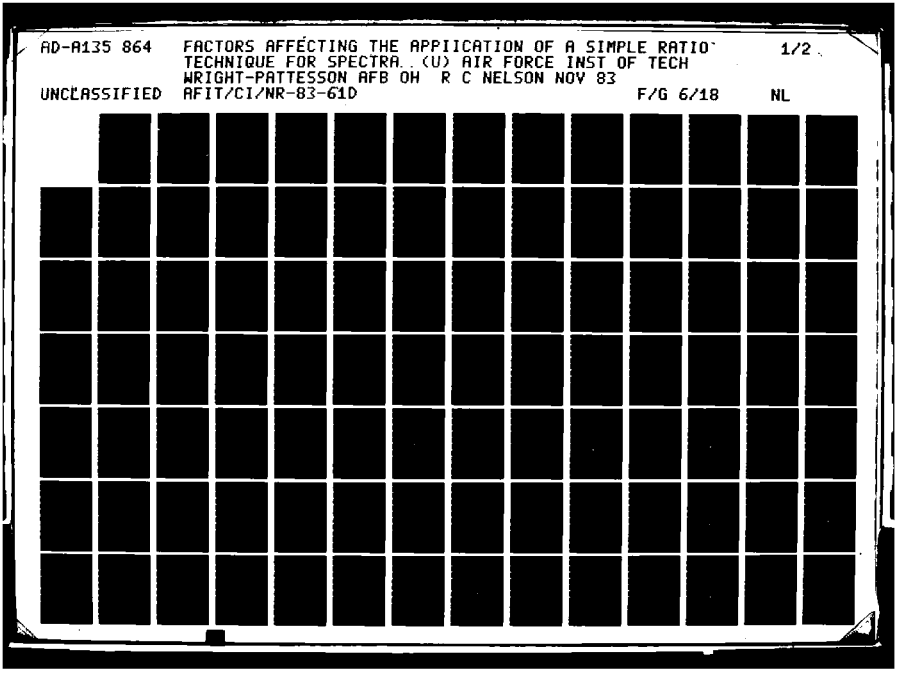
AD-A135 864 FACTORS AFFECTING THE APPLICATION OF A SIMPLE RATIO TECHNIQUE FOR SPECTRA.. (U) AIR FORCE INST OF TECH WRIGHT-PATTESSON AFB OH R C NELSON NOV 83
1/2
UNCLASSIFIED AFIT/CI/NR-83-61D
F/G 6/18
NL

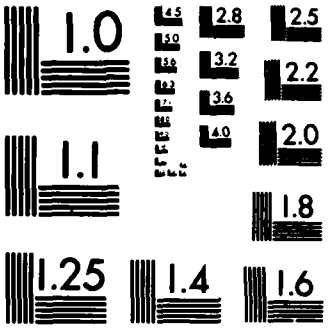

MICROCOPY RESOLUTION TEST CHART
NATIONAL BUREAU OF STANDARDS-1963-A

AD-A135 864

Factors Affecting the Application of A Simple Ratio Technique for Spectral Correction of a Neutron Personnel Albedo Dosimeter

BY

Robert C. Nelson
B.S.,University of Kansas, 1968
M.S.,University of Kansas, 1969

Submitted to the Department of Radiation Biophysics and the Faculty of the Graduate School of the University of Kansas in Partial Fulfillment of the Requirements for the Degree of Doctor of Philosophy

Copyright 1983
Robert C. Nelson

DTIC
ELECTE
DEC 15 1983
S D
D

Dissertation Committee:

Benjamin S Grosser
Chairman

Louis R. Milavickas

[illegible]

Russell Mesler

Edward L Kaan

Dissertation Defended: November 1983

DTIC FILE COPY

DISTRIBUTION STATEMENT A
Approved for public release;
Distribution Unlimited

83 12 14 010

UNCLASS

SECURITY CLASSIFICATION OF THIS PAGE (When Data Entered)

REPORT DOCUMENTATION PAGE	READ INSTRUCTIONS BEFORE COMPLETING FORM
1 REPORT NUMBER: AFIT/CI/NR 83-61D	2 GOVT ACCESSION NO. A135 864 / 3 RECIPIENT'S CATALOG NUMBER
4. TITLE (and Subtitle): Factors Affecting the Application of a Simple Ratio Technique for Spectral Correction of a Neutron Personnel Albedo Dosimeter	5 TYPE OF REPORT & PERIOD COVERED: THESIS/DISSERTATION
	6 PERFORMING ORG. REPORT NUMBER
7 AUTHOR(s): Robert C. Nelson	8. CONTRACT OR GRANT NUMBER(s)
9 PERFORMING ORGANIZATION NAME AND ADDRESS: AFIT STUDENT AT: University of Kansas	10. PROGRAM ELEMENT, PROJECT, TASK AREA & WORK UNIT NUMBERS
11 CONTROLLING OFFICE NAME AND ADDRESS: AFIT/NR WPAFB OH 45433	12. REPORT DATE: Nov 83
	13. NUMBER OF PAGES: 88
14. MONITORING AGENCY NAME & ADDRESS (if different from Controlling Office)	15. SECURITY CLASS. (of this report): UNCLASS
	15a. DECLASSIFICATION DOWNGRADING SCHEDULE

16. DISTRIBUTION STATEMENT (of this Report)

APPROVED FOR PUBLIC RELEASE; DISTRIBUTION UNLIMITED

17. DISTRIBUTION STATEMENT (of the abstract entered in Block 20, if different from Report)

18. SUPPLEMENTARY NOTES

APPROVED FOR PUBLIC RELEASE: IAW AFR 190-17

8 DEC 1983

LYNN E. WOLAVER
Dean for Research and
Professional Development

19. KEY WORDS (Continue on reverse side if necessary and identify by block number)

20 ABSTRACT (Continue on reverse side if necessary and identify by block number)

ATTACHED

DD FORM 1 JAN 73 1473 EDITION OF 1 NOV 65 IS OBSOLETE

UNCLASS

SECURITY CLASSIFICATION OF THIS PAGE (When Data Entered)

83 12 14 010

ABSTRACT

Factors Affecting the Application of A Simple Ratio Technique for Spectral Correction of a Neutron Personnel Albedo Dosimeter

Robert C. Nelson, Ph.D.

University of Kansas, 1983

To accurately assess the dose equivalent indicated by the albedo response of a neutron personnel dosimeter, additional knowledge is generally required in order to apply the needed spectral specific correction factors. This work was designed to evaluate the capability of the USAF Personnel Neutron Dosimeter to "self-calibrate" for moderated fission neutron spectra. The boron/bare ratio technique is compared with a simple theoretical model of the dosimeter and with the 23 cm (9 in) to 7.6 cm (3 in) Hankins' remmeter calibration technique. The overall goal was to provide dose-equivalent estimates comparable to those provided by the remmeter technique without the necessity of special on-site measurements.

Although the boron/bare technique with the present dosimeter design fails to provide calibration factors needed for moderated fission neutron spectra, theoretical predictions based upon the model and the measured dosimeter responses are used to propose a dosimeter design which might fulfil the desired goal. Ancillary data gathered during the study are also presented.

The University of Kansas
Lawrence

November 22, 1983

To Whom it May Concern:

This is to certify that Robert Clifton Nelson has completed all the requirements for the degree Doctor of Philosophy with a major in Radiation Biophysics and will be recommended for that degree at the next meeting of the faculty.

Signed:

Gilbert Dyck

Dean

Accession For	
NTIS GRA&I	☒
DTIC TAB	☐
Unannounced	☐
Justification	
By	
Distribution/	
Availability Codes	
Dist	Special
A/1	

DTIC COPY INSPECTED 3

ACKNOWLEDGEMENT

The time span involved in my work has made writing of an acknowledgement most difficult to accomplish. One is always afraid of forgetting to mention someone who was an ardent supporter in time of distress or who made significant suggestions or provided assistance along the way.

I am particularly grateful to my advisor, friend, and associate, Dr. Benjamin Friesen, whose patience, understanding and persistence has allowed this work to be completed. Additionally, my sincere thanks is extended to the faculty and staff of the Radiation Biophysics Department and to the University Graduate Staff. I must also acknowledge Dr. Curtis Graham and Dave Trombino of the Hazards Control Division, Lawrence Livermore National Laboratory, who provided radiation source time and operation at their facility, and Steve Sims, Dick Swaja, and Richard Greene at the Health Physics Research Reactor, Oak Ridge National Laboratory, who likewise provided special runs for available moderated fission spectra at their facility.

I must acknowledge the financial assistance of the Air Force Institute of Technology for assignment to the three years of on-campus study, along with the committment of my present supervisor,

Col. Roger Graham and Col. William Mabson, Laboratory Commander, who insured that time was available in my duty schedule to accomplish this work.

Finally, and most important, I am thankful for the fortitude of my wife and sons who have put up with me through my highs and lows these last few years. Without the constant encouragement and expert editing skills provided by my wife, it would have been very easy to have abandoned the task long ago.

TABLE OF CONTENTS

TABLE OF CONTENTS (Continued)

LIST OF TABLES

LIST OF FIGURES

LIST OF FIGURES (Continued)

LIST OF FIGURES (Continued)

LIST OF FIGURES (Continued)

LIST OF FIGURES (Continued)

I. INTRODUCTION

Thermoluminescent dosimeters are the most widely used type of personnel neutron dosimeters. These dosimeters are designed to respond to the incident neutron flux and the neutron flux scattered from the body. The main advantage of thermoluminescent dosimeters is that they do not have the energy threshold of around 1 MeV that exists with some other types of personnel neutron dosimeters. The main disadvantage of thermoluminescent dosimeters is the rapid loss of sensitivity as the incident neutron energy increases. To accurately measure dose, the thermoluminescent dosimeter must be calibrated in the field in which they are worn or sufficient information about the neutron energy spectrum must be known to establish an appropriate calibration factor.

Due to growing Congressional and public concern over the effects in man from exposures to radiation at levels at or below those recommended in National Council on Radiation Protection and Measurements (NCRP) and International Commission on Radiation Protection (ICRP) guidelines (NCRP71a, NCRP71b, ICRP69), the Department of Defense (DoD) under the direction of the Assistant Secretary of Defense for Atomic Energy established a working group on Intrinsic Radiation (INRAD). INRAD being the emissions eminating from nuclear weapons due to the inherent presence of radioactive material. This working group has recommended that, although exposures to United States

Air Force (USAF) nuclear weapons maintenance technicians from INRAD results in yearly exposures of less than 500 millirem per year, a monitoring program should be established to document the actual exposures to personnel.

Development of individual calibration factors for over one hundred additional INRAD facilities requiring personnel monitoring is a tremendously time consuming and manpower-intensive task. The possibility of utilizing the information provided by the USAF personnel dosimeter badge, a design similar to the badge developed at Sandia National Laboratory Albuquerque (SNLA) by Thompson (Th77), to provide "self-calibration" factors for each dosimeter in unknown environments was considered to have the potential to eliminate this need.

This work was undertaken to systematically study the USAF dosimeter in moderated fission spectra, both theoretically and by measurement, and to determine if the present dosimeter could be used to "self-calibrate". Special emphasis was placed on evaluation of the current capability to measure neutron dose in view of the questions regarding albedo dosimeter performance (Gr79) and the possible reduction of a factor of three to ten in accepted levels for occupational and general public exposure (FR79, NCRP80, FR81).

II. LITERATURE REVIEW

In recent years, several investigators have expended considerable effort in attempting to effectively model the neutron sensitivity of thermoluminescent dosimeters (Fu72,A174,Ho78,Lo80,He82,G183). Early attempts were dominated by calculational efforts to determine kerma in lithium fluoride and comparing the resultant values with the measured thermoluminescent response of ^{6}LiF. The objective of these studies was to explain in detail the response differential between ^{6}LiF and ^{7}LiF with regard to incident neutron energy. The $^{6}Li(n,\alpha)\ ^{3}H$ reaction dominates the ^{6}LiF response and results in a ^{6}LiF response more than two orders of magnitude greater than ^{7}LiF at 0.01 MeV. This differential decreases to a single order of magnitude at 1 MeV and to a roughly equal response by 10 MeV. Conceptually, accurate knowledge of the thermoluminescent response to neutrons as a function of the neutron energy for ^{6}LiF and ^{7}LiF could allow fine tuning of calibrations for known neutron spectra.

Unfortunately, although numerous dosimeter designs have been modeled, this has served only to verify response calibration spectra and sources. Calculated thermoluminescent response characteristics serve only to improve the dosimeter's usefulness for given spectra by improving precision by a few percent. Since in most cases for radiation protection purposes, errors in determining neutron dose

equivalent of the order of ten to twenty percent are considered excellent and errors of fifty percent regulatively acceptable, improvements by detailed response calculations for spectra where simple calibration yields similar results are not in order. Likewise, this knowledge generally yields little advantage for single element dosimeters in unknown spectra where deviations greater than an order of magnitude in predicted dose equivalent can occur.

In the case of the USAF Personnel Neutron Dosimetry Badge, the thermoluminescent response for two separate neutron spectra is actually measured, these being the actual incident/albedo neutron spectrum, and the spectrum measured after moderation through a Boron-10 impregnated pouch. This technique follows from the use of Boron-10 in personnel dosimeters as suggested by Griffith (Gr73). Substitution of Boron-10 impregnated plastic for the cadmium normally used in Hankins-type personnel dosimeters (Ha73) allows for concurrent gamma exposure determinations through the elimination of interference caused by the cadmium n,γ reaction (Ha79). The effect of the Boron-10 pouch can be theoretically calculated for known spectra by using the Boron-10 neutron absorption cross section curve (Ga76) to determine the secondary spectra (Figure 1).

Since the USAF Personnel Neutron Dosimeter will be used basically for monitoring sources which produce modified fission spectra, this ratio technique must allow for ascertainment of an appropriate neutron response calibration factor for evaluation of the true dose equivalent without the necessity of further detailed measurements in

Figure 1

Boron-10 Total Neutron Absorption Cross Sections versus Neutron Spectral Mid-Energy Values

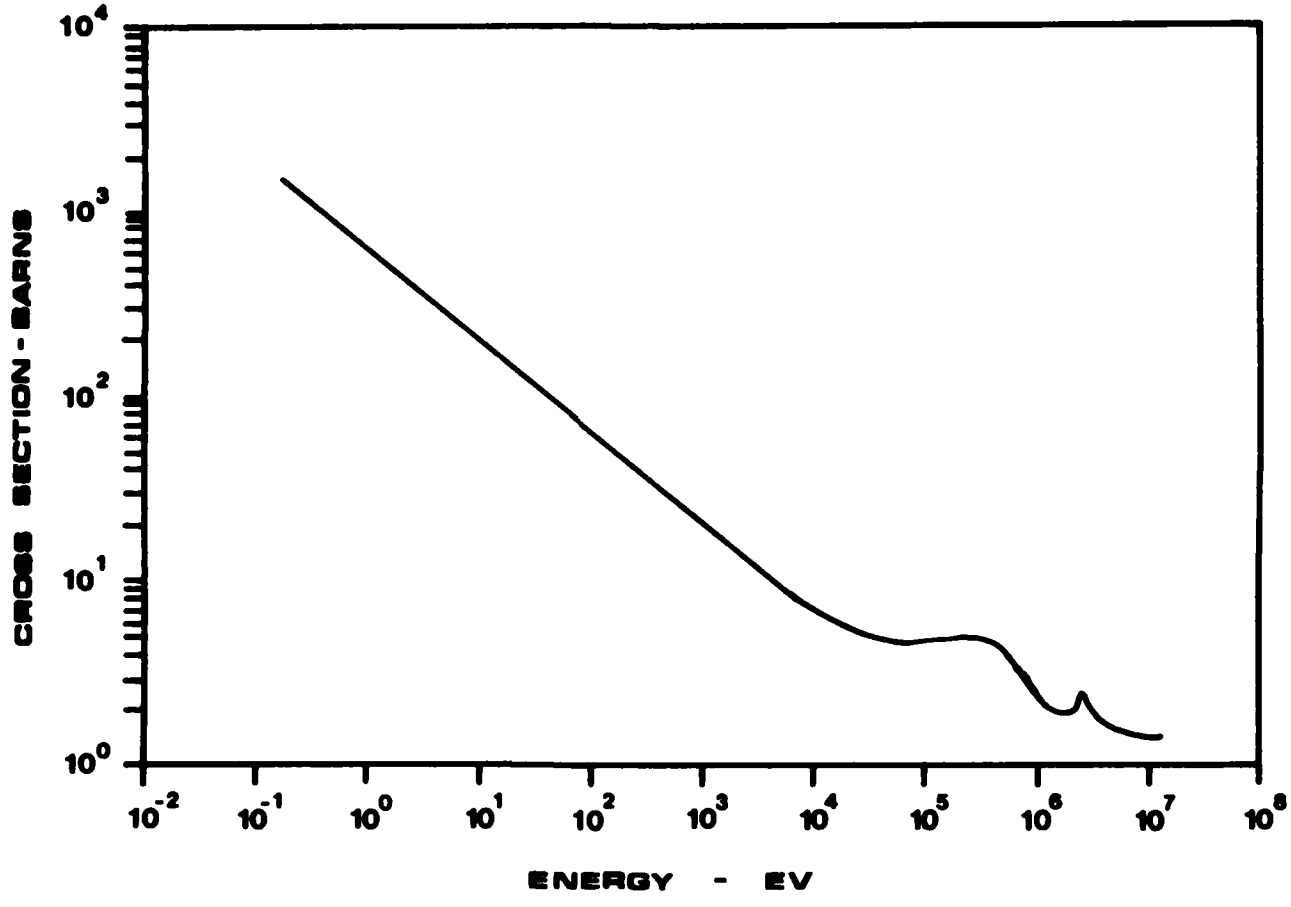
CROSS SECTION - BARNS
10^4
10^3
10^2
10^1
10^0
10^{-2}
10^{-1}
10^0
10^1
10^2
10^3
10^4
10^5
10^6
10^7
10^8
ENERGY - EV

the field. Below 14 MeV the ^{6}LiF response curve can be appropriately approximated by utilizing the Lithium-6 neutron absorption cross section curve (Ga76,G183) presented in Figure 2.

Criteria for performance of personnel neutron dosimeters are currently found in two documents by the American National Standards Institute and a Regulatory Guide published by the United States Nuclear Regulatory Commission (ANSI76, ANSI82, NRC77). The 1982 American National Standard for testing of dosimetric performance has recently been accepted by the United States Nuclear Regulatory Commission as criteria for license compliance with personnel dosimetry standards and testing taken over by the National Voluntary Laboratory Accreditation Program (NVLAP) administered by the National Bureau of Standards (FR83).

Shortly after attaining operational capability for personnel thermoluminescent dosimetry, the USAF participated in the preliminary test #3 of this standard as processor 138 (P182). Results of these tests showed the USAF easily capable of obtaining precision levels differing by less than ten percent from the accepted value for a specified neutron spectrum. The most significant result was the subsequent implementation of individual chip calibration techniques suggested by Zeman (Ze79) to reduce the reported standard deviation. Results of processor testing for neutrons show only the capability to accurately assess dose equivalents received from a specific Cf-252 source configuration for which reference calibration data is provided. Testing did not demonstrate the capability of meeting a 50

Figure 2

Lithium-6 Total Neutron Absorption Cross Sections versus Neutron Spectral Mid-Energy Values

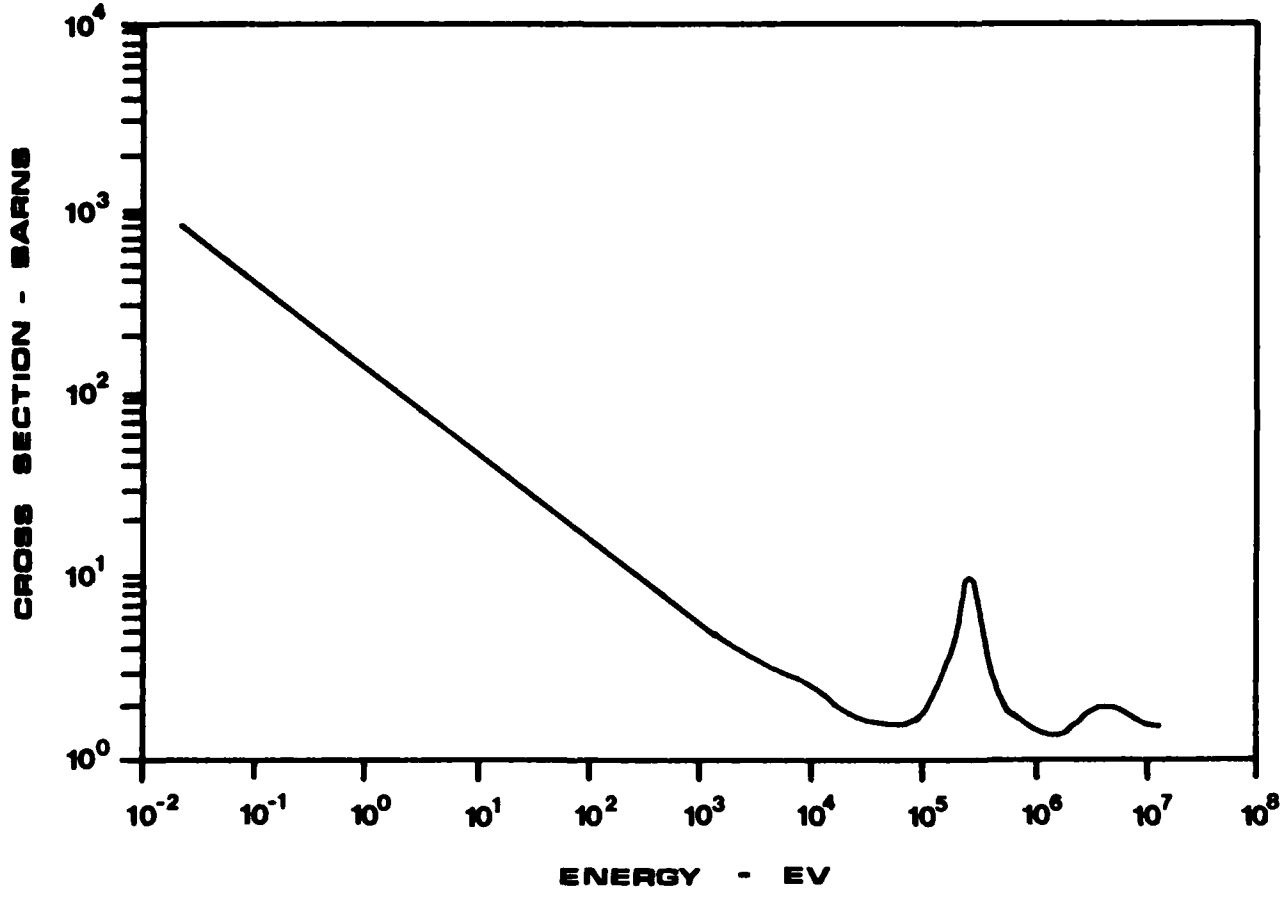
CROSS SECTION - BARNS
10^4
10^3
10^2
10^1
10^0
10^{-2}
10^{-1}
10^0
10^1
10^2
10^3
10^4
10^5
10^6
10^7
10^8
ENERGY - EV

percent performance criterion for all neutron spectra in which albedo response is shown to vary by more than two orders of magnitude.

III. THEORY

A. Neutron Interactions

The biological effects of nuclear radiations are attributed to ionization and electronic excitation in tissue which cause the destruction of various molecules such as proteins and DNA which play functional roles in living cells. In general, the greater the linear energy transfer (LET), the greater the damage for a given energy absorption. Although neutrons do not directly ionize, they are able to cause considerable biological damage through secondary interactions created by their passage through tissue.

Slow or thermal neutrons produce their primary effect through radiative capture reactions with hydrogen and nitrogen nuclei. The (n,α) capture of neutrons by hydrogen produces 2.2 MeV photons which either irradiate the surrounding tissue or escape from the body. The (n,p) reaction with nitrogen results in the production of protons which dissipate their energy in short high-LET paths. In addition, these reactions transform nitrogen atoms into atoms of carbon possibly destroying the identity of biologically important molecules which may result in significant alteration of cellular function. Other reactions exhibited by slow or thermal neutrons in living tissue are generally believed to be of minor significance.

When the body is exposed to intermediate or high energy (fast) neutrons, the particles lose their energy by elastic collisions with atoms of carbon, oxygen, nitrogen, and hydrogen present in living tissue. Interactions with hydrogen are generally considered to be the most important. In elastic collisions, the struck atom acquires kinetic energy which is dissipated by ionization, excitation, and elastic collisions with other atoms. Fast neutrons can sustain the (n,p) reaction with Nitrogen-14 indicated previously, or, given sufficient energy (greater than 1.5 MeV), the (n,α) reaction can occur. The recoil atoms, along with any protons or alpha particles produced, lose their energy within a very short distance of the point at which the initial reaction occurs. In considering the region in which neutron injury can occur, it is important to remember that neutrons can penetrate to considerable distances prior to sustaining an interaction.

Due to the high LET products of neutron interactions with tissue, the biological effectiveness of neutrons with tissue is not only generally higher than X or gamma rays but also depends markedly on neutron energy. It is assumed that differences in the LET of secondary products produced from neutron reactions are directly related to biological effects of the absorbed dose. Personnel limits are therefore stated in terms of the dose equivalent (DE) which is defined as the product of absorbed dose (D) and a LET-dependent

quality factor (QF) (NCRP54,ICRP63). Since dose is delivered over a range of values of LET (L), the dose equivalent is given by:

$$DE = \int_{L_{min}}^{L_{max}} D(L)QF(L)dL$$

where D(L) is the distribution of absorbed dose in LET, L, and QF (L) is the quality factor at L.

The relationship of neutron interactions at a given energy to the LET of the secondary interactions results directly in the determination of dose equivalent (DE). Sims (Si83) recently reviewed the use of five different sets of neutron fluence-to-dose equivalent (DE) conversion factors as a function of energy. Although differences in these conversion sets are generally considered minor, values for referenced spectra were found to deviate up to 41 percent dependent on the conversion factor set and interpolation method utilized. The point is that the dosimetrist must always be aware of what conversion factors were utilized prior to making any direct comparisons.

Early in the DoD INRAD effort, this possibility was recognized and a common set of conversion factors agreed upon which are followed in this work (Fa82). Conversion factors utilized (Figure 3) result from the calculations of Snyder (Sn57) as presented in ICRP Report # 21 (ICRP73). Calculation of conversion factors not directly given are obtained by the logarithmic interpolation method suggested by Eisenhauer and Schwartz (Ei81). A survey of Figure 3 will quickly show

Figure 3

Neutron Dose-Equivalent Conversion Factors

(Unidirectional Broad Beam, Normal Incidence)

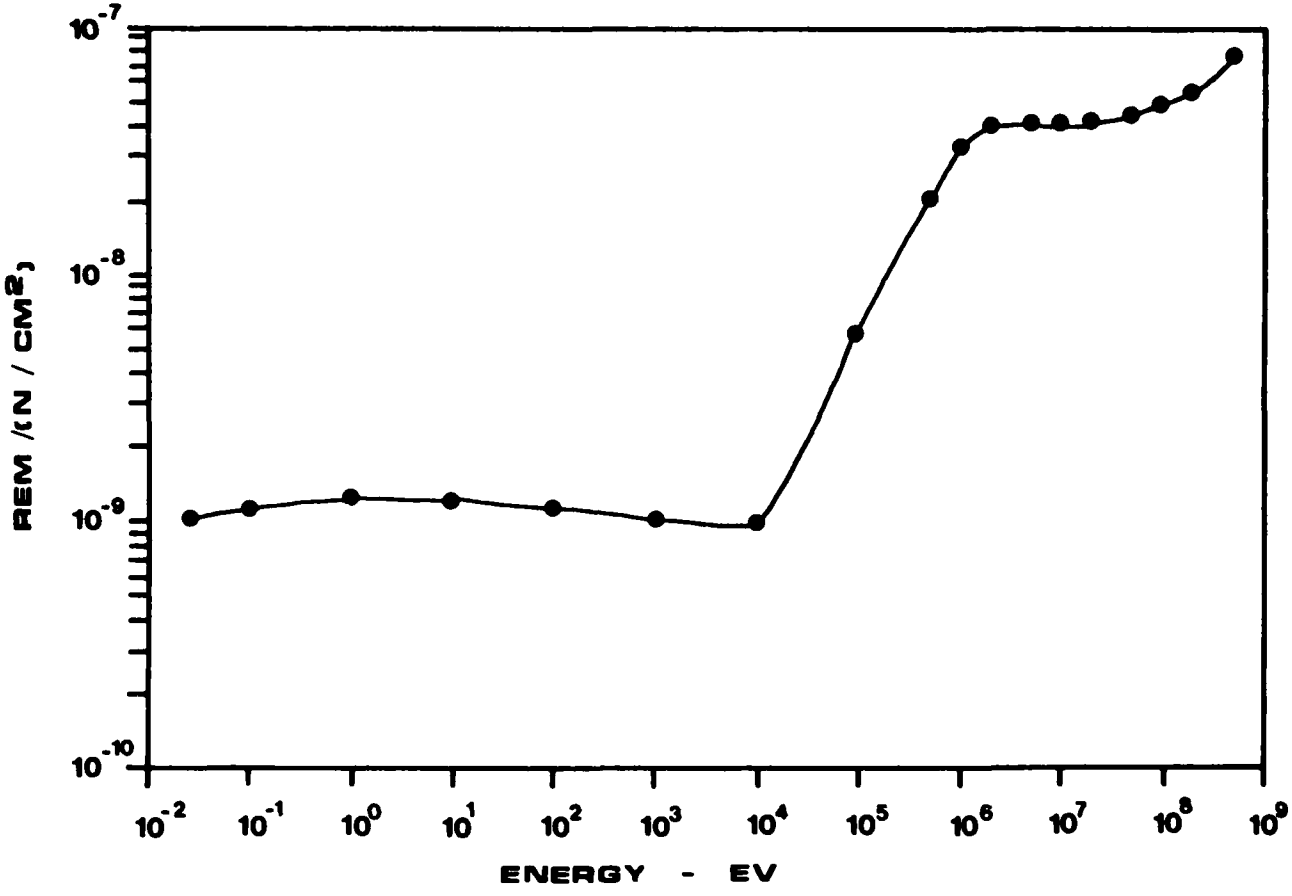
REM /(N / CM²)
10⁻⁷
10⁻⁸
10⁻⁹
10⁻¹⁰
10⁻² 10⁻¹ 10⁰ 10¹ 10² 10³ 10⁴ 10⁵ 10⁶ 10⁷ 10⁸ 10⁹
ENERGY - EV

the major deficiency of LiF thermoluminescent dosimeters in that although the majority of the dose equivalent is contributed by neutrons whose energies are greater than 10 KeV, these neutrons produce relatively little response in lithium fluoride.

B. Personnel Dosimeter Design

The design of the USAF Personnel Neutron Dosimetry Badge is an adaptation of a design originally developed for routine use at Sandia National Laboratories in Alburquerque, New Mexico (Th77). The intent of the Sandia design was to ascertain if individuals had been exposed to drastically different neutron spectra from those for which the individual's badge calibration factor had been assigned. This would allow for further investigation of the actual dose equivalent for these cases and the establishment of necessary direct calibration factors. The only basic difference lies in utilization of the four-chip card holder compatible with the Harshaw 2276 system in place of the two two-chip card holders used by Sandia for readout on their Harshaw 2271 systems. The four-chip card has a definite advantage since the two-chip card holders have a thin aluminum backing which interferes with the filtration for the chips on the companion card. The badge design is shown pictorially in Figure 4.

The four-chip TLD card insert contains two each ^{6}LiF (TLD-600) and ^{7}LiF (TLD-700) dosimeter chips placed in the positions shown. The TLD-600 chips are sensitive to neutron and gamma exposure while the TLD-700 chips are gamma sensitive only. Differential filtration is provided for energy correction of both the gamma and neutron

Figure 4

United States Air Force Personnel Neutron Dosimeter

Badge Design

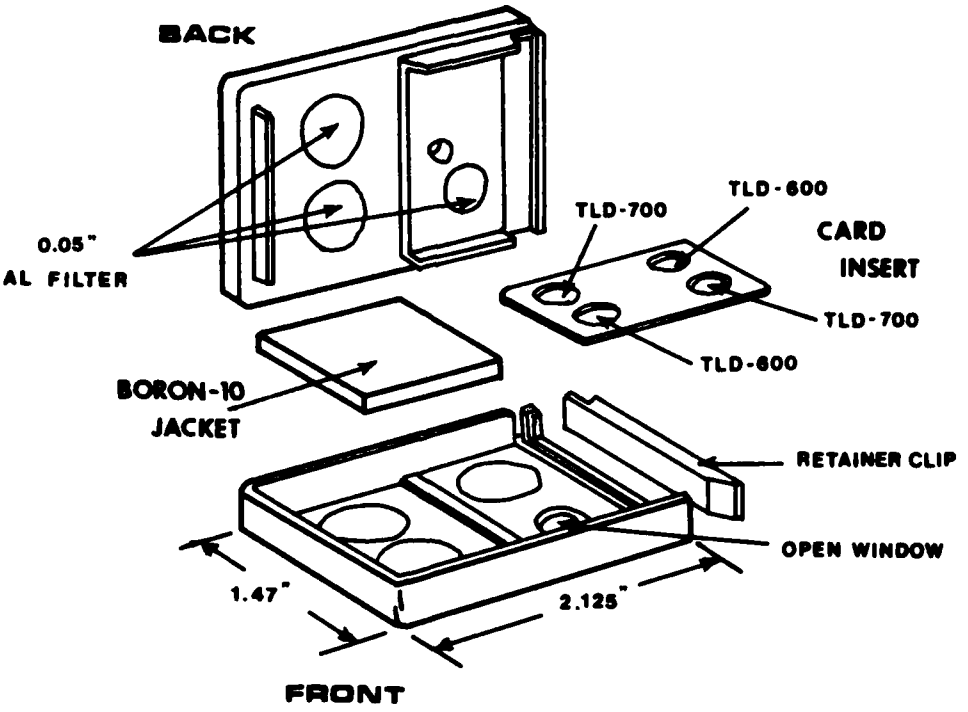

DOSIMETER BADGE
0.5" THICK

sensitive components. Standard open window/aluminum filtration correction is provided for photon energy correction while a Boron-10 impregnated pouch provides basic information concerning the neutron spectrum. The pouch allows the top TLD-600 chip to be utilized to measure incident thermal neutrons and albedo neutrons while the bottom TLD-600 chip measures both incident and backscattered intermediate-energy neutrons.

The use of the TLD-600 "Boron/Bare" ratio allows the identification of neutrons whose energies are below 1 eV. As the neutron energy drops below the 1 eV threshold, the "Boron/Bare" ratio decreases from approximately 0.2 to 0.025. Dosimeter response to neutrons between 1 eV and 10 keV is relatively independent, increasing by only a factor of 2 over this range. Over 10 keV, neutron sensitivity drops rapidly. Information provided through knowledge of the ratio of neutrons in these different energy ranges could allow additional data beyond the qualitative level to produce direct cross reference to appropriate calibration factors. This is especially important since, for proper neutron dosimetry evaluation, it is necessary to know the source of the neutrons and, if possible, to calibrate to that source.

C. TLD Dose Calculations

Dose calculations are made via interpretation of the thermoluminescent light output of all four lithium fluoride chips present in the USAF Personnel Neutron Dosimeter Badge. Considering the open window as chip position number one and numbering the remaining chips

clockwise from the badge front results in dosimeter filter/tld chip combinations as given in Table 1.

To eliminate the inherent chip to chip variations of thermoluminescent dosimeters (overall variations of ±15 percent have been noted), all responses are first normalized using individual chip normalization factors. These factors are obtained by exposing each chip to a Strontium-90 calibration source for sufficient time to obtain the equivalent response of 100 mR Cs-137. Calibration exposures are made immediately after each readout of every dosimeter card and all readings maintained in a computer data base. Any noted trend or gross deviation from standard chip calibration factors is evaluated prior to any actual dose assignments.

The response of chips one and three are used to establish the shallow and deep dose resulting from exposure to beta, gamma or X-radiation. The response ratio between chips one and three provides a correction factor to compensate for the over-response of the lithium fluoride to photons of energies less than 100 KeV. A typical energy response curve, along with Cesium-137 and Cobalt-60 calibration curves, are provided for reference in the Appendix. The photon response of chip three, corrected for the response differential noted between supplied batches of TLD-600 and TLD-700 (See Appendix), is subtracted from the response of chips two and four to eliminate photon response for neutron calculations.

The use of chips two and four to obtain neutron dose equivalent is the detailed subject of the remainder of this report. Due to the

Table 1

USAF Personnel Neutron Dosimeter Configuration

Chip Position	TLD Type	Filtration (mg/cm2)	Type	Purpose
1	TLD-700	8	Mylar	Photon Dose (Shallow)
2	TLD-600	343	Aluminum	Neutron Dose
		226	Plastic	
3	TLD-700	343	Aluminum	Photon Dose
		332	Plastic	(Deep)
		26	Boron	
4	TLD-600	343	Aluminum	Neutron
		332	Plastic	Spectral
		26	Boron	Correction

higher sensitivity of the bare chip, the raw response of chip two corrected for gamma interference is generally utilized for obtaining neutron response. This reading is extremely dependent upon the thermal component of the incident spectra and relies upon detailed characterization of that spectra for appropriate calibration factors. Although the response of the boron covered chip eliminates the majority of the influence of thermal neutrons, the sensitivity is reduced by at least a factor of ten and calibration factors are still required for spectra of interest.

D. Dosimeter Response Modeling

The theory behind potential utilization of the USAF Personnel Neutron Dosimetry Badge described previously for "self-calibration", is that within the range of neutron environments encountered routinely at USAF facilities (moderated fission spectra), the dosimeter badge in itself could serve as a crude spectrometer to allow determination of the correct dose equivalent to be assigned. In the same manner as the 9 to 3 ratio used extensively by Hankins (Ha75), the dose equivalent can be considered proportional to the ratio of the light outputs of the filtered TLD 4 (N_4) and unfiltered TLD 2 (N_2). Figure 5 is a schematic diagram of the USAF Personnel Neutron Dosimetry Badge and its response parameters. The light output from TLD 2 will be the result of the sum of $N_I + N_A + \gamma$; the light output from TLD 4 will be the result of the sum of $N_{IB} + N_{AB} + \gamma$; or

Figure 5.

Theoretical Schematic Representation of the United States Air Force Personnel Neutron Dosimeter Badge Design.

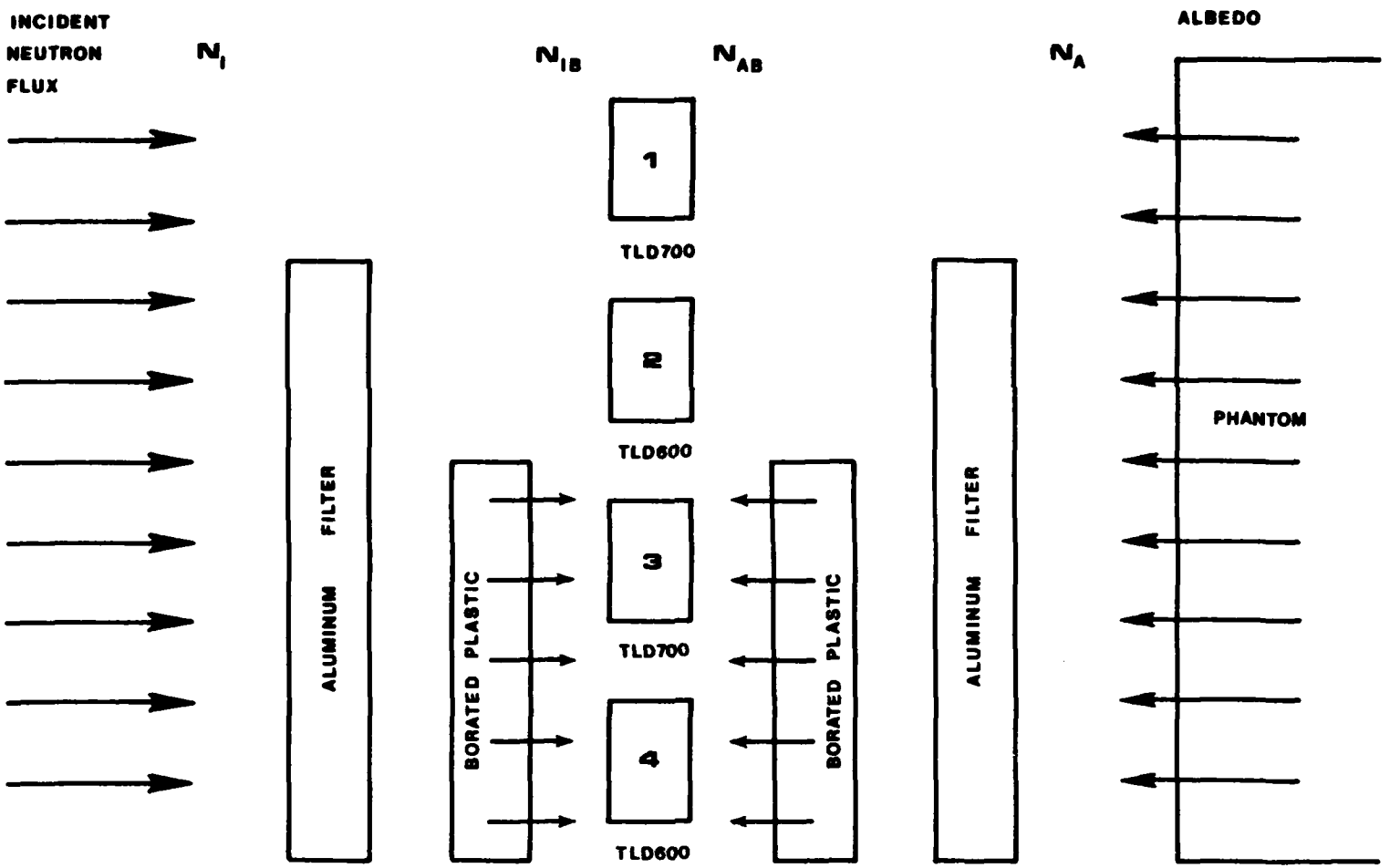
INCIDENT
NEUTRON
FLUX
N_I
ALUMINUM FILTER
N_{IB}
BORATED PLASTIC
1
TLD700
2
TLD600
3
TLD700
4
TLD600
N_{AB}
BORATED PLASTIC
ALUMINUM FILTER
N_A
ALBEDO
PHANTOM

$$N_2 = N_I + N_A + \gamma \quad = N_I + N_A + N_3 \tag{1}$$

$$N_3 = \gamma \tag{2}$$

$$N_4 = N_{IB} + N_{AB} + \gamma \quad = N_{IB} + N_{AB} + N_3 \tag{3}$$

where

N_I = Light output produced by the incident neutron flux

γ = Light output produced by the incident gamma flux

N_A = Light output produced by the reflected (albedo) neutron flux

N_{IB} = Light output produced by the epithermal and fast portions of the incident neutron flux

N_{AB} = Light output produced by the epithermal and fast portions of the reflected (albedo) neutron flux

Therefore, a proportionality constant is chosen which is equal to the ratio of the two light outputs, or

$$\frac{N_4}{N_2} = \frac{N_{IB} + N_{AB} + N_3}{N_I + N_A + N_3} \tag{4}$$

Since it is most common to work with the response of ^{6}LiF for neutrons corrected for gamma respon[illegible] by subtraction of ^{7}LiF response, we can define the gamma free response ratio as follows:

$$\frac{N_4'}{N_2'} = \frac{N_4 - N_3}{N_2 - N_3} = \frac{N_{IB} + N_{AB}}{N_I + N_A} \tag{5}$$

The response of ^{6}LiF is a result of neutron interactions with the Lithium-6 nucleus. The reaction of interest is the splitting of the lithium into an alpha particle (Helium-4 nucleus) and a triton (Tritium nucleus), which is written $^{6}Li(n,\alpha)^{3}H$. The α and ^{3}H recoiling particles ionize atoms in their path thus freeing electrons which will then become trapped. The normal difficulty in correctly interpreting this interaction is that a thermal neutron will interact with ^{6}Li approximately one thousand times more frequently than a neutron with a million times the energy. ^{6}LiF can be considered to act as a differential flux detector responsive mainly at thermal energies. For this reason, thermoluminescent dosimeters are extremely energy dependent in their response to neutrons. The true ^{6}LiF response could thus be considered to be

$$N_R = C \int_0^\infty \phi_E (1 - e^{-\Sigma_{Li_E} X_C}) dE \qquad (6)$$

where

ϕ_E = Incident neutron flux of energy E

Σ_{Li_E} = Lithium macroscopic absorption cross section at energy E (cm^{-1})

X_C = Thickness of thermoluminescent dosimeter chip (cm)

C = Response conversion factor

N_R = Neutron response (Light output)

Similarly, the effect of the boron absorber on the neutron spectrum incident to the dosimeter pouch can be represented as

$$\phi_{ET} = \phi_E \bullet^{-\Sigma_{B_E} X_P} \qquad (7)$$

where

ϕ_{ET} = Transmitted neutron flux of energy E

ϕ_E = Incident neutron flux of energy E

Σ_{B_E} = Boron macroscopic absorption cross section at energy E (cm-1)

X_P = Thickness of Boron impregnated dosimeter pouch

The final factor, the reflected or albedo flux from the phantom can be approximated in two different ways. The first approximation considers the albedo flux as a fraction of the incident flux as a consequence of simple diffusion theory (GL52) as follows

$$\beta_E = \frac{1 - 2KD}{1 + 2KD} \qquad (8)$$

where

β_E = Albedo factor for energy E

K = Reciprocal of the diffusion length

D = Diffusion coefficient.

Utilization of β_E to approximate the albedo spectrum is recognized to underestimate the true low energy albedo spectrum since this factor considers the fraction of reflected neutrons to be equal in energy to the incident neutron. Albedo neutrons are in fact reflected in a continuum of energies with the incident energy being the maximum reflected energy.

Combining equations 5, 6, 7 and 8, we obtain the following equation for the schematic representation of the USAF Personnel Neutron Dosimeter Badge:

$$\frac{N_4'}{N_2'} = \frac{C\int_0^\infty \phi_{ET}(1-e^{-\Sigma_{Li_E}X_C})dE + C\int_0^\infty \beta_E\phi_{ET}(1-e^{-\Sigma_{Li_E}X_C})dE}{C\int_0^\infty \phi_E(1-e^{-\Sigma_{Li_E}X_C})dE + C\int_0^\infty \beta_E\phi_E(1-e^{-\Sigma_{Li_E}X_C})dE}$$

$$= \frac{\int_0^\infty \phi_E e^{-\Sigma_{B_E}X_P}(1-e^{-\Sigma_{Li_E}X_C})dE + \int_0^\infty \beta_E\phi_E e^{-\Sigma_{B_E}X_P}(1-e^{-\Sigma_{Li_E}X_C})dE}{\int_0^\infty \phi_E(1-e^{-\Sigma_{Li_E}X_C})dE + \int_0^\infty \beta_E\phi_E(1-e^{-\Sigma_{Li_E}X_C})dE} \quad (9)$$

The second approximation to the albedo flux results from direct modeling of the reflected spectrum using functions calculated by Glickstein (G183). This calculation can be expressed as

$$\phi_{E_{AB}} = \int_0^E f(E, E_{AB})\phi_E \, dE \tag{10}$$

where:

$\phi_{E_{AB}}$ = Albedo neutron flux of Energy E

ϕ_E = Incident neutron flux of Energy E

$f(E, E_{AB})$ = Neutron scattering function

Combining equations 5, 6, 7 and 10 we obtain the following second equation for the schematic representation of Personnel Neutron Dosimeter Badge.

$$\frac{N_4'}{N_2'} = \frac{\int_0^\infty \phi_E \, e^{-\Sigma_{B_E} X_P (1-e^{-\Sigma_{Li_E} X_C})} dE + \int_0^\infty \phi_{E_{AB}} e^{-\Sigma_{B_E} X_P (1-e^{-\Sigma_{Li_E} X_C})} dE}{\int_0^\infty \phi_E (1-e^{-\Sigma_{Li_E} X_C}) dE + \int_0^\infty \phi_{E_{AB}} (1-e^{-\Sigma_{Li_E} X_C}) dE} \tag{11}$$

IV. MATERIALS AND METHODS

A. Calibration Facility Descriptions

1. Dosar Facility - Oak Ridge National Laboratory

The Dosimetry Applications Research (DOSAR) Facility is a part of the Oak Ridge National Laboratory (ORNL) located in Oak Ridge, Tennessee where irradiations took place utilizing the Health Physics Research Reactor (HPRR). The HPRR is an unmoderated fast reactor which is capable of operation in either low power steady-state (0.1 w to 10 kw) or pulse mode (10^{16} to 10^{17} fissions). The reactor core is a right circular cylinder (20 cm diameter and 23 cm high) of enriched uranium (93.14 wt % U-235) alloyed with 10 wt % molybdenum.

The reactor building is a low-scatter aluminum structure 23 m long, 9 m wide, and 15 m high. Within the reactor building, the HPRR is supported by a 10 m high positioning device mounted on tracks which extend the length of the building and 21 meters beyond on an external concrete pad. This positioning device allows the reactor to be moved horizontally along the track and be positioned vertically along the centerline of the track to within 1 cm of any preselected height up to 5 meters above the concrete floor. Two concrete pits are available for reactor placement allowing access to the reactor building approximately 15 minutes after HPRR operation.

The reactor control building is located 274 meters from the reactor building behind an intervening ridge which provides shielding from direct radiation. The two buildings are connected by a multiconduit above-ground cable distribution network which links the facilities for reactor control, remote positioning, remote radiation monitoring, closed circuit television and experimental device monitoring. Within the control building, protection from scattered radiation is provided by the roof, exterior walls, and some interior walls all of which consist of poured concrete ranging from 20 to 60 centimeters thick. Reactor operations, experimental monitoring, and remote positioning of the HPRR is performed from the control room.

Dosimeter irradiations were carried out on the HPRR on three separate occasions:

(1) during attendance at an ORNL sponsored Personnel Neutron Dosimetry course 9-14 November 1982;

(2) in conjunction with the 9th Personnel Dosimetry Intercomparison Study (PDIS) 6-9 April 1983; and

(3) during reactor utilization time provided 25-27 April 1983 by the DOSAR staff.

Dosimeters were exposed while mounted on standard bomab or lucite phantoms. Phantoms were placed to coincide with the horizontal centerline of the HPRR (1 meter above the concrete floor) at variable distances from the vertical centerline. The energy distribution (neutron spectra) of neutrons reaching the dosimeters was

varied via a lucite, steel, concrete, or steel/concrete shield interposed between the HPRR and the phantom position. Reference dosimetry data for each of the shield configurations is available in the literature (Si81). Desired exposure levels were predetermined for each reactor run and appropriate power levels and exposure times calculated. Exposure time was started when the reactor attained 1/e of the desired power level and terminated at the predetermined time. This procedure compensated for the variable power levels (and resultant neutron flux) that occur during reactor startup and shutdown. Final dose determinations were made by reference to sulphur activation pellets placed at a standard calibration point on the HPRR for each individual reactor run. Gamma exposure levels were determined by integration of the output from a Shonka-Wycoff chamber mounted on a phantom adjacent to the dosimeter phantom and equidistant from the reactor centerline.

2. Willow Run Facility - University of Michigan

The University of Michigan (UM) Willow Run Facility was established under contract with the Nuclear Regulatory Commission for testing of the Personnel Dosimetry Performance Standard (P180,P182). The facility is located within an old vehicle maintenance garage of a former United States Air Force Base. The moderator sphere is suspended via four chains from the ceiling of the facility approximately 250 cm above the concrete floor, 205 cm from the wooden ceiling, and 400 cm from the nearest concrete block wall. This NBS developed moderator sphere (Sc80) is designed to provide a neutron spectrum which

would simulate the type of spectra encountered in the vicinity of a power reactor. The sphere consists of a 30 cm diameter, 0.8 cm thick, stainless steel shell filled with D_2O. Additionally, the sphere is covered with an outer layer of cadmium, 0.5 mm thick. The cadmium is present to avoid calculational difficulties posed by thermal neutrons during source modeling. Although these thermal neutrons do not contribute significantly to the dose equivalent, they do generally contribute a significant portion of the thermoluminescent response.

The bare Cf-252 source capsule, when not in use, is stored in a water filled pit approximately 120 cm in diameter and 120 cm in depth, directly below the moderator sphere.

3. Hazards Control Calibration Facility - Lawrence Livermore National Laboratory

The Lawrence Livermore National Laboratory Hazards Control Calibration Facility is a concrete room 12.2 m long, 9.14 m wide, and 7.32 m high. Individual sources are moved from storage shields to the irradiation position through a pair of pneumatic "rabbit" systems. The exposure end of each of the transfer tubes is one meter above an aluminum false floor in the center of the calibration room and approximately two meters apart. The two transfer tubes are used for gamma and neutron sources respectively, and allow for simultaneous source irradiations. Exposures are controlled through a computer console located in an adjacent control room. Remote instrumentation and interlocks are utilized to insure personnel safety.

Multiple sources are available to provide various source strengths of PuBe, Cf-252, Cs-137 and Co-60. To provide various neutron spectra, moderator spheres of deuterium oxide, polyethylene, and aluminum are available for placement over the end of the transfer tube. Characterizations of the neutron fields available have been accomplished and are available in the literature (Gr78).

B. Equipment Description and Use

1. Multisphere Neutron Spectrometer

Neutron spectrum determinations were made utilizing a Ludlum Model 42-5 Neutron Spectrometer. The spectrometer consists of a 4 mm x 4 mm LiI(Eu) scintillation crystal coupled through an optical light pipe to a photomultiplier tube. High density polyethylene moderating spheres 2, 3, 5, 8, 10, and 12 inches in diameter are provided for measuring individual spectral responses. Each sphere is machined and drilled to place the LiI(Eu) crystal in the geometric center of the selected moderator.

High voltage was supplied to the photomultiplier tube with a Ludlum Model 2500 scaler/rate meter which also served as a gross monitor of the output of the detector system. The amplified output of the scaler/rate meter was fed directly into the signal input of a Nuclear Data ND-Six portable multichannel analyzer. For each measurement, the output spectrum was collected and stored on tape for subsequent retrieval and data reduction.

2. Portable Neutron Remmeters

Eberline Model PRS-2P "RASCAL" portable neutron Rem counters were utilized to measure the neutron fields encountered. The "RASCAL" system consisted of a portable, digital display, scaler/rate meter connected to a Nancy Wood BF_3 detector probe. Measurements were made utilizing the bare BF_3 tube for determination of the thermal neutron component, the BF_3 tube inserted into an Eberline HP-280 7.6 cm (3 in) diameter cadmium covered polyethelene sphere for estimation of intermediate neutrons, and with the BF_3 tube inserted into an Eberline 23 cm (9 in) NRD cadmium loaded polyethelene sphere for estimation of neutron dose equivalent.

3. Harshaw Advanced Thermoluminescent Dosimetry System

The Harshaw Advanced Thermoluminescent Dosimetry System utilized by the USAF for processing of exposed thermoluminescent dosimeter cards is a custom designed combination of the Harshaw Model 2276 Automated TL Dosimetry System and a Harshaw Model 2080 Glow Curve Analyzer. The Model 2080 Glow Curve Analyzer replaces the Harshaw Model 2000B Automatic Integrating Picoammeter in the 2276 system which further includes a Model 2276T Transport Module, a Model 2276L Logic Module, and a Texas Instruments Model KSR-820 printing terminal. The thermoluminescent dosimetry system is further controlled via custom applications software running on a Hewlett-Packard Model 1000 Series F computer system. The overall system provides for remote programming of the 2276L Logic Module, and collection of both the integrated current output and the digitized glow

curve for every thermoluminescent chip processed. Data collected are analyzed for dose computation and validation purposes using data processing programs. For this work, all dosimeter chips were read out during a 40 second heating cycle without any preliminary preheat cycle. The heating cycle consisted of an initial instantaneous heating to 120 degrees centigrade followed by a 5 degrees centigrade per second ramp until a final temperature of 300 degrees centigrade was reached. This final temperature was thus established in order to prevent damage to the thin teflon sheeting supporting the LiF crystals in the card holder. Readouts were performed under a continuous flow of prepurified dry nitrogen in order to reduce the influence of triboluminescence. A typical card glow curve readout is presented in Figure 6.

C. Computational Techniques

Numerical calculations necessary for this work were conducted either on a Digital Equipment Corporation (DEC) PDP 11/34 or a Hewlett Packard (HP) 1000 Series F computer available within the Radiation Services Division of the United States Air Force Occupational and Environmental Health Laboratory. All graphical presentations were constructed utilizing the standard plotting package available on the DEC PDP 11/34. Data analysis was conducted using software available through the Statistical Analysis System (SAS) (He78) or standard statistical equations (So69).

Calculation of neutron spectra from bonner sphere measurements was accomplished utilizing an unfolding program developed at

Figure 6.

Typical Glow Curve Readout of Four Chip

Dosimeter Card.

GLOW CURVE PLOTS FOR 184384

CHIP 1

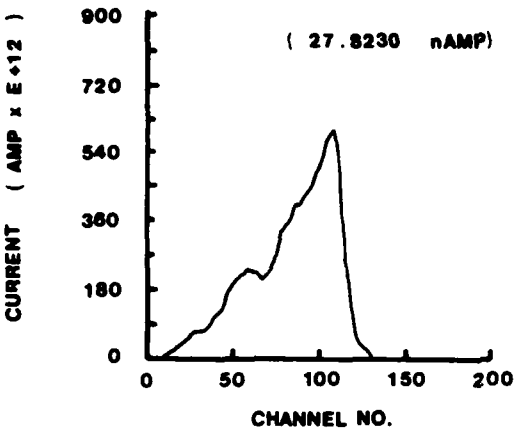

CHIP 2

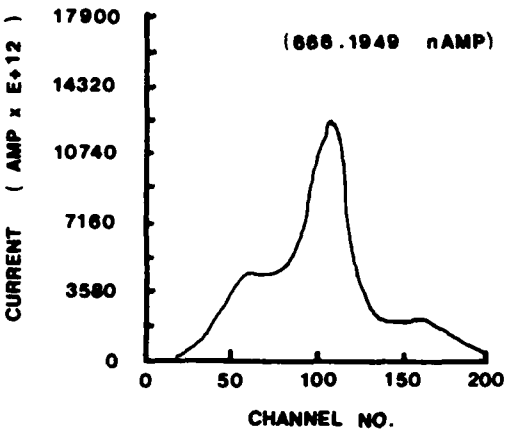

CHIP 3

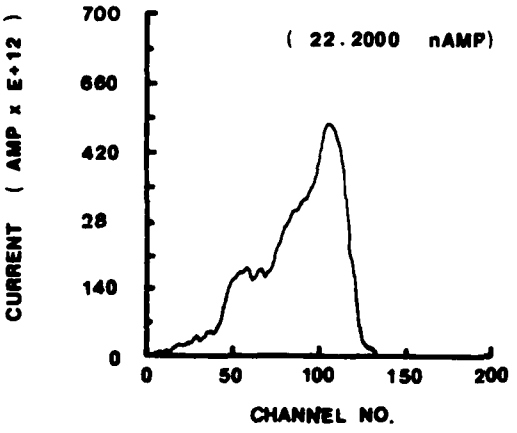

CHIP 4

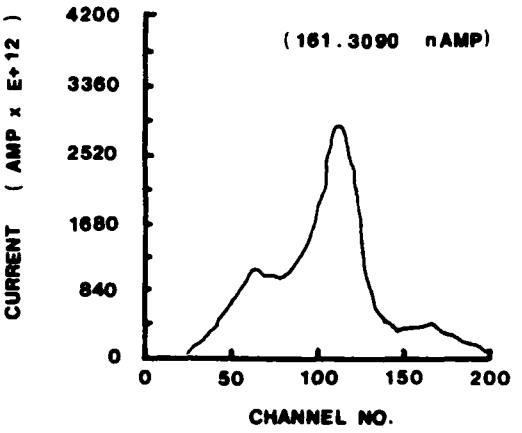

the Lawrence Livermore National Laboratory (Ho83). This program assumes an initial spectrum and then procedes to change the input spectrum utilizing response functions for the 4 mm X 4 mm LiI(Eu) detector developed by Sanna (Sa73) until the calculated counts from each detector match the measured counts per second. The program continues to iterate until the detector residuals reach a minimum.

D. Other Measurements

Throughout the duration of this work, many ancillary measurements were made other than direct measurement of Lithium Fluoride thermoluminescent response in the various neutron environments. These measurements are included where appropriate for completeness.

Rascal calibration measurements were completed for all neutron calibration spectra encountered along with 23 cm (9 in) to 7.6 cm (3 in) or 7.6 cm to bare ratios whenever source or facility time was available. Complete bonner sphere measurements were taken for all source configurations used at the Lawrence Livermore National Laboratory Hazards Control Calibration Facility to allow calculation of the theoretical response parameters of the USAF Personnel Neutron Dosimeter. Bonner sphere spectra are presented in the Appendix (Figures 40 to 48).

In order to identify the effect, if any, of the USAF Personnel Neutron Dosimeter Badge in itself on the input neutron spectra, measurements were made with the TLD card insert placed in air and directly upon the lucite phantom without any modifying effect of the

badge. Resultant albedo response factors are presented in the Appendix (Figures 34 and 35). A discussion of the moderating effect of the badge can be found in the results.

V. RESULTS

As previously stated, this work was designed to determine if the USAF Personnel Neutron Albedo Dosimeter could be used to "self-correct" for spectral dependent response in environments of moderated fission spectra. Common practice is to take work-place calibration measurements with auxiliary instrumentation such as a remmeter and relate actual dosimeter results to these values by the application of a correction factor. Tables 2 and 3 present the measured remmeter 23 cm (9 in) to 7.6 cm (3 in) or 7.6 cm (3 in) to bare ratios either acquired during this work or available in the literature for the sources and spectra measured. Accuracy of remmeter measurements is dependent upon relating this ratio to the ratio measured with the calibration source of choice. Calibration curves for each of the remmeters used are presented in the Appendix (Figures 32 and 33). Linear regression calibration curves were found to be log(Ratio) = -2.57E-2 x (CPM/(MR / HR)) + 1.41 and log(Ratio) = -2.85E-2 x (CPM/(MR / HR)) + 1.69 for Rascal/NRD serial numbers 212 and 215 respectively. Correlation coefficients were 0.902 and 0.881 ($P < 0.001$).

Figures 7 and 8 present the integral and peak response in pico-coulombs per millisievert for the USAF Personnel Neutron Albedo Dosimeter versus the remmeter ratio. Correlation coefficients were found to be 0.904 and 0.906 for the integral and peak curves respec-

TABLE 2

Ratios of the Counting Rates of a BF_3 Detector Inside 23 cm (9 in) and 7.6 cm (3 in) Polyethylene Spheres

Source	Distance m.	Ratio 23 cm/7.6 cm Spheres Hankins (Po72,Ha77)	Greene (Gr82)	This Work
LLNL PuBe (Bare)	1	----	----	2.67
LLNL Cf252 (Bare)	1	----	----	1.99
LLNL Cf252 (Bare)	2	----	----	1.21
ORNL HPRR (Bare)	2	1.09	1.10	1.14
ORNL HPRR (Bare)	3	1.00	1.00	----
ORNL HPRR (Bare)	6	0.89	0.85	0.86
LLNL Cf252 (5 cm D_2O)	1	----	----	0.84
ORNL HPRR (13 cm Steel)	3	0.74	0.72	0.74
ORNL HPRR (12 cm Lucite)	3	0.57	0.53	0.58
ORNL HPRR (12 cm Lucite)	9	----	0.42	0.47
ORNL HPRR (20 cm Concrete)	3	----	0.39	0.41
LLNL Cf252 (10 cm D_2O)	1	----	----	0.38
ORNL HPRR (15 cm Concrete + 5 cm Steel)	3	----	0.34	----
UM Cf252 (15 cm D_2O + 0.5 mm Cd)	0.5	----	----	0.29
LLNL Cf252 (15 cm D_2O)	1	----	----	0.26
LLNL Cf252 (15 cm D_2O + 0.5 mm Cd)	1	----	----	0.23
LLNL Cf252 (25 cm D_2O)	1	----	----	0.20
LLNL Cf252 (20 cm Al)	1	----	----	0.17

TABLE 3

Ratios of the Counting Rates of a BF_3 Detector Inside and Outside a 7.6 cm (3 in) Polyehylene Sphere

Source	Distance	Ratio 7.6 cm/Bare
UM Cf252 (15 cm D_2O + 0.5 mm Cd)	0.5	8.21
LLNL Cf252 (5 cm D_2O)	1	6.94
LLNL Cf252 (15 cm D_2O + 0.5 mm Cd)	1	5.98
LLNL Cf252 (10 cm D_2O)	1	4.88
LLNL Cf252 (Bare)	1	4.81
LLNL PuBe (Bare)	1	3.86
LLNL Cf252 (Bare)	2	2.40
LLNL Cf252 (15 cm D_2O)	1	2.19
LLNL Cf252 (20 cm Al)	1	1.03
LLNL Cf252 (25 cm D_2O)	1	0.54

Figure 7

Total Integral Thermoluminescent Response (Picocoulombs per Millisievert) versus Ratio of Counting Rate of a BF_3 Detector Inside 23 cm (9 in) and 7.6 cm (3 in) Polyethelene Spheres. Response is for TLD-600 Chip Exposed in USAF Personnel Neutron Dosimeter Above the Boron-10 Pouch.

———— First Order Least Square Curve Fit

---------- Second Order Least Square Curve Fit

Slope: -0.529 ± 0.038

Intercept: 2.625 ± 0.203

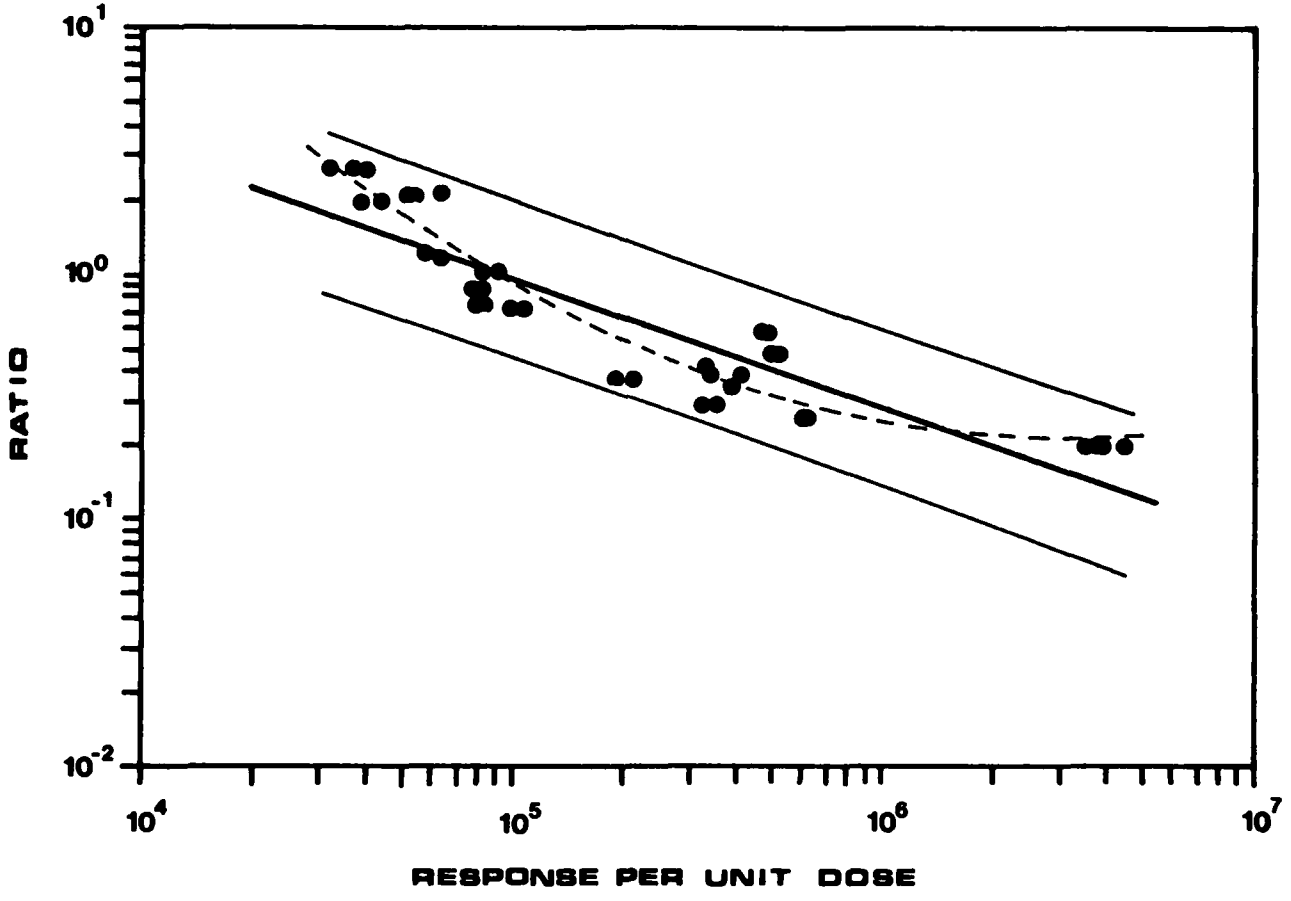
10^1
10^0
10^{-1}
10^{-2}
RATIO
10^4
10^5
10^6
10^7
RESPONSE PER UNIT DOSE

Figure 8

Peak Thermoluminescent Response (Picocoulombs per Millisievert) versus Ratio of Counting Rates of a BF_3 Detector Inside 23 cm (9 in) and 7.6 cm (3 in) Polyethelene Spheres. Response is for TLD-600 Chip Exposed in USAF Personnel Neutron Dosimeter Above the Boron-10 Pouch.

———— First Order Least Square Curve Fit

---------- Second Order Least Square Curve Fit

Slope: -0.529 ± 0.038

Intercept: 1.705 ± 0.135

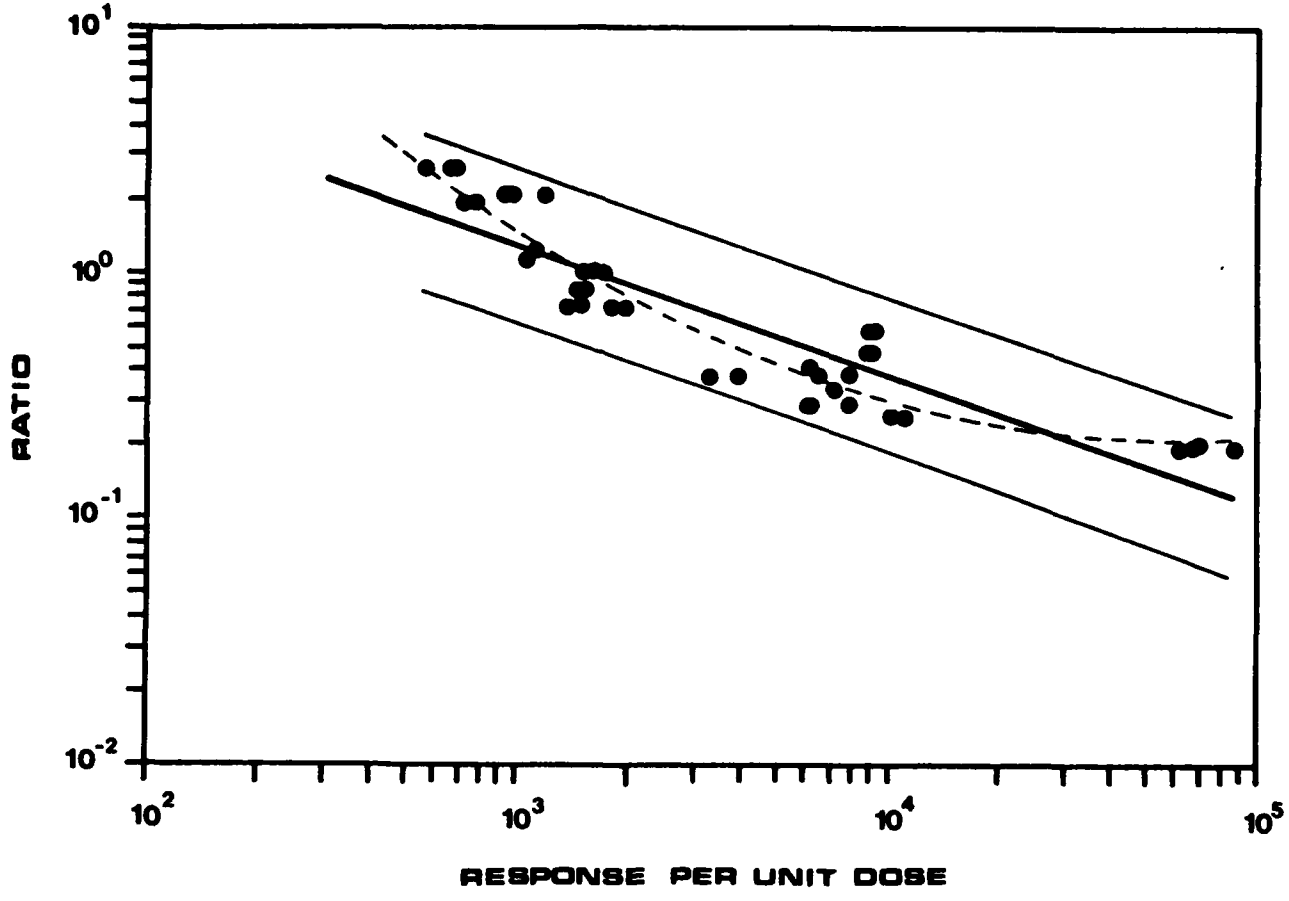
10^1
10^0
10^{-1}
10^{-2}
RATIO
10^2
10^3
10^4
10^5
RESPONSE PER UNIT DOSE

tively ($P < 0.005$). Figures 9 and 10 present the identical response factors in picocoulombs per millisievert versus the internal badge boron/bare ratios. Correlation coefficients of 0.654 and 0.717 were obtained for the integral and peak curves respectively ($P < 0.001$). Both the linear and second order regression curves have been plotted. Empirical observation that the second order equation results in a better fit for the data presented is not supported by the data of Hankins (Ha75) over a much broader energy range. Utilization of this second order fit would present the problem of requiring additional data about the spectrum measured when the second order solution yielded double valued calibration factors. Resultant regression curves for integral and peak evaluation versus nine to three response factors were log(Ratio) = -0.529 x log(Response) + 2.625 and log(Ratio) = -0.529 x log(Response) + 1.705 respectively. The internal boron/bare (four to two) ratio yielded regressions of log(Ratio) = -0.154 x log(Response) - 7.83E-3 and log(Ratio) = - 0.168 x log(Response) - 0.215 for the integral and peak evaluation techniques.

Data taken to help ascertain the true neutron albedo effect on the USAF Personnel Neutron Albedo Dosimeter are presented in the Appendix (Figures 34 and 35). For all spectra evaluated, the badge holder/card combination exposed on a lucite phantom was found to yield approximately 90 percent of the response of the card exposed directly on the phantom without the badge holder. This most likely is a result of the air separation caused by the badge attachment clip.

Figure 9

Total Integral Thermoluminescent Response (Picocoulombs per Millisievert) for TLD-600 Chip Exposed in USAF Personnel Neutron Dosimeter Above the Boron-10 Pouch versus Ratio of Integral Responses of TLD-600 Surrounded by and Above the Boron-10 Pouch.

———— First Order Least Square Curve Fit

---------- Second Order Least Square Curve Fit

Slope: -0.154 ± 0.027

Intercept: 0.008 ± 0.142

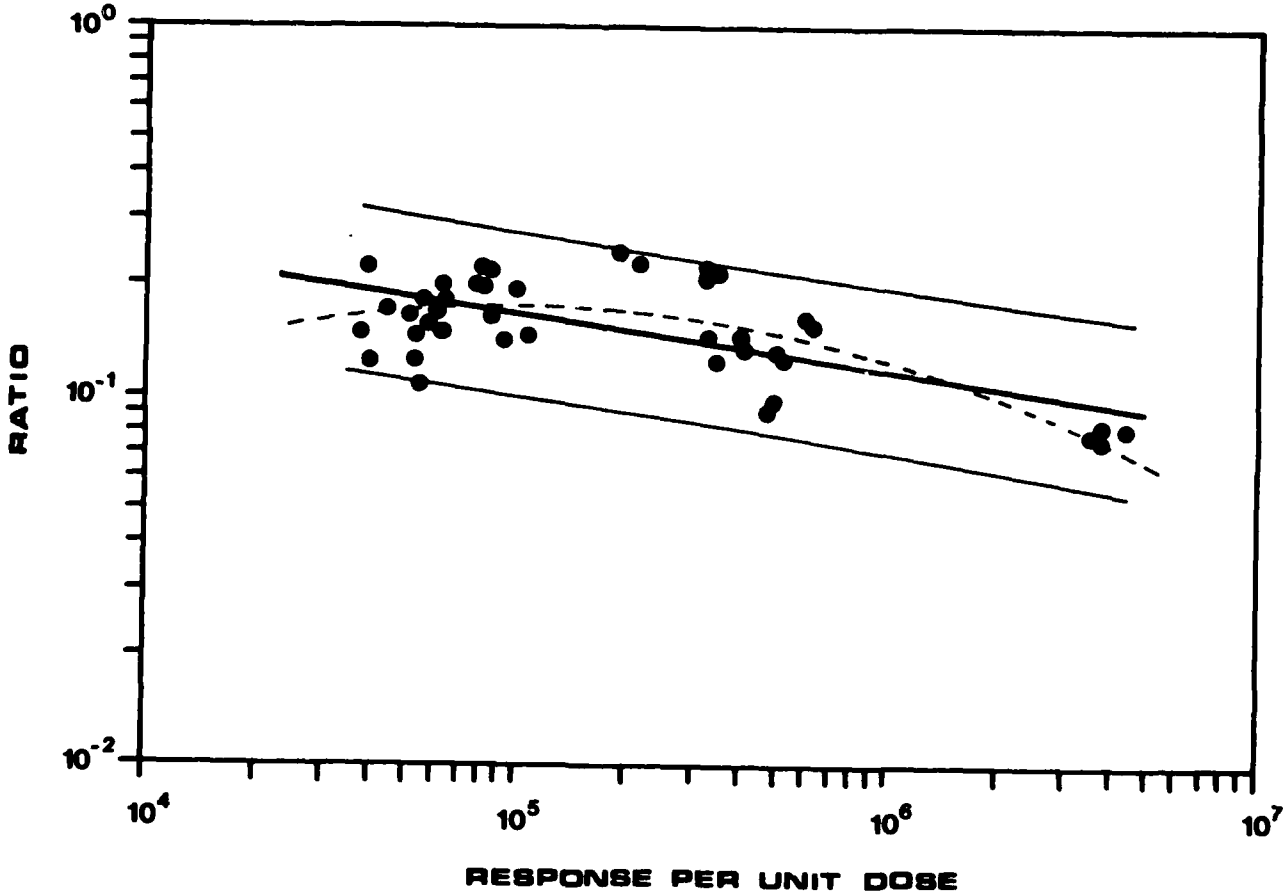
10^0
10^{-1}
10^{-2}
RATIO
10^4
10^5
10^6
10^7
RESPONSE PER UNIT DOSE

Figure 10

Peak Thermoluminescent Response (Picocoulombs per Millisievert) for TLD-600 Chip Exposed in USAF Personnel Neutron Dosimeter Above the Boron-10 Pouch versus Ratio of Peak Response of TLD-600 Surrounded by and Above the Boron-10 Pouch.

———— First Order Least Square Curve Fit

---------- Second Order Least Square Curve Fit

Slope: -0.168 ± 0.025

Intercept: 0.215 ± 0.088

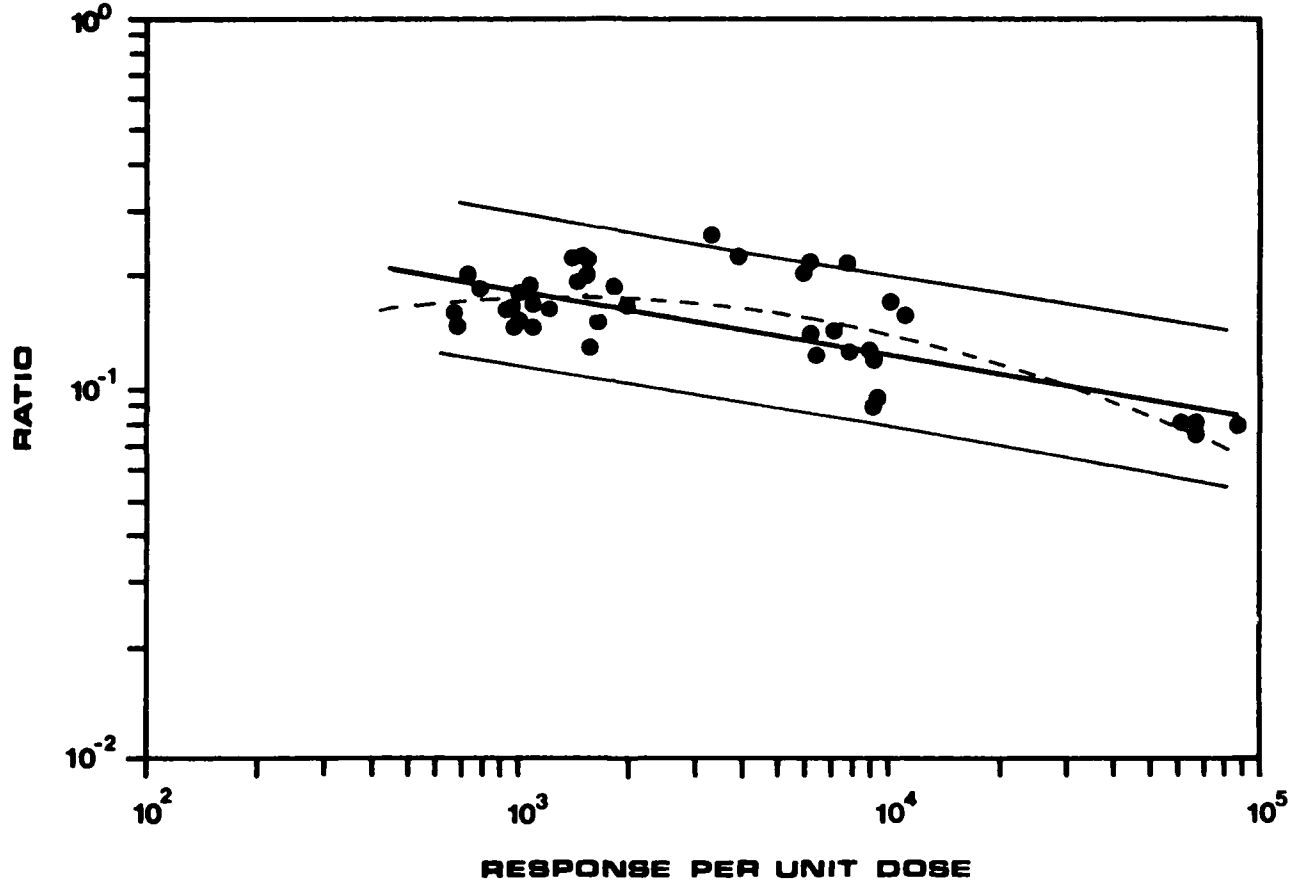
RATIO
10^0
10^{-1}
10^{-2}
10^2
10^3
10^4
10^5
RESPONSE PER UNIT DOSE

To test the theoretical model for the simple boron/bare (four to two) badge ratio, results of predicting the ratio through the simple models presented earlier in this work are compared to the actual measured ratios in Figures 11 and 12. The predicted versus actual ratio yields correlation coefficients of 0.572 ($P < 0.005$) and 0.503 ($P < 0.05$) respectively.

Figure 11

Modeled Spectral Correction Ratio versus Actual Measured Ratio. Data Presented for Spectra Shown in the Appendix. (Albedo Reflection Factor)

A.	HPRR (Bare at 3m)	Figure 36
B.	HPRR (13 cm Steel at 3m)	Figure 37
C.	HPRR (20 cm Concrete at 3m)	Figure 38
D.	HPRR (15 cm Concrete + 5 cm Steel at 3m)	Figure 39
E.	PuBe (Bare at 1m)	Figure 40
F.	Cf-252 (Bare at 1m)	Figure 41
G.	Cf-252 (Bare at 2m)	Figure 42
H.	Cf-252 (5 cm D_2O at 1m)	Figure 43
I.	Cf-252 (10 cm D_2O at 1m)	Figure 44
J.	Cf-252 (15 cm D_2O at 1m)	Figure 45
K.	Cf-252 (15 cm D_2O + 0.5 mm Cd at 1m)	Figure 46
L.	Cf-252 (25 cm D_2O at 1m)	Figure 47
M.	Cf-252 (20 cm Al at 1m)	Figure 48

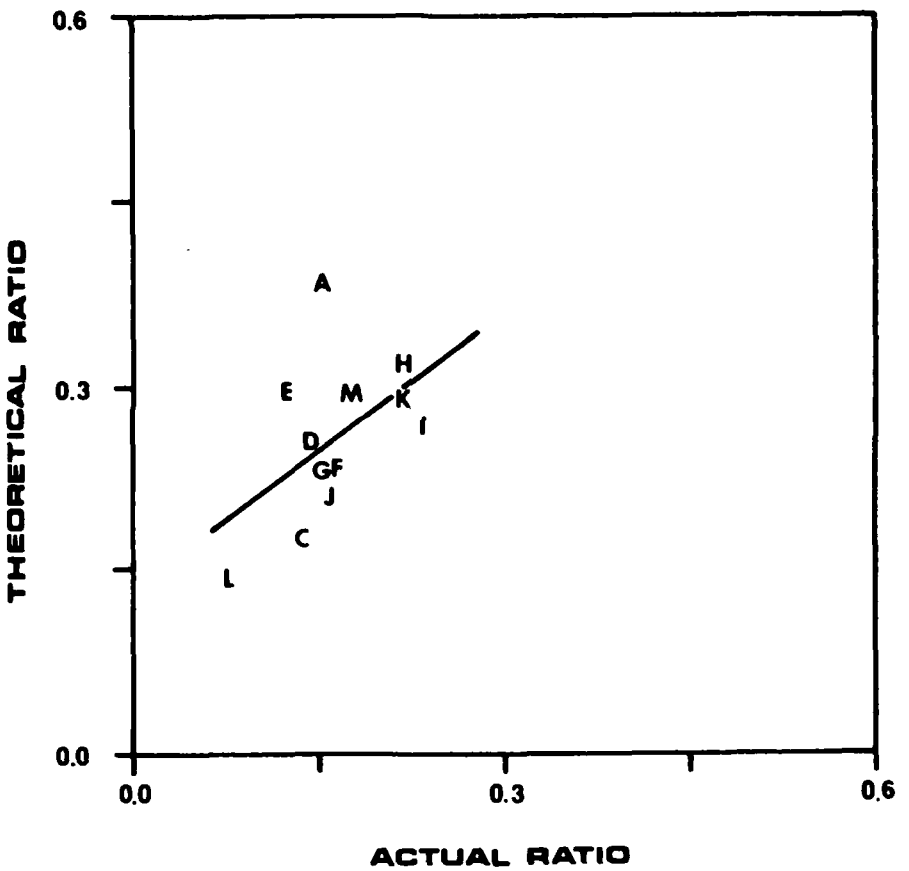
0.6
0.3
0.0
THEORETICAL RATIO
A
H
E
M
K
I
D
GF
J
C
L
0.0
0.3
0.6
ACTUAL RATIO

Figure 12

Modeled Spectral Correction Ratio versus Actual Measured Ratio. Data Presented for Spectra Shown in the Appendix. (Modeled Albedo Spectrum)

A.	HPRR (Bare at 3m)	Figure 36
B.	HPRR (13 cm Steel at 3m)	Figure 37
C.	HPRR (20 cm Concrete at 3m)	Figure 38
D.	HPRR (15 cm Concrete + 5 cm Steel at 3m)	Figure 39
E.	PuBe (Bare at 1m)	Figure 40
F.	Cf-252 (Bare at 1m)	Figure 41
G.	Cf-252 (Bare at 2m)	Figure 42
H.	Cf-252 (5 cm D_2O at 1m)	Figure 43
I.	Cf-252 (10 cm D_2O at 1m)	Figure 44
J.	Cf-252 (15 cm D_2O at 1m)	Figure 45
K.	Cf-252 (15 cm D_2O + 0.5 mm Cd at 1m)	Figure 46
L.	Cf-252 (25 cm D_2O at 1m)	Figure 47
M.	Cf-252 (20 cm Al at 1m)	Figure 48

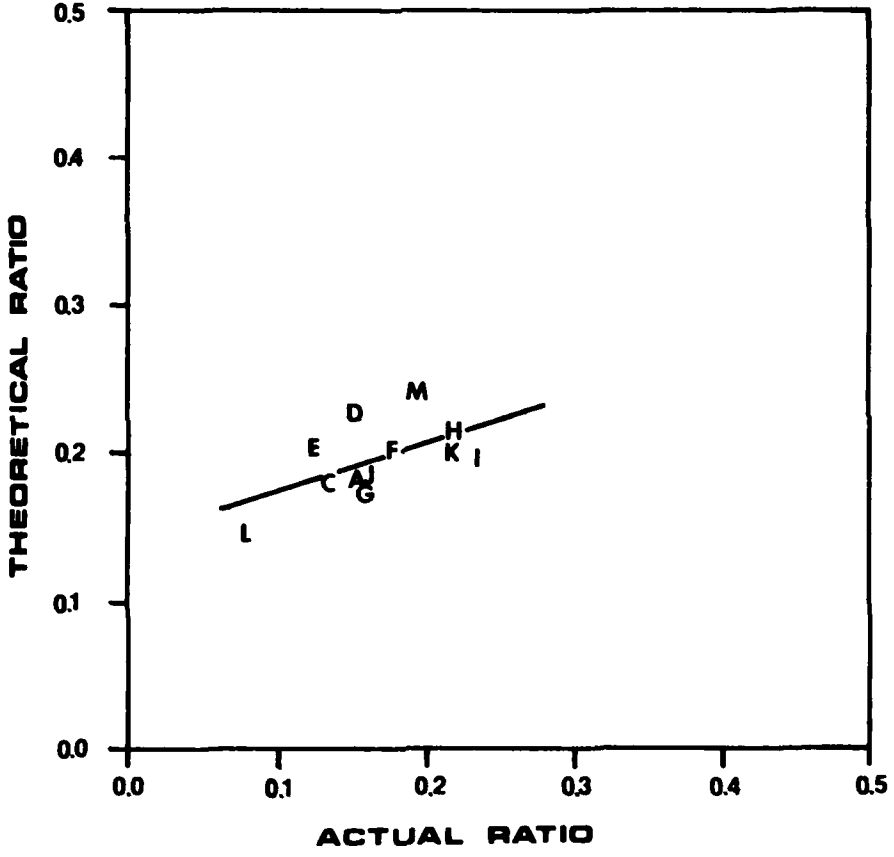
THEORETICAL RATIO
ACTUAL RATIO
0.0
0.1
0.2
0.3
0.4
0.5
M
D
H
E
F
K
I
C
A
J
G
L

VI. DISCUSSION

It is quite clear from the results of this study that a self calibrating Personnel Neutron Albedo Dosimeter is not yet available. The internal boron/bare ratio technique as applied to the thermoluminescent responses of the USAF Personnel Neutron Albedo Dosimeter is unable to provide a calibration factor for the response of the bare chip in an unknown moderated fission spectrum. This is clearly demonstrated in Figures 9 and 10 which show that the calibration factor selected by the observed ratio could be in error by three orders of magnitude at the 95% confidence level.

The albedo dosimeter's inability to be "self calibrating" is apparently due to the bare chip's high sensitivity to small changes in the fluence of low energy neutrons which do not contribute significantly to the dose equivalent. When the "boron to bare ratios" or the "23 cm (9 in) to 7.6 cm (3 in) ratios" are plotted against the albedo factor, no correlation of data is found (Figures 34 and 35). This also holds true when the above named ratios are divided by the albedo factor and plotted against the bare chip response (Figures 13 and 14). A further comparison of the location of the points representing a specific spectrum in these figures demonstrates that the albedo factor also does not correlate with the bare chip response. These results clearly show that the bare chip

Figure 13

Ratio of Counting Rates of a BF_3 Detector Inside 23 cm (9 in) and 7.6 cm (3 in) Polyethylene Spheres Divided by Albedo Factor versus Total Integral Thermoluminescent Response of Bare Chip (Picocoulombs per Millisievert) for Various Incident Spectra.

A.	HPRR (Bare at 3m)	Figure 36
B.	HPRR (13 cm Steel at 3m)	Figure 37
C.	HPRR (20 cm Concrete at 3m)	Figure 38
D.	Cf-252 (Bare at 1m)	Figure 41
E.	Cf-252 (Bare at 2m)	Figure 42
F.	Cf-252 (5 cm D_2O at 1m)	Figure 43
G.	Cf-252 (10 cm D_2O at 1m)	Figure 44
H.	Cf-252 (15 cm D_2O at 1m)	Figure 45
I.	Cf-252 (20 cm Al at 1m)	Figure 48
J.	HPRR (Bare at 6m)	
K.	HPRR (12 cm Lucite at 3m)	
L.	HPRR (12 cm Lucite at 9m)	

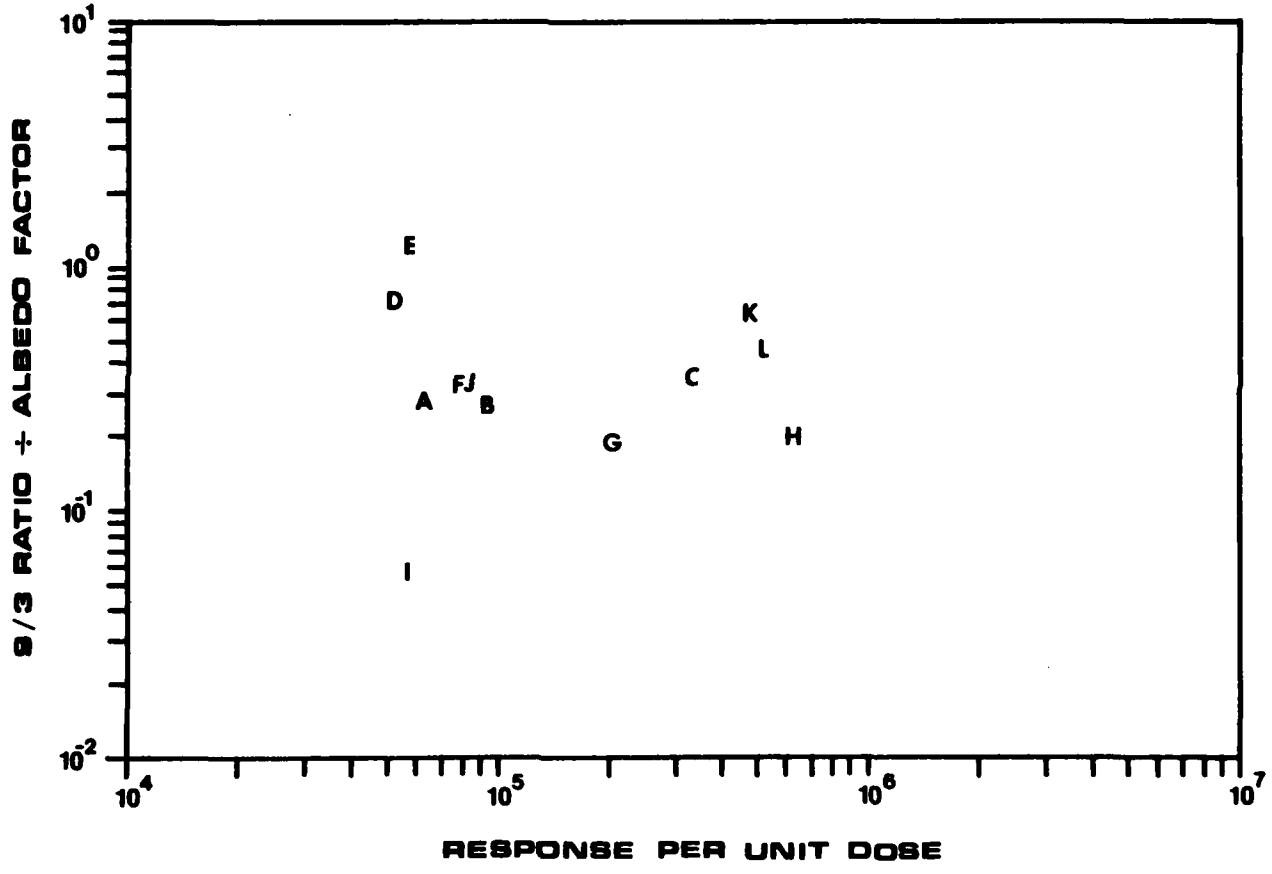
9/3 RATIO ÷ ALBEDO FACTOR
10^1
10^0
10^{-1}
10^{-2}
E
D
K
L
C
FJ
A
B
G
H
I
10^4
10^5
10^6
10^7
RESPONSE PER UNIT DOSE

Figure 14

Ratio of Counting Rates of a BF_3 Detector Inside and Outside a 7.6 cm (3 in) Polyethylene Sphere Divided by Albedo Factor versus Total Integral Thermoluminescent Response of Bare Chip (Picocoulombs per Millisievert) for Various Incident Spectra.

A. Cf-252 (Bare at 1m)	Figure 41
B. Cf-252 (Bare at 2m)	Figure 42
C. Cf-252 (5 cm D_2O at 1m)	Figure 43
D. Cf-252 (10 cm D_2O at 1m)	Figure 44
E. Cf-252 (15 cm D_2O at 1m)	Figure 45
F. Cf-252 (20 cm Al at 1m)	Figure 48

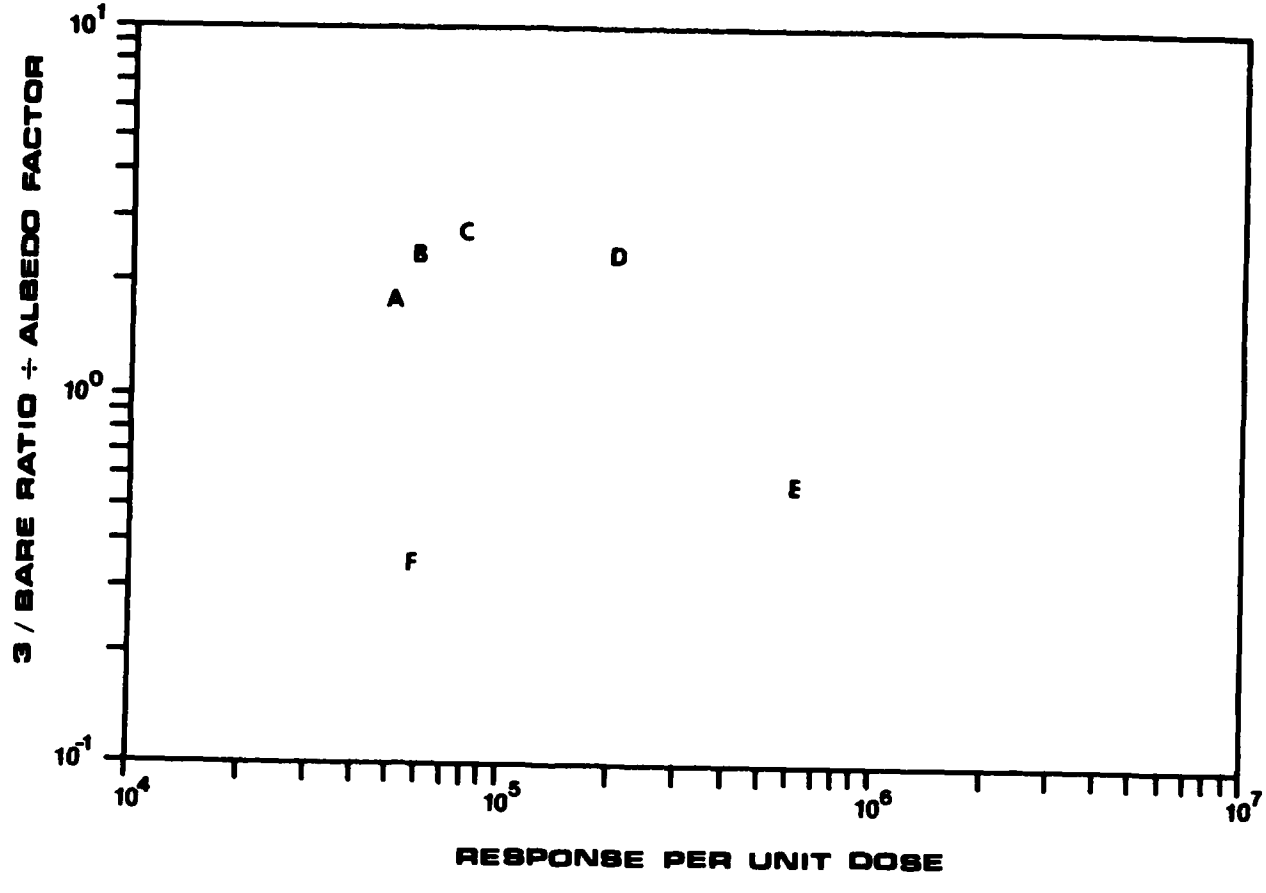
3 / BARE RATIO ÷ ALBEDO FACTOR
10^1
10^0
10^{-1}
A
B
C
D
E
F
10^4
10^5
10^6
10^7
RESPONSE PER UNIT DOSE

response is of no value in measuring the dose eqivalent unless it is used for a spectrum for which a calibration factor has been obtained in some other fashion and that spectrum is invariant in time and location within the work area occupied by the assigned wearer.

One can then ask whether or not the data gathered can be used as a guide for the design of a personel dosimeter that might be "self-calibrating". To accomplish this goal, the design must provide a system which essentially will ignore the low energy neutrons which do not contribute significantly to the dose. This means that the higher energy neutrons must govern the response of the dosimeter. Since thermoluminescent chips are mostly responsive to low energy neutrons, one can accomplish this only by placing moderators around the chips. Some of the data needed to check the feasibility of this approach have been made available in this investigation. The responses of a bare chip and a chip covered with a specific amount of boron in each of the different moderated fission spectra and the nature of these spectra has been obtained.

The theoretical models (Equations 9 and 10) may be used to make crude predictions of what might be expected of neutron dosimeters that contained additional amounts of a moderator in front of the chips. It should be emphasized that the theoretical models have inherrent assumptions. In considering the model utilizing an albedo relfection factor, the model assumes that the reflected neutrons (albedo) for each energy interval are at the same emergy as that of the incident neutrons. Since the reflected neutrons are clearly of a lower energy,

the model underestimates the change in the ratio as a function of neutron energy. The model utilizing a calculated albedo neutron spectrum relies on the parameters determined by Glickstein (G183) and the calculated bonner sphere spectra. Inherrent errors in assigning energy groupings and in calculating the incident thermal component of the spectrum from bonner spheres will emphasize the intermediate energy region of the albedo spectrum and underestimate the thermal albedo flux which would yield the highest thermoluminescent response. Figures 11 and 12 reflect that underestimation.

Since it is predicted that better results would be obtained if the amount of moderator surrounding the chips were increased, the effect of increasing the boron content by a factor of two and four was investigated. The theoretical response of the chips with the additional boron was calculated and appropriate ratios were plotted against either the response of the bare chip or the response of the chip covered with boron. Figures 15 through 20 show the predicted effect of increasing the boron content of the "boron pouch". In these figures the boron/bare theoretical ratio is plotted against the response of the bare chip. It is noted that the slope of the line increases as the boron content increases but the scatter that is introduced by using the bare chip remains. Since Boron-10 is very expensive, the effect of using Lithium-6 fluoride as a moderator is also shown (Figures 21 and 22).

In order to reduce the influence of low energy neutrons, the response under boron was further studied. "High Boron to Low Boron"

Figure 15

Theoretical Ratio using Albedo Reflection Factor of Chip Surrounded by and Above the Boron-10 Pouch (Normal Loading) versus Measured Total Integral Thermoluminescent Response of Bare Chip (Picocoulombs per Millisievert).

Slope: -1.179 ± 0.130

Intercept: 0.344 ± 0.191

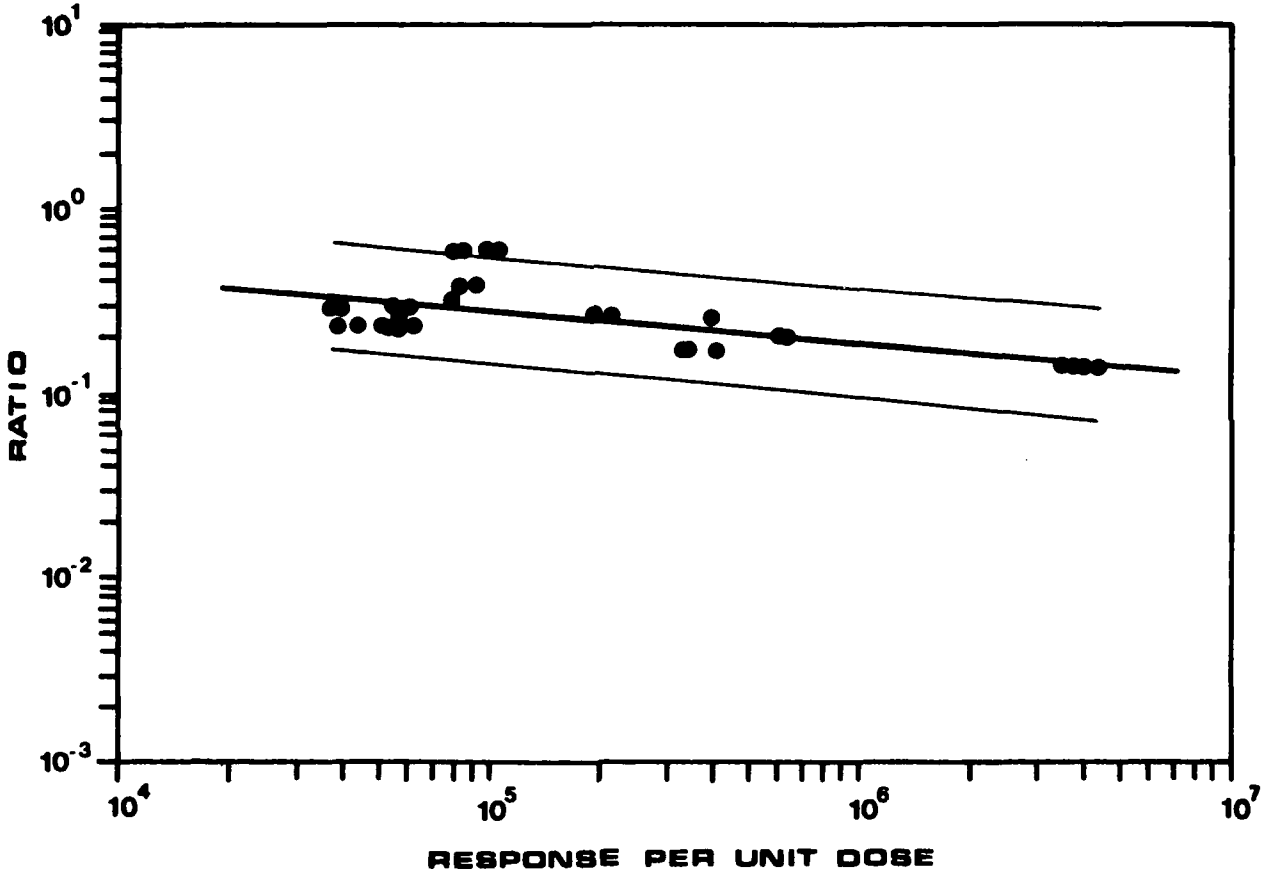
10^1
10^0
10^{-1}
10^{-2}
10^{-3}
RATIO
10^4
10^5
10^6
10^7
RESPONSE PER UNIT DOSE

Figure 16

Theoretical Ratio using Modeled Albedo Spectrum of Chip Surrounded by and Above the Boron-10 Pouch (Normal Loading) versus Measured Total Integral Thermoluminescent Respnse of Bare Chip (Picocoulombs per Millisievert).

Slope: -0.068 ± 0.013

Intercept: -0.358 ± 0.068

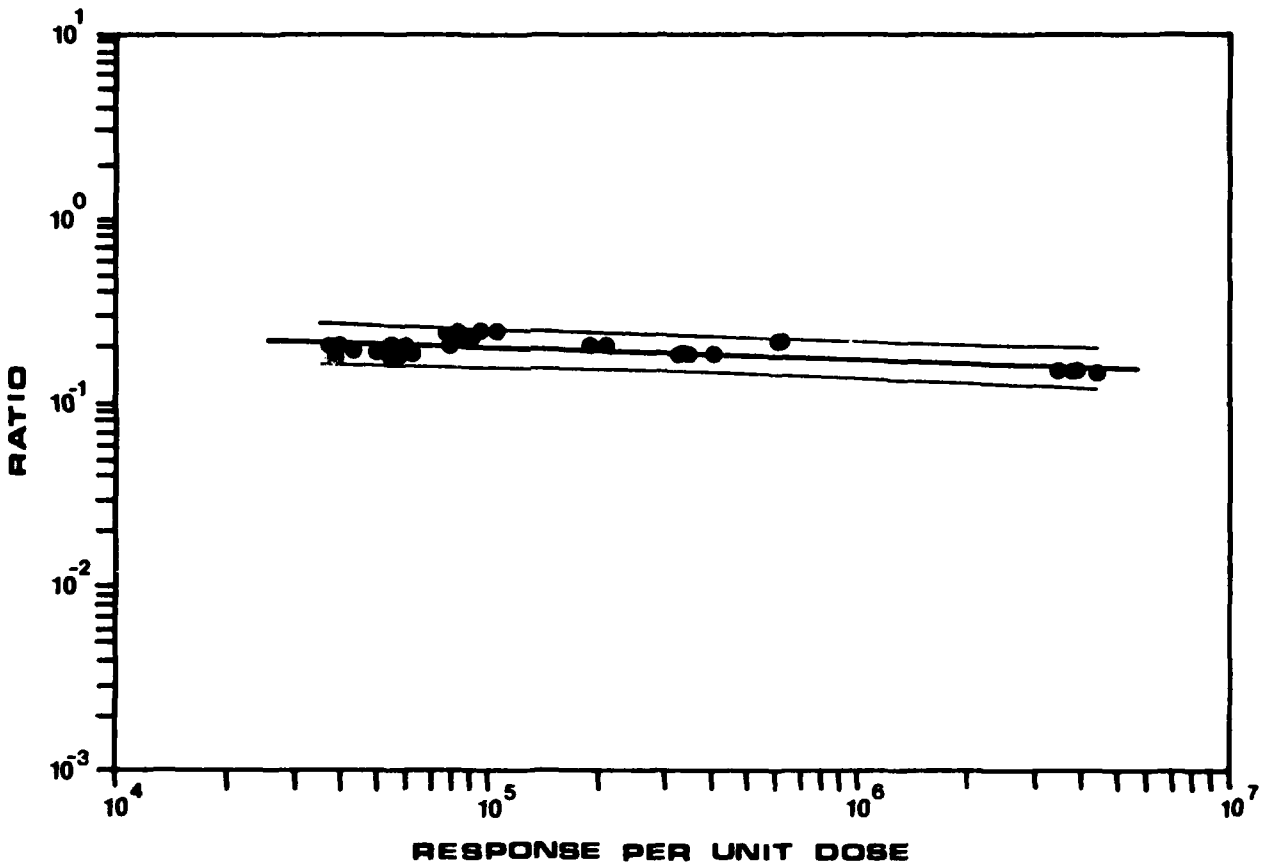
RATIO
10^{1}
10^{0}
10^{-1}
10^{-2}
10^{-3}
10^{4}
10^{5}
10^{6}
10^{7}
RESPONSE PER UNIT DOSE

Figure 17

Theoretical Ratio using Albedo Reflection Factor of Chip Surrounded by and Above the Boron-10 Pouch (Twice Normal Loading) versus Measured Total Integral Thermoluminescent Response of Bare Chip (Picocoulombs per Millisievert).

Slope: -0.410 ± 0.060

Intercept: 1.301 ± 0.318

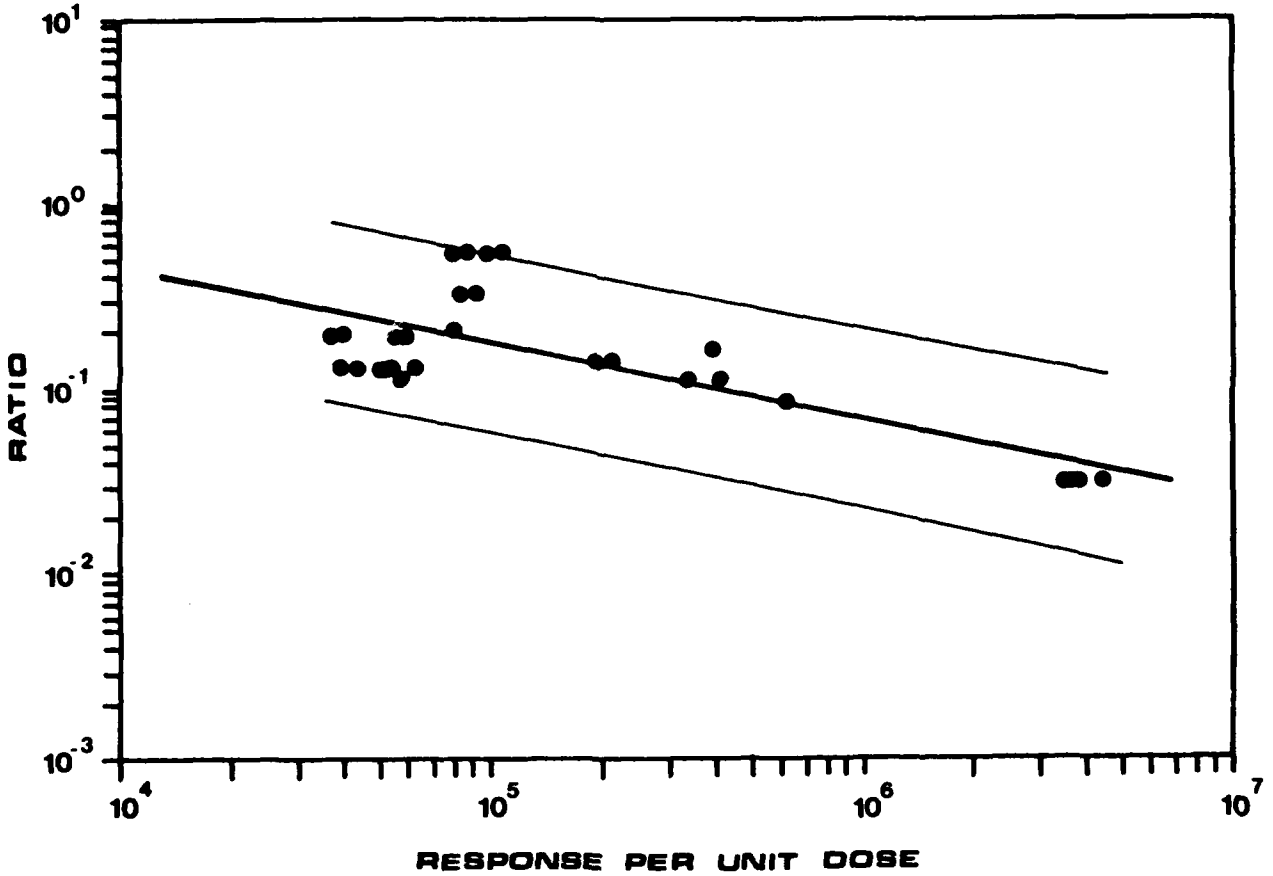
10^1
10^0
10^{-1}
10^{-2}
10^{-3}
RATIO
10^4
10^5
10^6
10^7
RESPONSE PER UNIT DOSE

Figure 18

Theoretical Ratio using Modeled Albedo Spectrum of Chip Surrounded by and Above the Boron-10 Pouch (Twice N· ~mal Loading) versus Measured Total Integral Thermoluminescent Response of Bare Chip (Picocoulombs per Millisievert).

Slope: -0.141 ± 0.069

Intercept: -0.367 ± 0.367

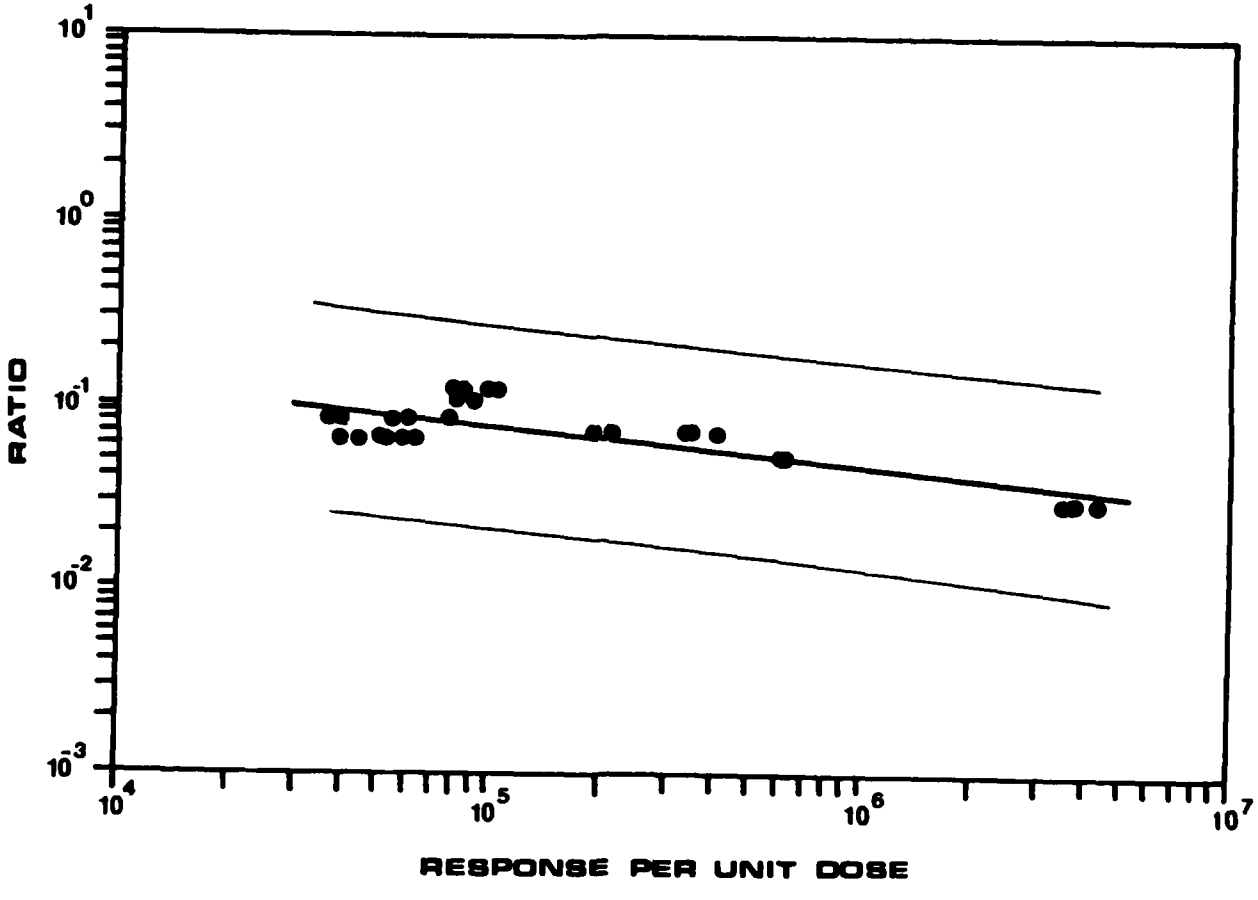
RATIO
10^{1}
10^{0}
10^{-1}
10^{-2}
10^{-3}
10^{4}
10^{5}
10^{6}
10^{7}
RESPONSE PER UNIT DOSE

Figure 19

Theoretical Ratio using Albedo Reflection Factor of Chip Surrounded by and Above the Boron-10 Pouch (Four Times Normal Loading) versus Measured Total Integral Thermoluminescent Response of Bare Chip (Picocoulombs per Millisievert).

Slope: -0.633 ± 0.072

Intercept: 2.318 ± 0.380

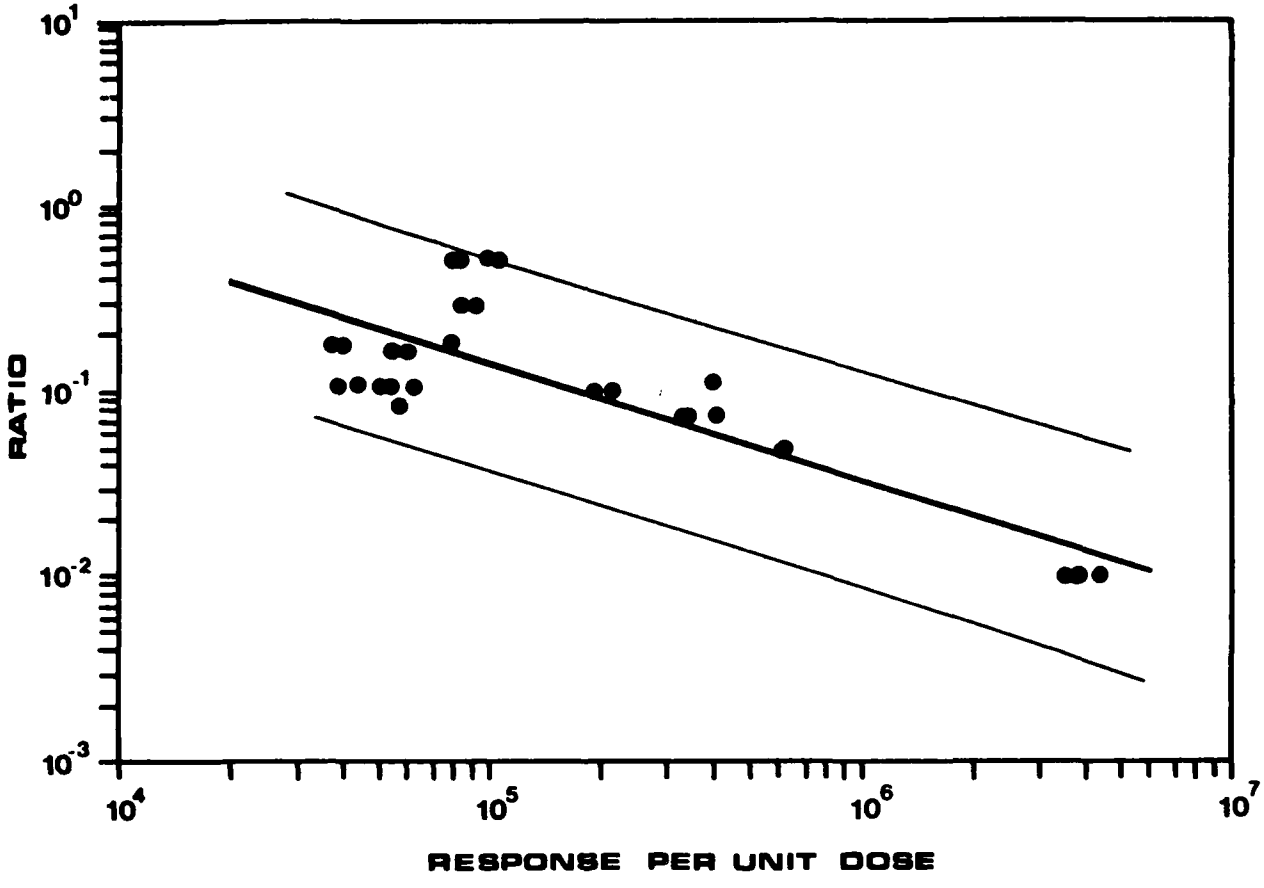
RATIO
10^{1}
10^{0}
10^{-1}
10^{-2}
10^{-3}
10^{4}
10^{5}
10^{6}
10^{7}
RESPONSE PER UNIT DOSE

Figure 20

Theoretical Ratio using Modeled Albedo Spectrum of Chip Surrounded by and Above the Boron-10 Pouch (Four Times Normal Loading) versus Measured Total Integral Thermoluminescent Response of Bare Chip (Picocoulombs per Millisievert).

Slope: -0.382 ± 0.042

Intercept: 0.538 ± 0.225

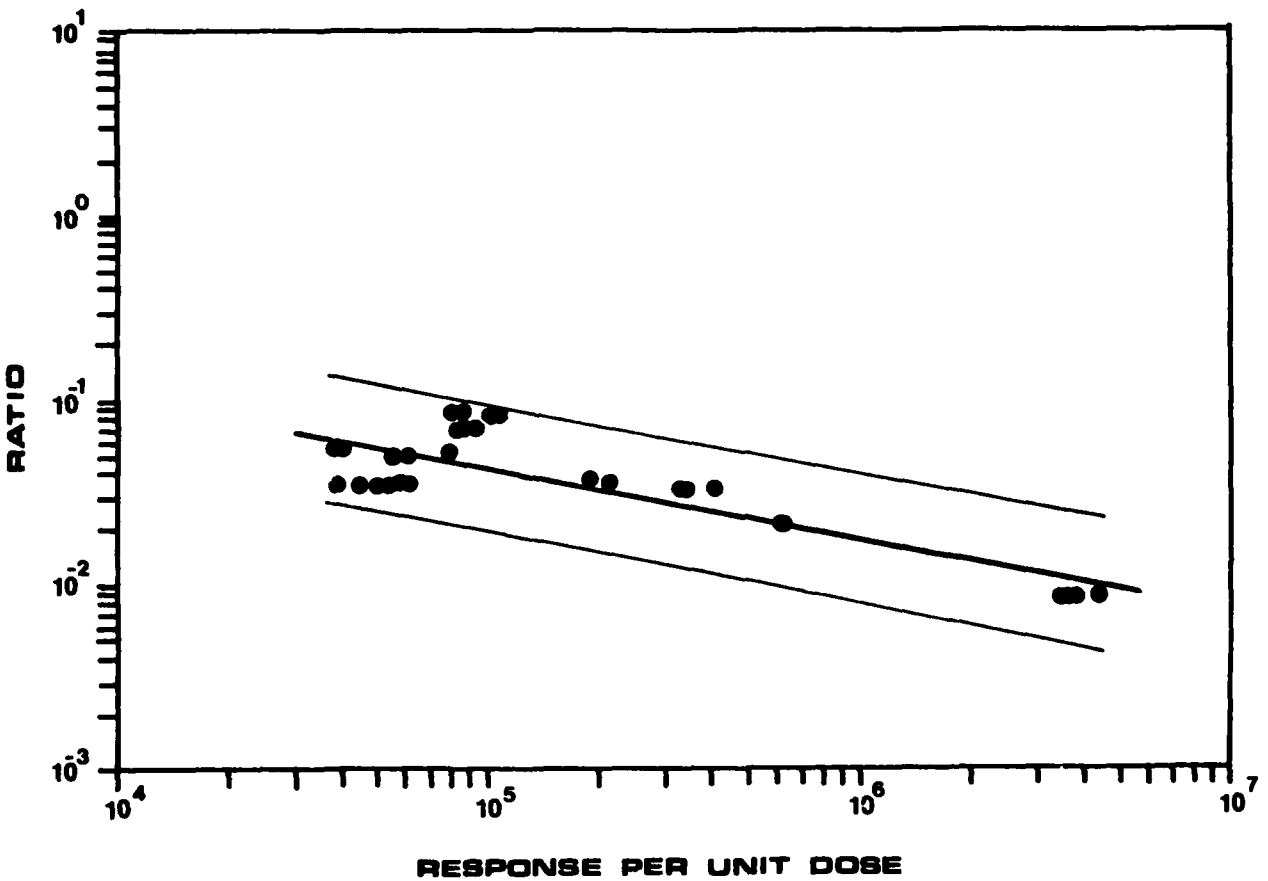
RATIO
10^{1}
10^{0}
10^{-1}
10^{-2}
10^{-3}
10^{4}
10^{5}
10^{6}
10^{7}
RESPONSE PER UNIT DOSE

Figure 21

Theoretical Ratio using Albedo Reflection Factor of Chip Surrounded by and Above a Lithium-6 Fluoride Shield (0.5 inch thick) versus Measured Total Integral Thermoluminescent Response of Bare Chip (Picocoulombs per Millisievert).

Slope: -0.437 ± 0.061

Intercept: 1.408 ± 0.321

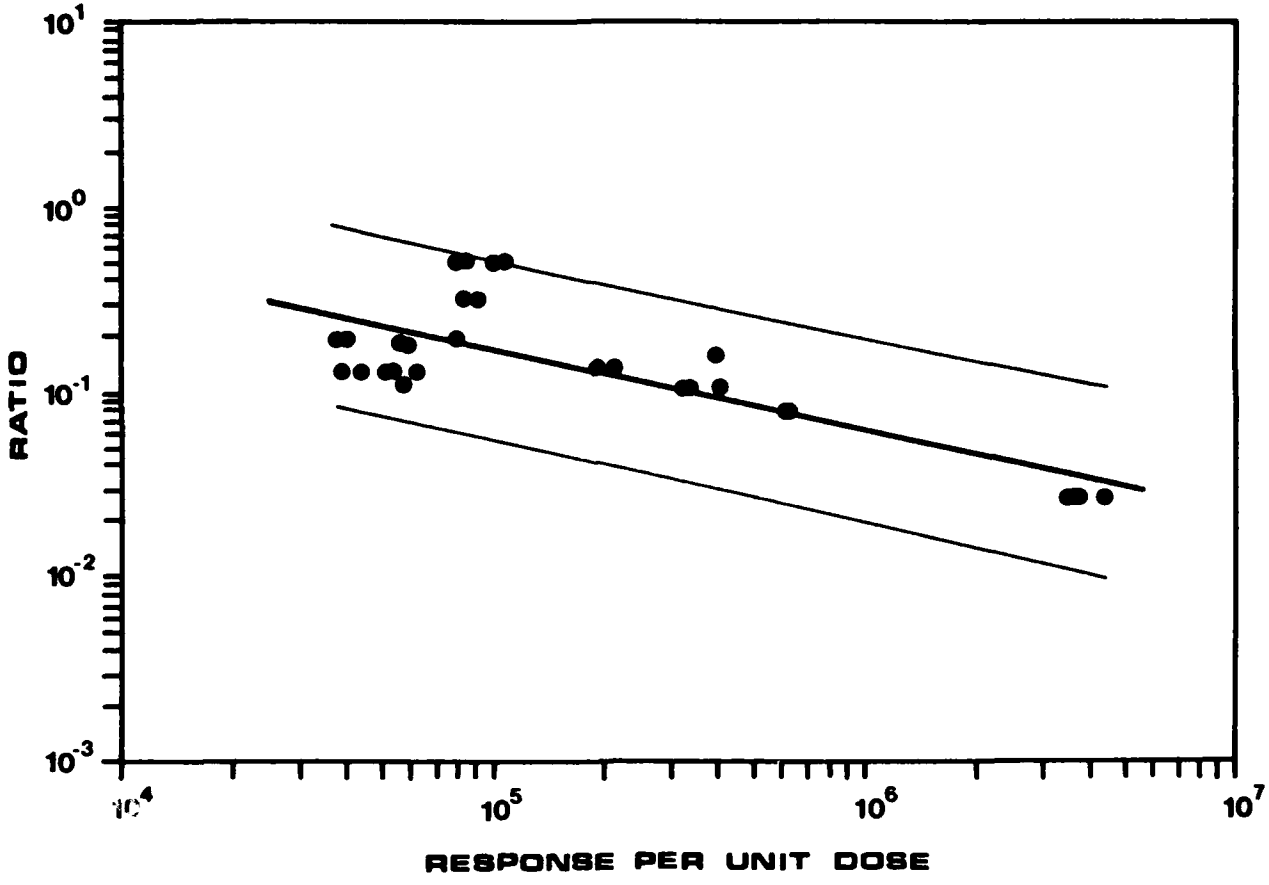
10^1
10^0
10^{-1}
10^{-2}
10^{-3}
RATIO
10^4
10^5
10^6
10^7
RESPONSE PER UNIT DOSE

Figure 22

Theoretical Ratio using Albedo Reflection Factor of Chip Surrounded by and Above a Lithium-6 Fluoride Shield (0.5 inch thick) versus Measured Total Integral Thermoluminescent Response of Bare Chip (Picocoulombs per Millisievert).

Slope: -0.081 ± 0.013

Intercept: -0.336 ± 0.068

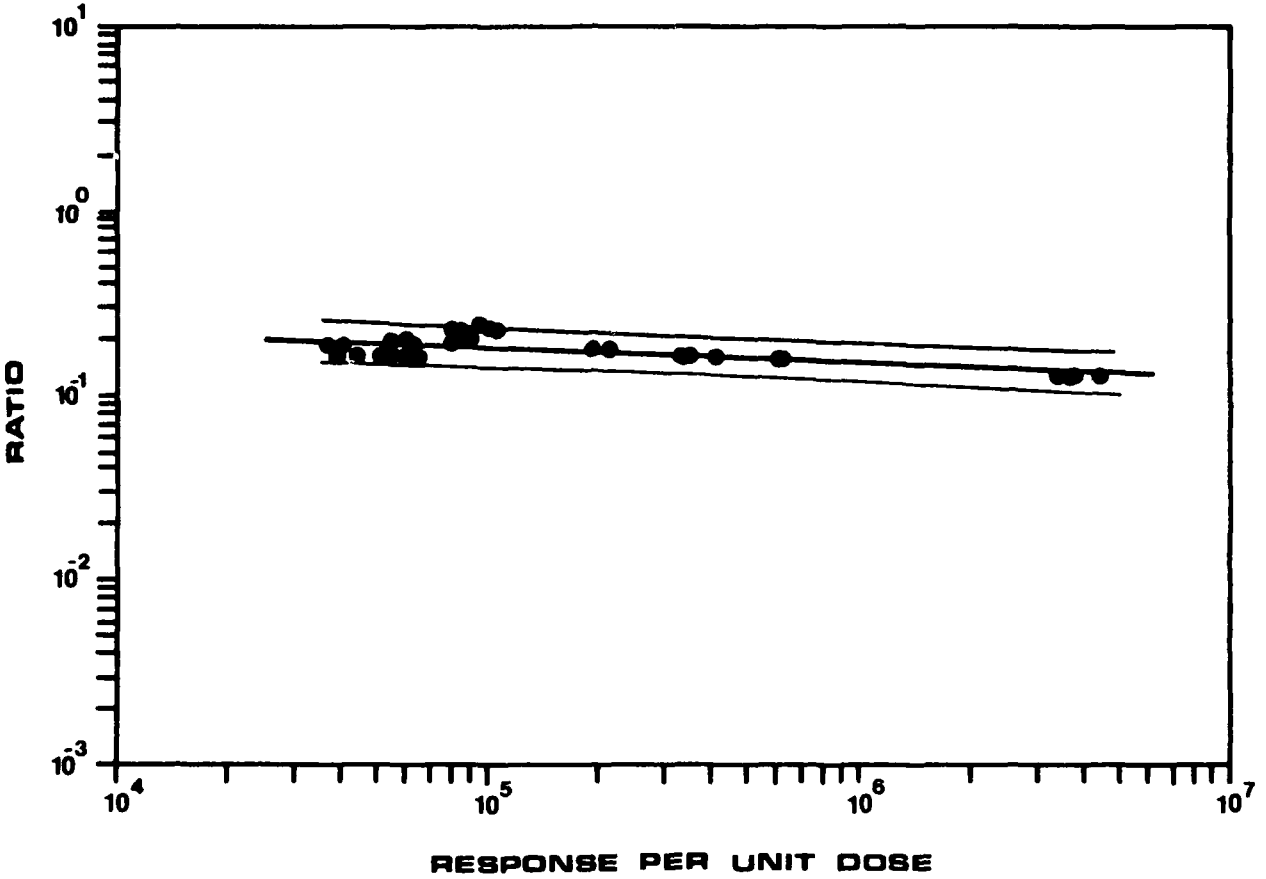
RATIO
10^{1}
10^{0}
10^{-1}
10^{-2}
10^{-3}
10^{4}
10^{5}
10^{6}
10^{7}
RESPONSE PER UNIT DOSE

ratios were established from the regression lines given in Figures 15 through 20. The theoretical "High to Bare" ratio and "Low to Bare" ratio obtained from the regression line for each experimental data point were used to obtain a "High Boron to Low Boron" ratio which is plotted against the measured response of the chip under "Low Boron" in Figures 23 to 26. Although these curves do not reflect the scatter that will be introduced by actual measurement of the ratios, they may be compared with the previous figures to illustrate the expected increase in correlation of the data. However, sensitivity is ten times lower.

From these calculations, one may propose a badge with five thermoluminescent chips. Of these, three would be ^{6}LF. One chip would be bare, one covered with 1X Boron and one with 4X Boron. The bare chip response could be used for low dose accumulations where some uncertainty in the calibration factor does not have serious consequences. At higher doses the response of the 1X boron covered chip would be used for more accurate results. In no case, however, should the dosimeter completely replace the evaluation of the exposure environment by an experienced dosimitrist.

Figure 23

Theoretical Ratio using Albedo Reflection Factor of Chip Covered by Normal Boron to Chip Covered by Twice Normal Boron versus Measured Total Integral Thermoluminescent Response of Normal Boron Covered Chip (Picocoulombs per Millisievert).

Slope: -0.263 ± 0.008

Intercept: 0.909 ± 0.037

AD-A135 864 FACTORS AFFECTING THE APPLICATION OF A SIMPLE RATIO TECHNIQUE FOR SPECTRA..(U) AIR FORCE INST OF TECH WRIGHT-PATTESSON AFB OH R C NELSON NOV 83 2/2

UNCLASSIFIED AFIT/CI/NR-83-61D F/G 6/18 NL

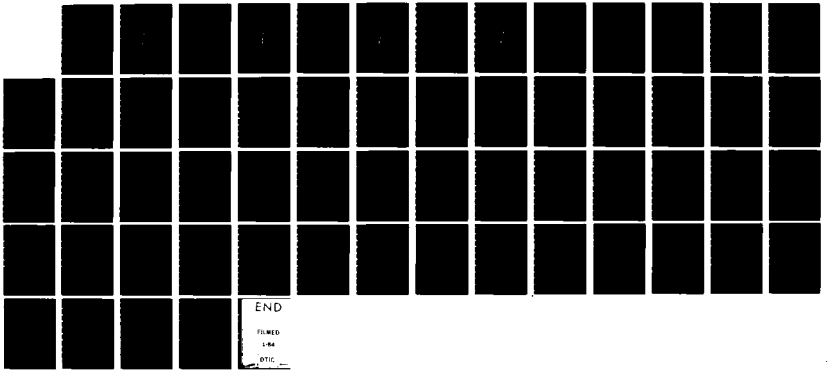

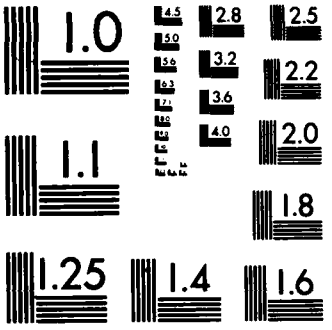

MICROCOPY RESOLUTION TEST CHART
NATIONAL BUREAU OF STANDARDS-1963-A

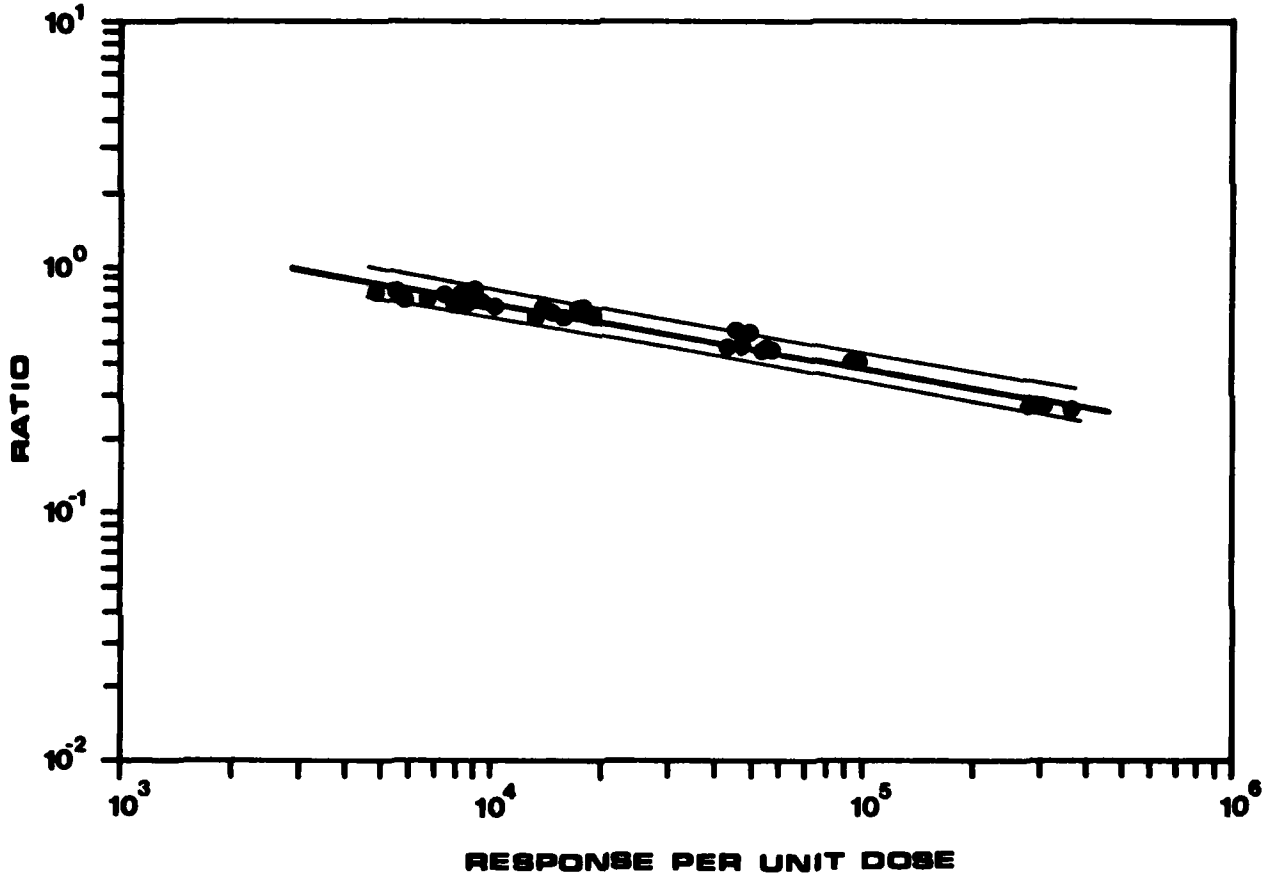
10^1
10^0
10^{-1}
10^{-2}
RATIO
10^3
10^4
10^5
10^6
RESPONSE PER UNIT DOSE

Figure 24

Theoretical Ratio using Modeled Albedo Spectrum of Chip Covered by Normal Boron to Chip Covered by Twice Normal Boron versus Measured Total Integral Thermoluminescent Response of Normal Boron Covered Chip (Picocoulombs per Millisievert).

Slope: -0.170 ± 0.005

Intercept: -0.299 ± 0.024

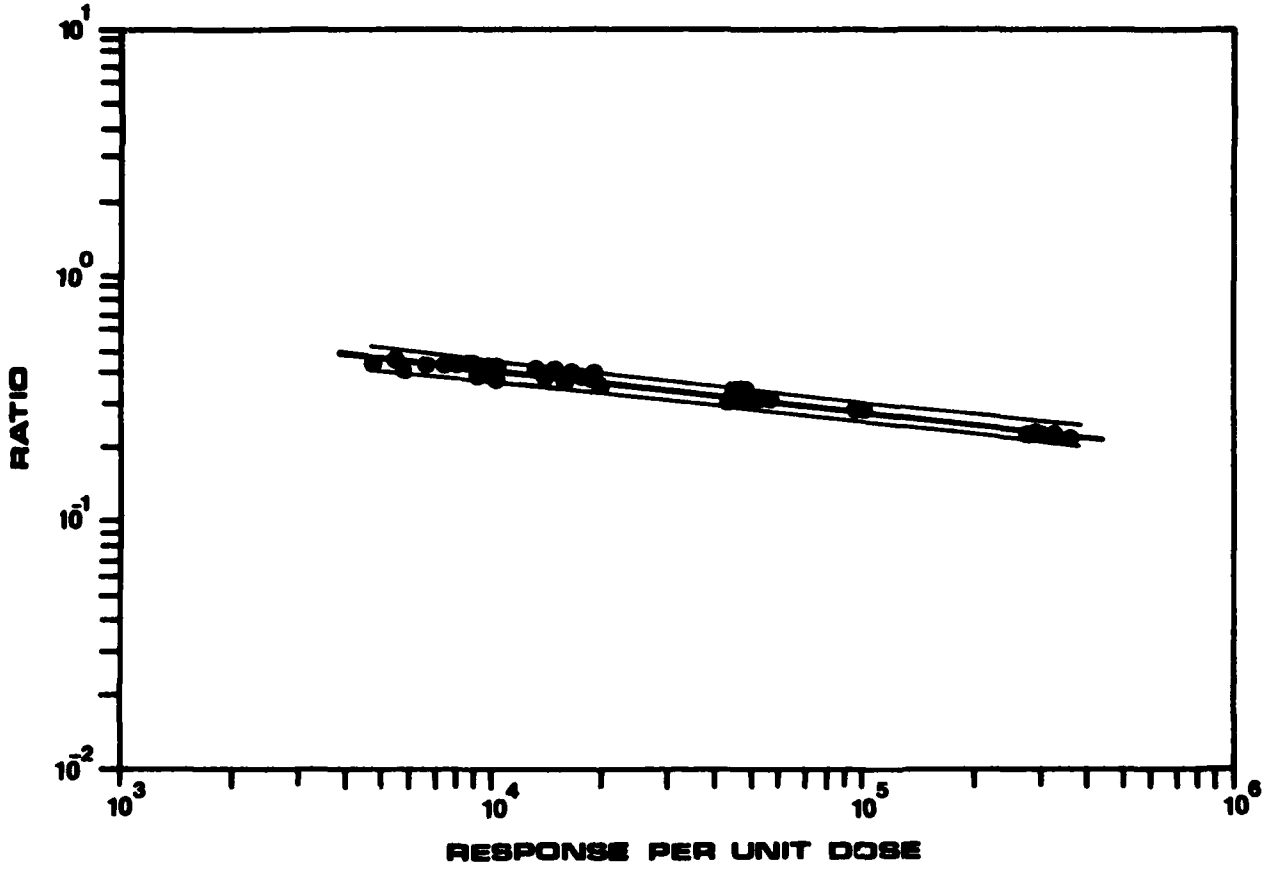
RATIO
10^{1}
10^{0}
10^{-1}
10^{-2}
10^{3}
10^{4}
10^{5}
10^{6}
RESPONSE PER UNIT DOSE

Figure 25

Theoretical Ratio using Albedo Reflection Factor of Chip Covered by Normal Boron to Chip Covered by Four Times Normal Boron versus Measured Total Integral Thermoluminescent Response of Normal Boron Covered (Picocoulombs per Millisievert).

Slope: -0.518 ± 0.016

Intercept: 1.877 ± 0.073

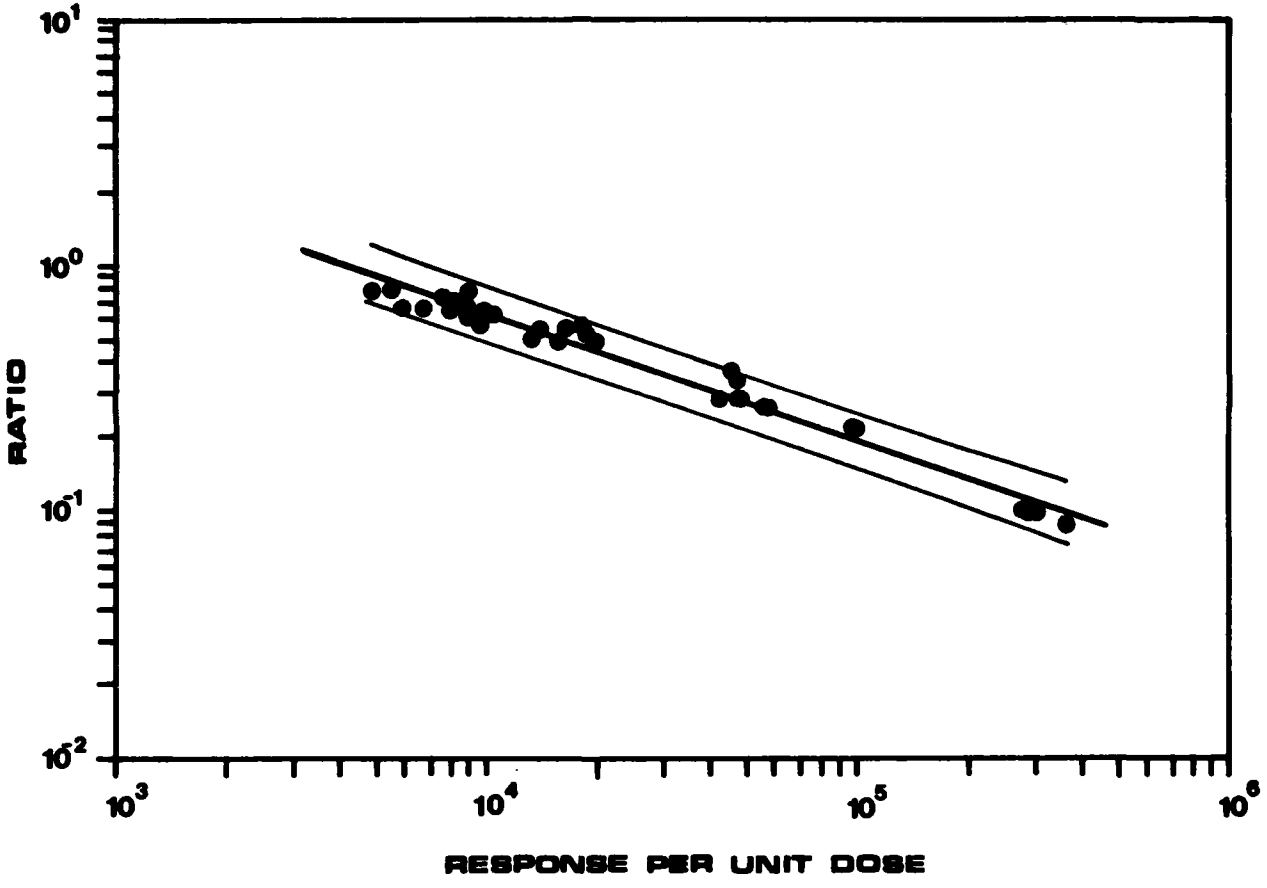
10^1
10^0
10^{-1}
10^{-2}
RATIO
10^3
10^4
10^5
10^6
RESPONSE PER UNIT DOSE

Figure 26

Theoretical Ratio using Modeled Albedo Spectrum of Chip Covered by Normal Boron to Chip Covered by Four Times Normal Boron versus Measured Total Integral Thermoluminescent Response of Normal Boron Covered (Picocoulombs per Millisievert).

Slope: -0.358 ± 0.011

Intercept: -0.831 ± 0.050

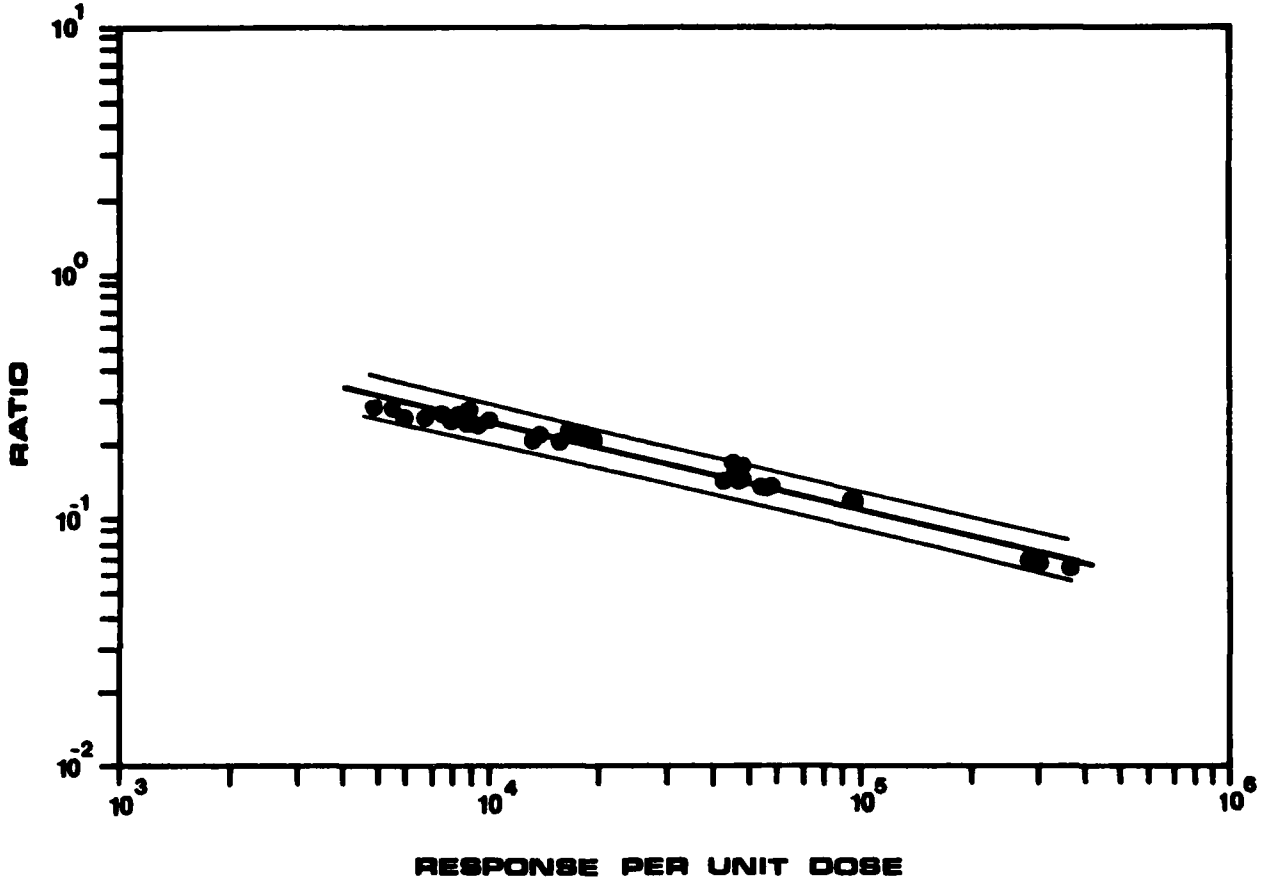
RATIO
10^{1}
10^{0}
10^{-1}
10^{-2}
10^{3}
10^{4}
10^{5}
10^{6}
RESPONSE PER UNIT DOSE

VII. SUMMARY

In an attempt to utilize existing technology while examining potential dosimeter designs, the USAF has developed a thermoluminescent neutron dosimetry capability based on a personnel neutron albedo dosimeter badge originally designed at SNLA. The dosimeter has been evaluated in multiple moderated neutron spectral environments to ascertain the capability of the badge to provide "self-calibration."

It has been found that ratios produced by the badge itself fail to allow a "self-calibration" for dose equivalent in moderated fission neutron spectra. The simple theoretical model presented shows, however, that the use of different moderators over thermoluminescent chips results in a badge ratio which yields direct correlation to changes in input neutron spectra. Utilizing the model along with additional data gathered during this work to provide background from which to predict the effect of changes in the monitoring environment on dosimeter results, a dosimeter design which can potentially meet the goal of "self-calibration" is proposed. In order to eliminate the effects of thermal and near thermal neutrons, which greatly affect dosimeter response without providing any significant contribution to the dose equivalent, utilization of two chips shielded by two differing boron concentrations is proposed. Shields equivalent to the boron

pouch in the present dosimeter and four times that amount show promise of yielding results similar to the Hankins' remmeter technique.

The major drawback of this design is that an approximate loss of a factor of ten in sensitivity results. If sensitivity is of a necessity, a five chip dosimeter could be designed allowing the use of three TLD-600 chips (bare and under two different boron shields). In the low exposure range, the bare response could be utilized with a conservative calibration factor. As higher exposures are recorded where sensitivity no longer is a problem, the boron ratio could provide a calibration factor to eliminate potential order of magnitude errors in the estimation of dose equivalent.

Evaluation of data with respect to both integral and peak glow curve values has additionally been found to be a valuable technique. Whenever values so obtained are found to be significantly in disagreement, an immediate indication of a possible dosimeter miss-read is obtained.

APPENDIX

Figure 27

Typical Energy Response Factors for Lithium Fluoride.

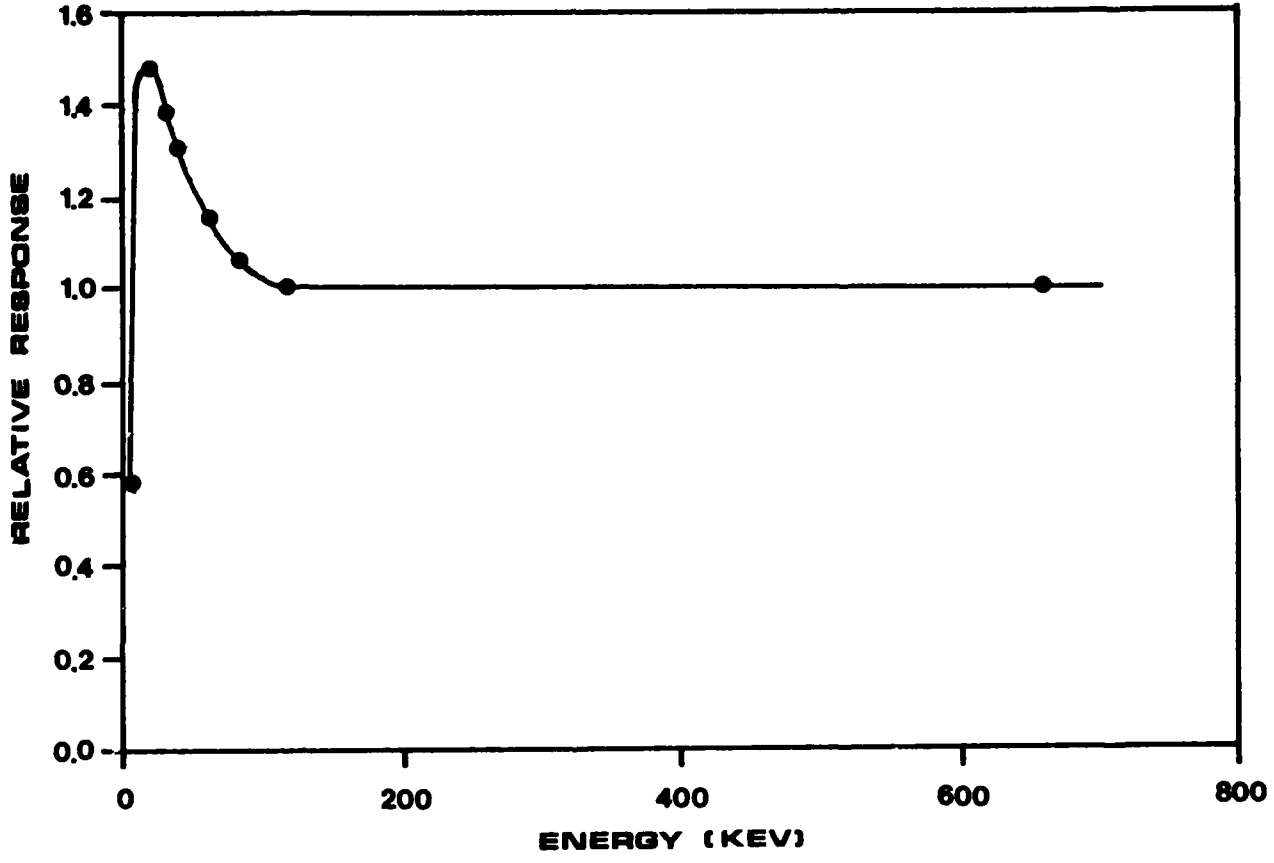
1.6
1.4
1.2
1.0
0.8
0.6
0.4
0.2
0.0
RELATIVE RESPONSE
0
200
400
600
800
ENERGY (KEV)

Figure 28

Total Integral Thermoluminescent Response (Picocoulombs per Millisievert) for TLD-600 and TLD-700 Chips Exposed in USAF Personnel Neutron Dosimeter versus Exposure (Millisieverts) to Cesium-137.

———— TLD-600 (^{6}LiF - Harshaw)

---------- TLD-700 (^{7}LiF - Harshaw)

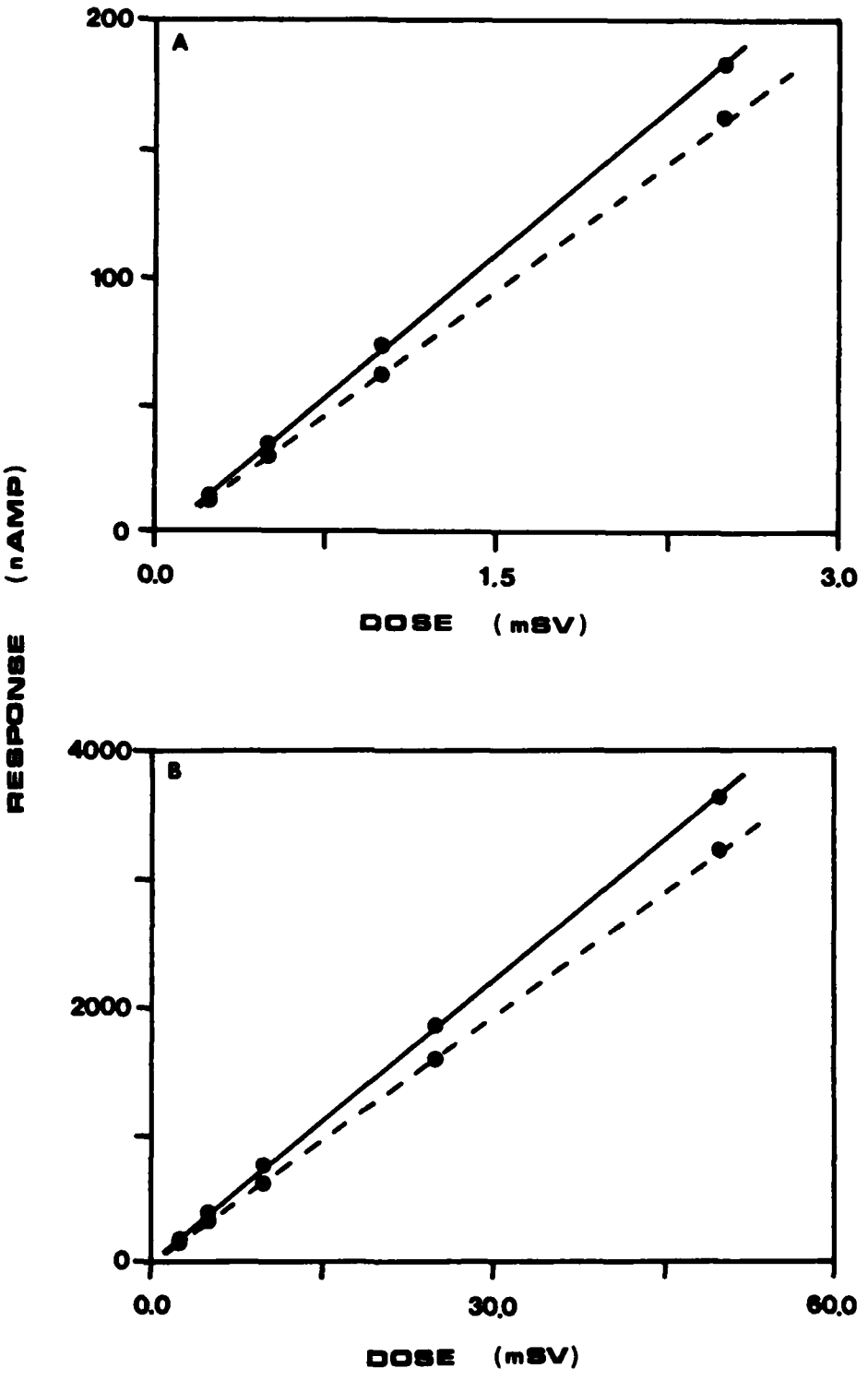
A
200
100
0
0.0
1.5
3.0
DOSE (mSV)
RESPONSE (nAMP)
B
4000
2000
0
0.0
30.0
60.0
DOSE (mSV)

Figure 29

Peak Thermoluminescent Response (Picocoulombs per Millisievert) for TLD-600 and TLD-700 Chips Exposed in USAF Personnel Neutron Dosimeter versus Exposure (Millisieverts) to Cesium-137.

———— TLD-600 (^{6}LiF - Harshaw)

---------- TLD-700 (^{7}LiF - Harshaw)

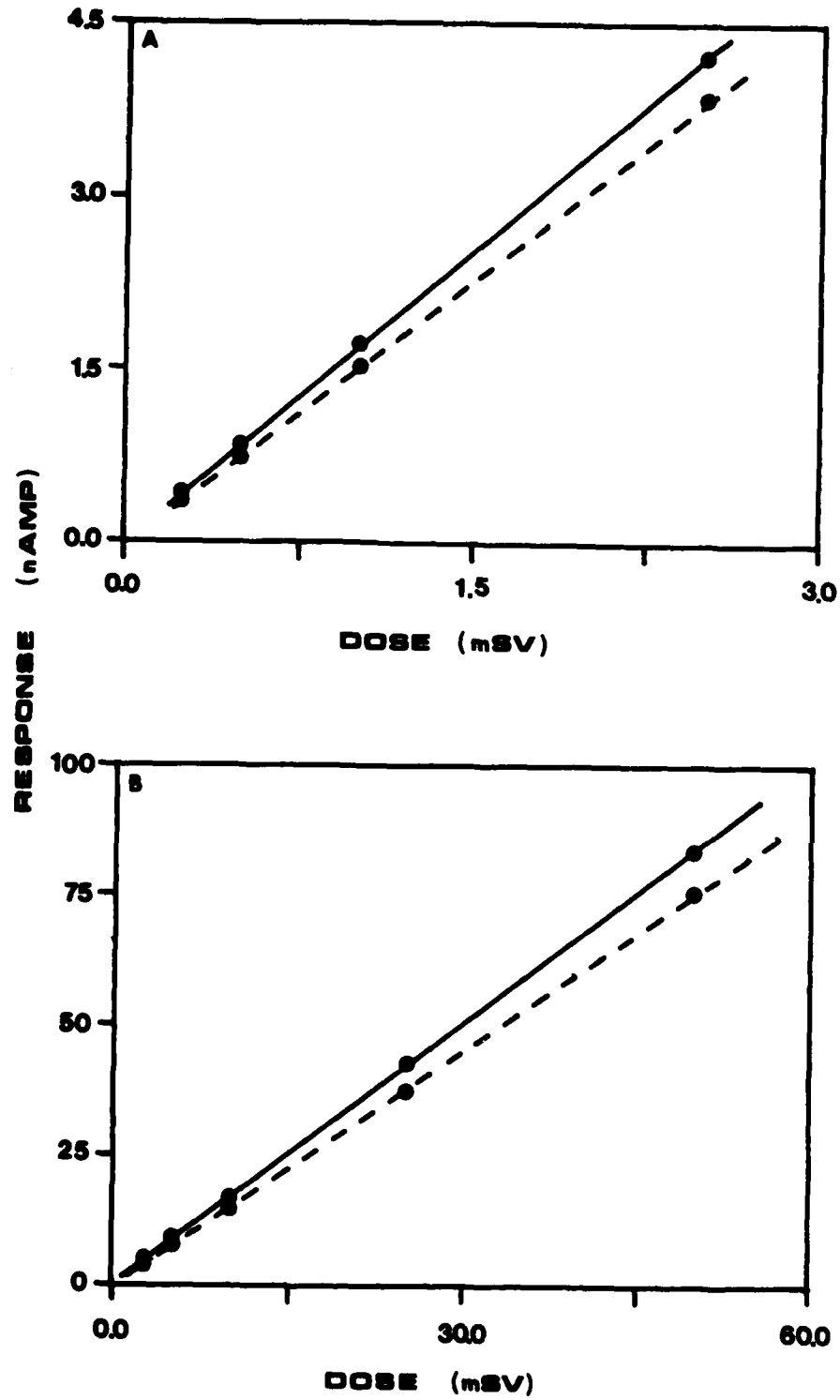
A
4.5
3.0
1.5
0.0
0.0
1.5
3.0
RESPONSE (nAMP)
DOSE (mSV)
B
100
75
50
25
0
0.0
30.0
60.0
DOSE (mSV)

Figure 30

Total Integral Thermoluminescent Response (Picocoulombs per Millisievert) for TLD-600 and TLD-700 Chips Exposed in USAF Personnel Neutron Dosimeter versus Exposure (Millisieverts) to Cobalt-60.

———— TLD-600 (^{6}LiF - Harshaw)

---------- TLD-700 (^{7}LiF - Harshaw)

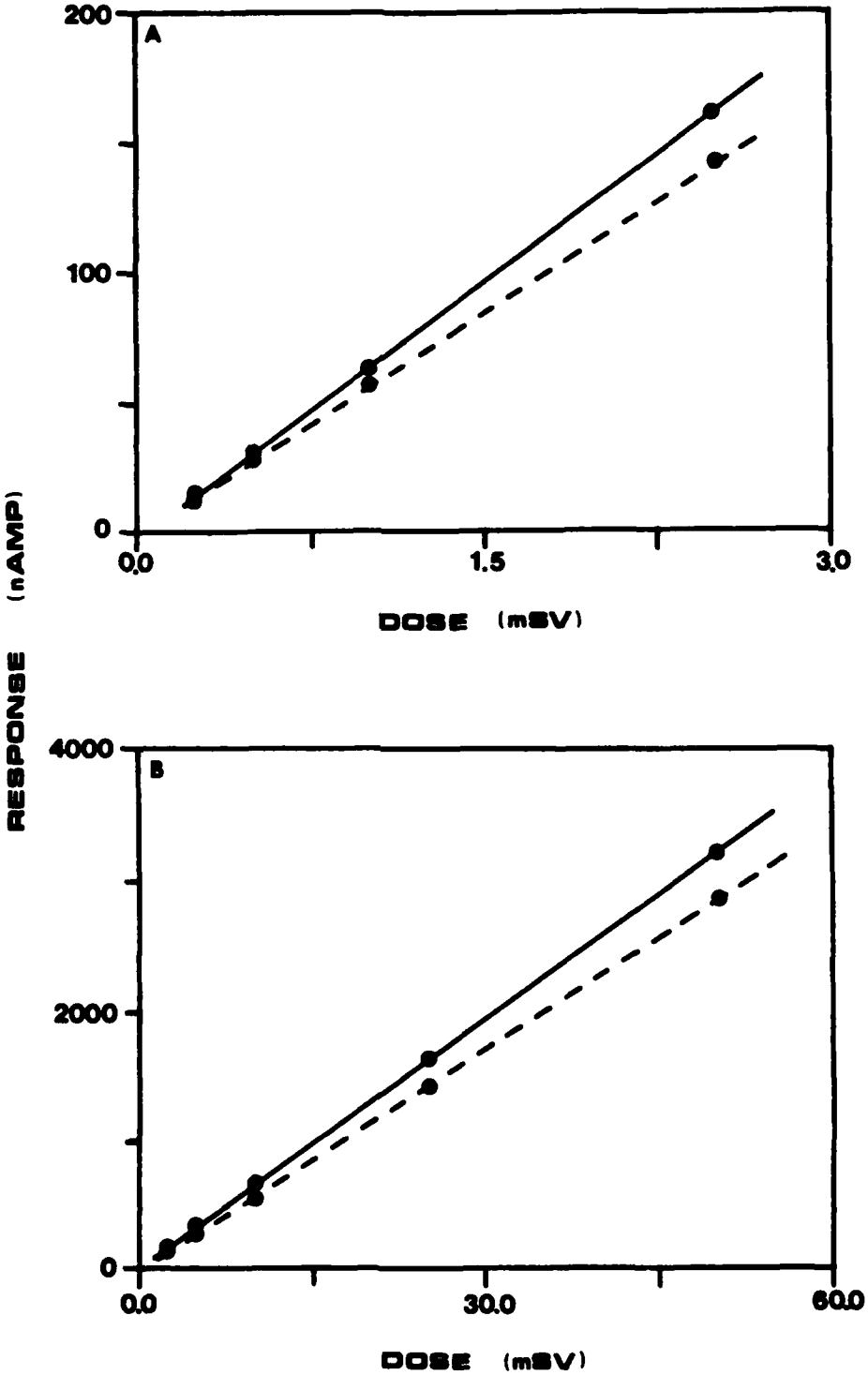
A
200
100
0
0.0
1.5
3.0
DOSE (mSV)
RESPONSE (nAMP)
B
4000
2000
0
0.0
30.0
60.0
DOSE (mSV)

Figure 31

Peak Thermoluminescent Response (Picocoulombs per Millisievert) for TLD-600 and TLD-700 Chips Exposed in USAF Personnel Neutron Dosimeter versus Exposure (Millisieverts) to Cobalt-60.

_____ TLD-600 (^{6}LiF - Harshaw)

_____ TLD-700 (^{7}LiF - Harshaw)

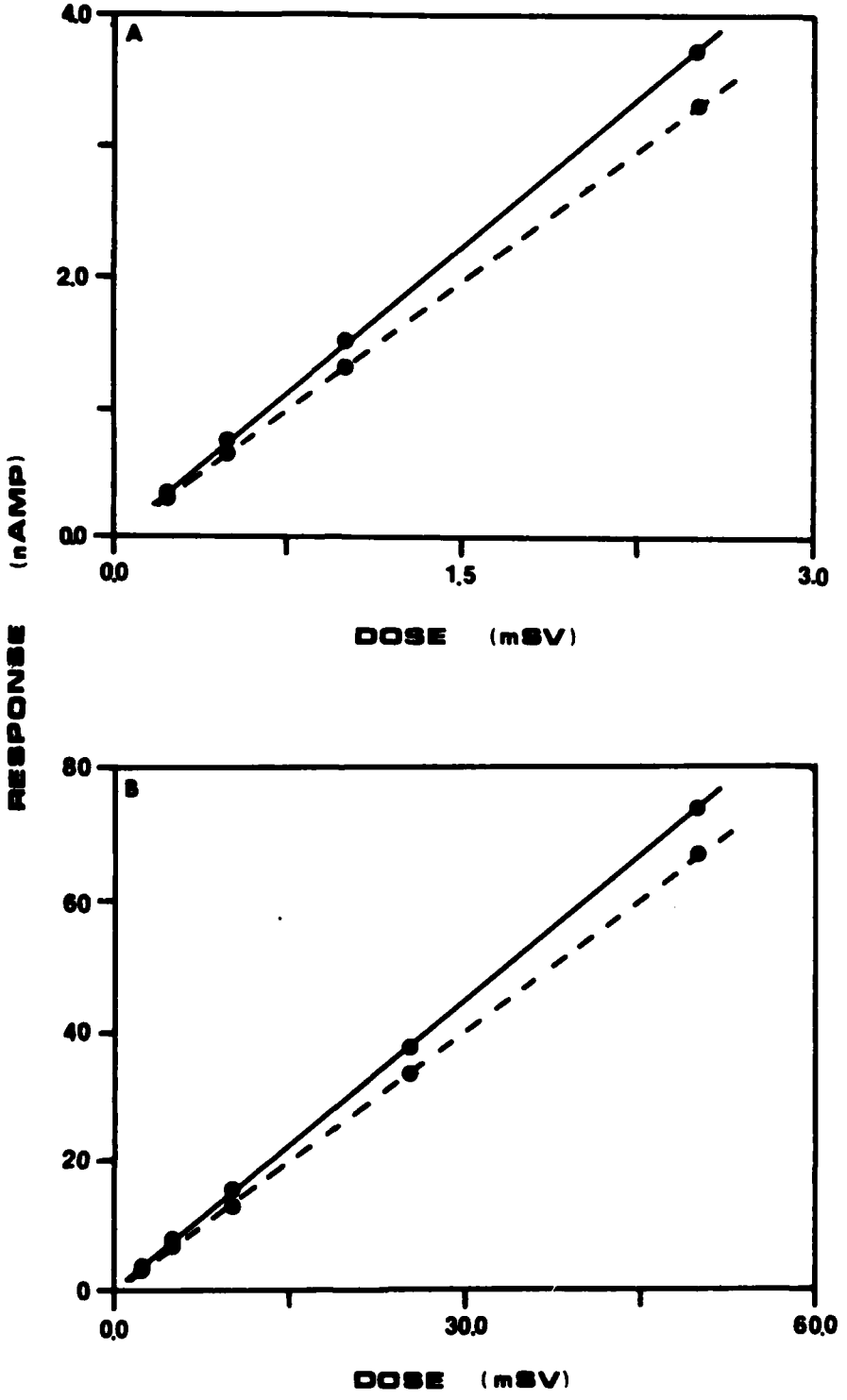
A
4.0
2.0
0.0
0.0
1.5
3.0
RESPONSE (nAMP)
DOSE (mSV)
B
80
60
40
20
0
0.0
30.0
60.0
DOSE (mSV)

Figure 32

Calibration Factors (Counts per Minute per Millirem per Hour) for Rascal/NRD 23 cm Remmeter System Serial 212. Calibration Factors are Plotted versus Ratio of Counting Rates of the BF_3 Detector Inside 23 cm (9 in) and 7.6 cm (3 in) Polyethelene Spheres.

Slope: -0.026 ± 0.004

Intercept: 1.408 ± 0.248

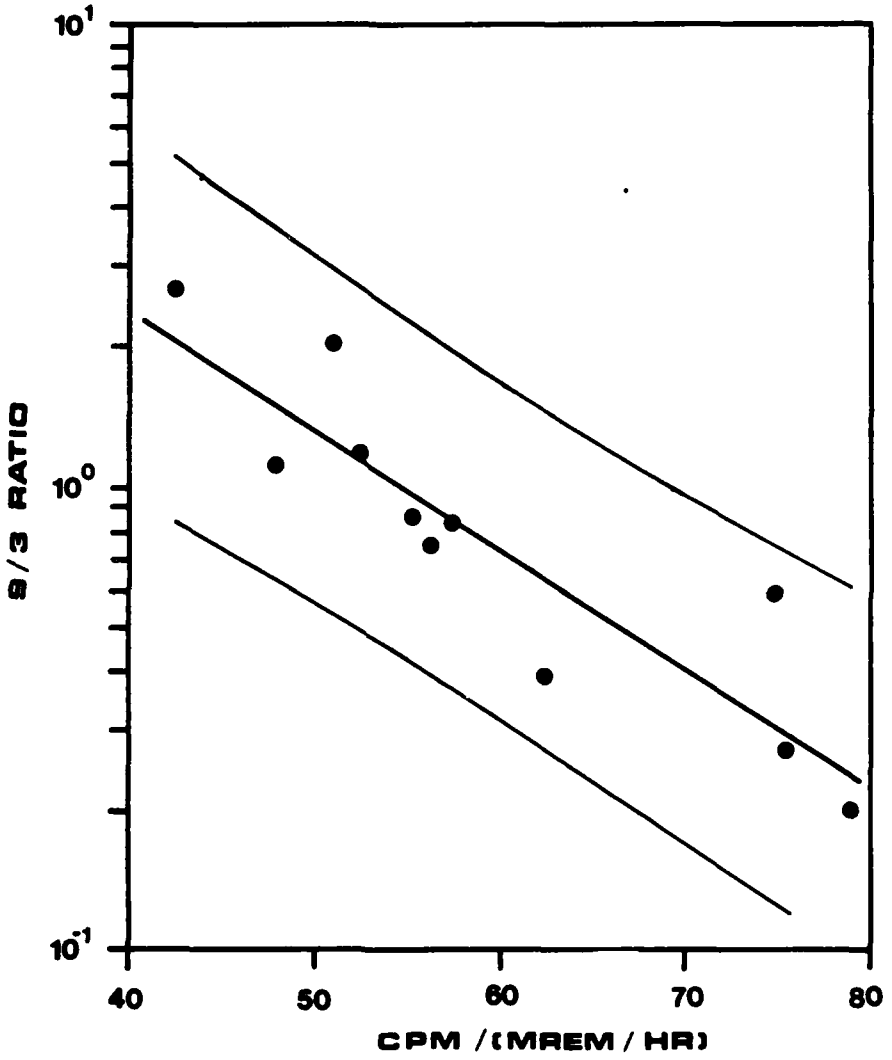
10^1
10^0
10^{-1}
S/3 RATIO
40
50
60
70
80
CPM /(MREM / HR)

Figure 33

Calibration Factors (Counts per Minute per Millirem per Hour) for Rascal/NRD 23 cm Remmeter System Serial 215. Calibration Factors are Plotted versus Ratio of Counting Rates of the BF_3 Detector Inside 23 cm (9 in) and 7.6 cm (3 in) Polyethelene Spheres.

Slope: -0.028 ± 0.005

Intercept: 1.688 ± 0.312

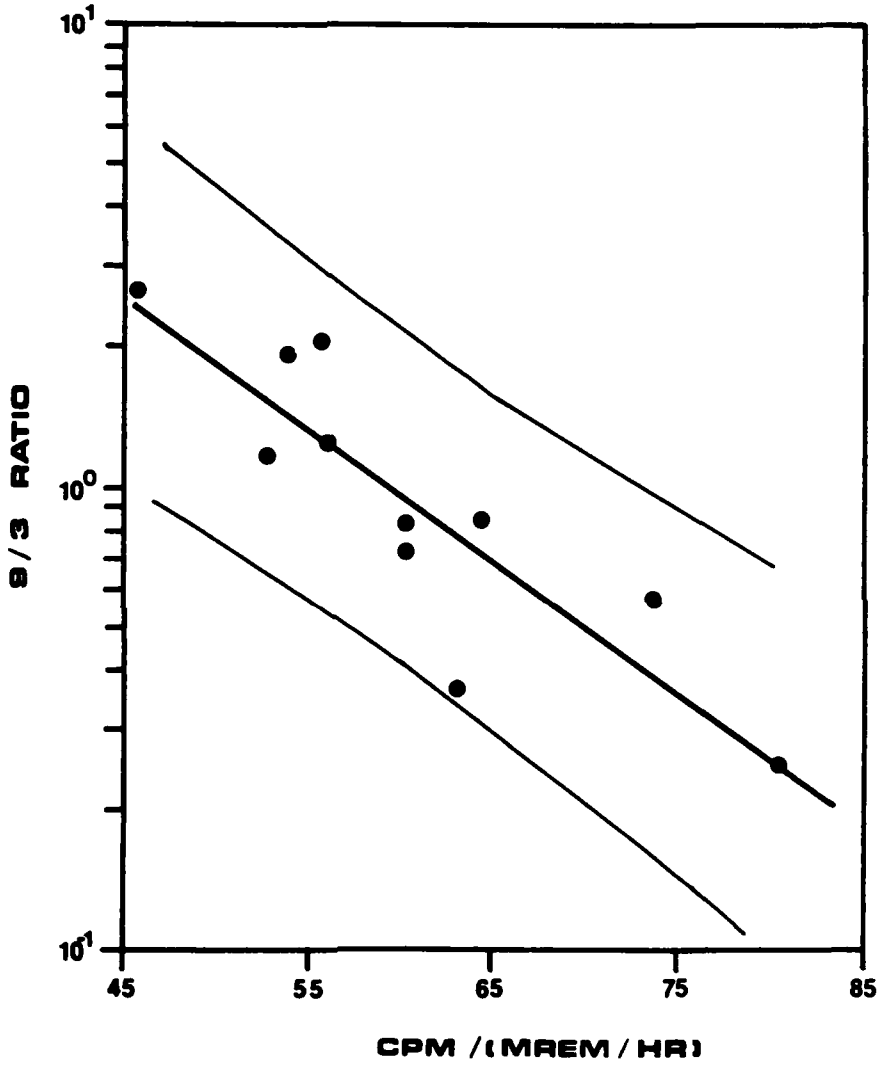
10^1
10^0
10^{-1}
9/3 RATIO
45
55
65
75
85
CPM /(MREM / HR)

Figure 34

Measured Albedo Factor versus Ratio of Counting Rates of a BF_3 Detector Inside 23 cm (9 in) and 7.6 cm (3 in) Polyethelene Spheres.

A.	HPRR (13 cm Steel at 3 m)	Figure 37
B.	HPRR (20 cm Concrete at 3 m)	Figure 38
C.	Cf-252 (Bare at 1 m)	Figure 41
D.	Cf-252 (Bare at 2 m)	Figure 42
E.	Cf-252 (5 cm D_2O at 1 m)	Figure 43
F.	Cf-252 (10 cm D_2O at 1 m)	Figure 44
G.	Cf-252 (15 cm D_2O at 1 m)	Figure 45
H.	Cf-252 (15 cm D_2O + 0.5 mm Cd at 1 m)	Figure 46
I.	Cf-252 (20 cm Al at 1 m)	Figure 48
J.	HPRR (Bare at 6 m)	
K.	HPRR (12 cm Lucite at 3m)	
L.	HPRR (12 cm Lucite at 9m)	
M.	HPRR (Bare at 2m)	

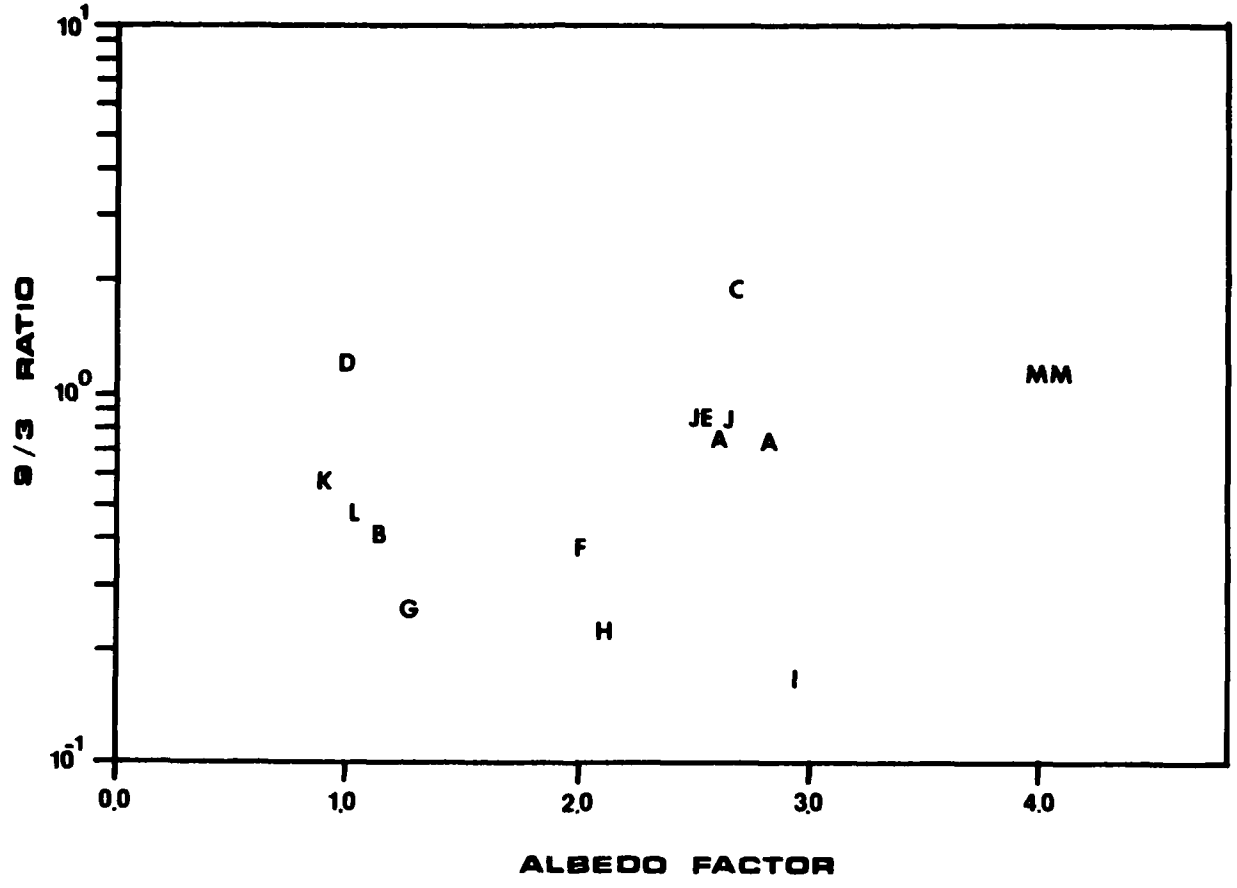
10^1
10^0
10^{-1}
B/3 RATIO
C
D
MM
JE
J
A
A
K
L
B
F
G
H
I
0.0
1.0
2.0
3.0
4.0
ALBEDO FACTOR

Figure 35

Measured Albedo Factor versus Ratio of Counting Rates of a BF_3 Detector Inside and Outside a 7.6 cm (3 in) Polyethylene Sphere.

A.	Cf-252 (Bare at 1 m)	Figure 41
B.	Cf-252 (Bare at 2 m)	Figure 42
C.	Cf-252 (5 cm D_2O at 1 m)	Figure 43
D.	Cf-252 (10 cm D_2O at 1 m)	Figure 44
E.	Cf-252 (15 cm D_2O at 1 m)	Figure 45
F.	Cf-252 (15 cm D_2O + 0.5 mm Cd at 1 m)	Figure 46
G.	Cf-252 (20 cm Al at 1 m)	Figure 48

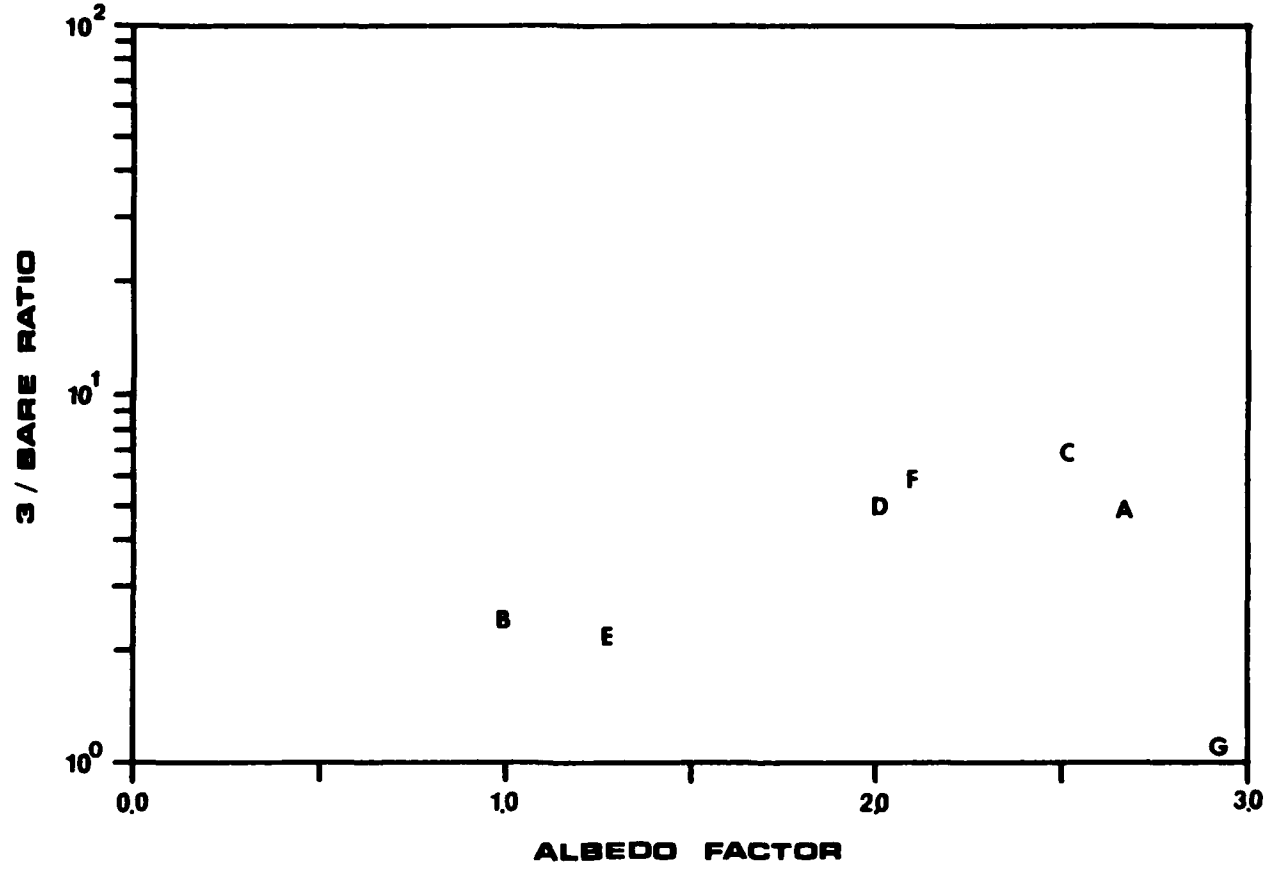
10^2
10^1
10^0
3 / BARE RATIO
0.0
1.0
2.0
3.0
ALBEDO FACTOR
A
B
C
D
E
F
G

Figure 36

Reference Neutron Spectrum for Unshielded Health Physics Research Reactor. Spectrum Calculated at 3 Meters from Reactor Centerline (Si81)

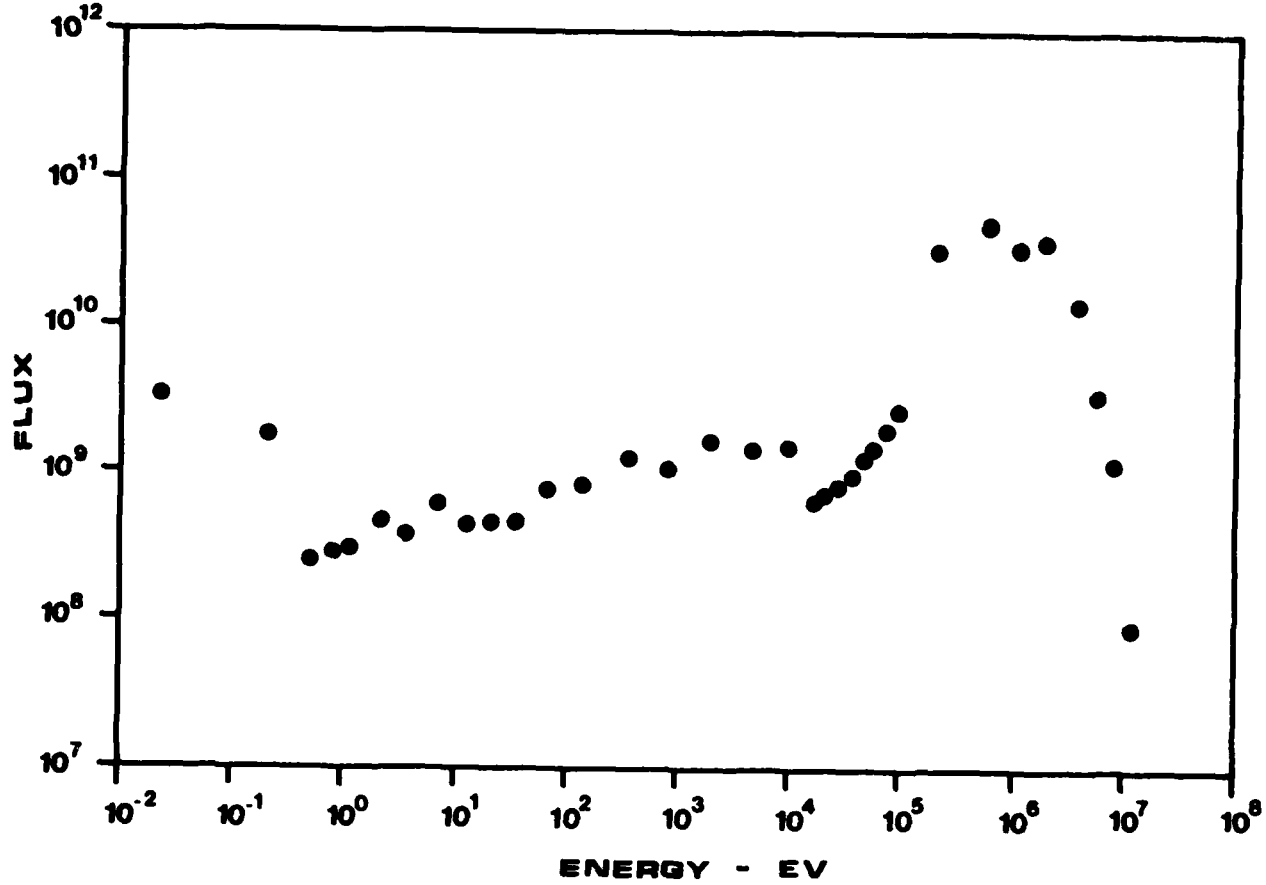
FLUX
10^{12}
10^{11}
10^{10}
10^{9}
10^{8}
10^{7}
10^{-2}
10^{-1}
10^{0}
10^{1}
10^{2}
10^{3}
10^{4}
10^{5}
10^{6}
10^{7}
10^{8}
ENERGY - EV

Figure 37

Reference Neutron Spectrum for Health Physics Research Reactor with 13 cm Steel Shield. Spectrum Calculated at 3 Meters from Reactor with Inside of Shield Placed 2 Meters from Centerline (S181).

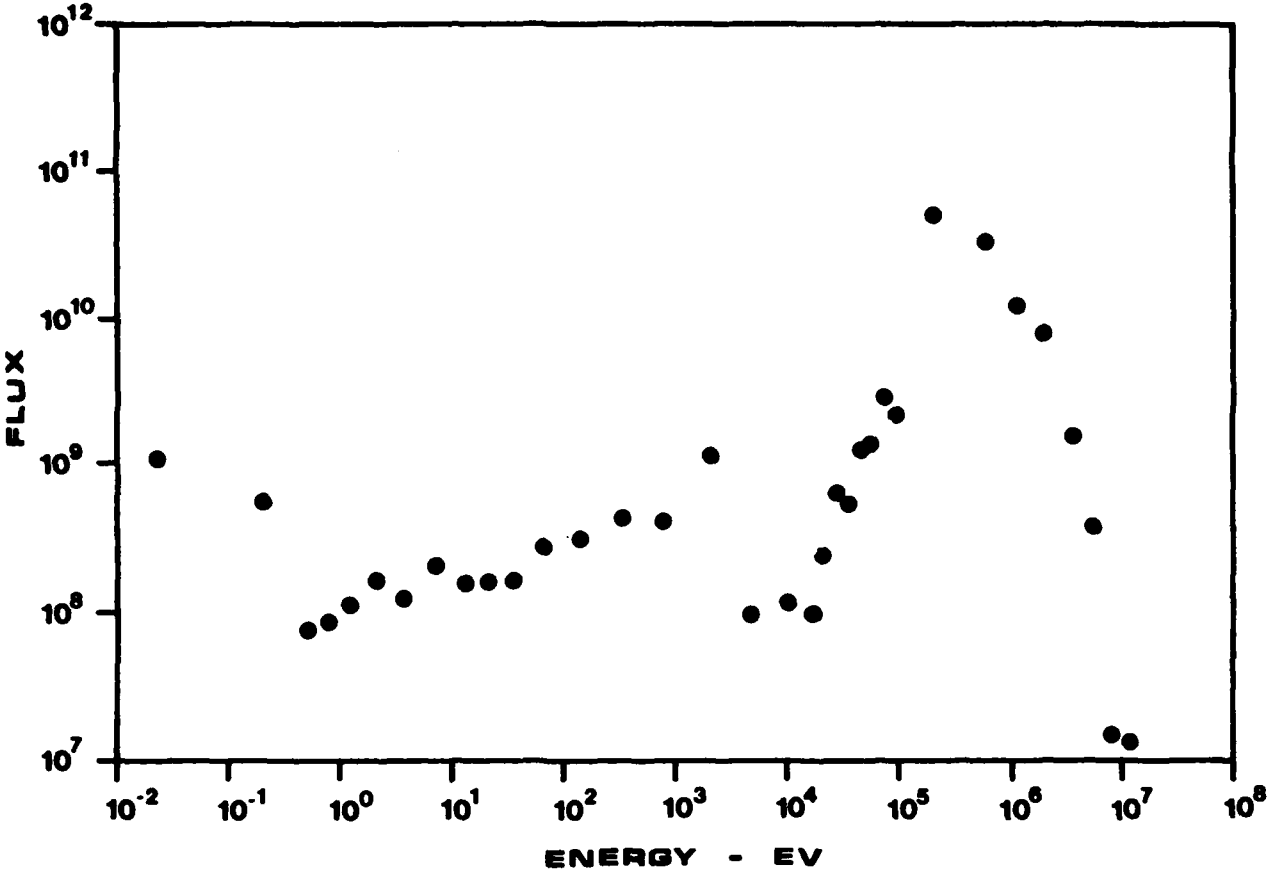
FLUX
10^{12}
10^{11}
10^{10}
10^{9}
10^{8}
10^{7}
10^{-2}
10^{-1}
10^{0}
10^{1}
10^{2}
10^{3}
10^{4}
10^{5}
10^{6}
10^{7}
10^{8}
ENERGY - EV

Figure 38

Reference Neutron Spectrum for Health Physics Research Reactor with 20 cm Concrete Shield. Calculated at 3 Meters from Reactor with Inside of Shield Placed at 1 Meter from Centerline (Si81)

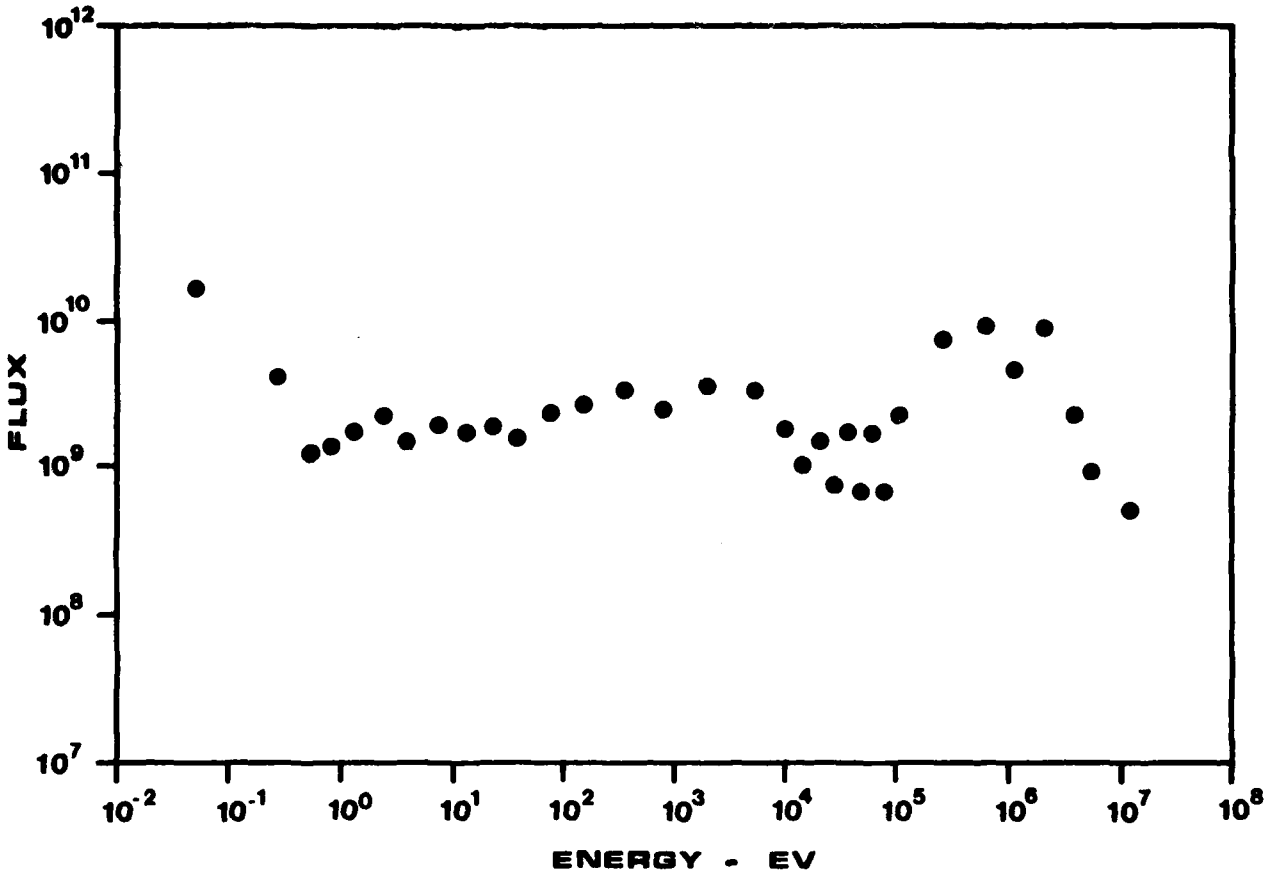
FLUX
10^{12}
10^{11}
10^{10}
10^{9}
10^{8}
10^{7}
10^{-2}
10^{-1}
10^{0}
10^{1}
10^{2}
10^{3}
10^{4}
10^{5}
10^{6}
10^{7}
10^{8}
ENERGY - EV

Figure 39

Reference Neutron Spectrum for Health Physics Research Reactor with 5 cm Steel/15 cm Concrete Shield. Spectrum Calculated at 3 Meters from Reactor with Inside of Shield Placed 1 Meter from Centerline (Si81)

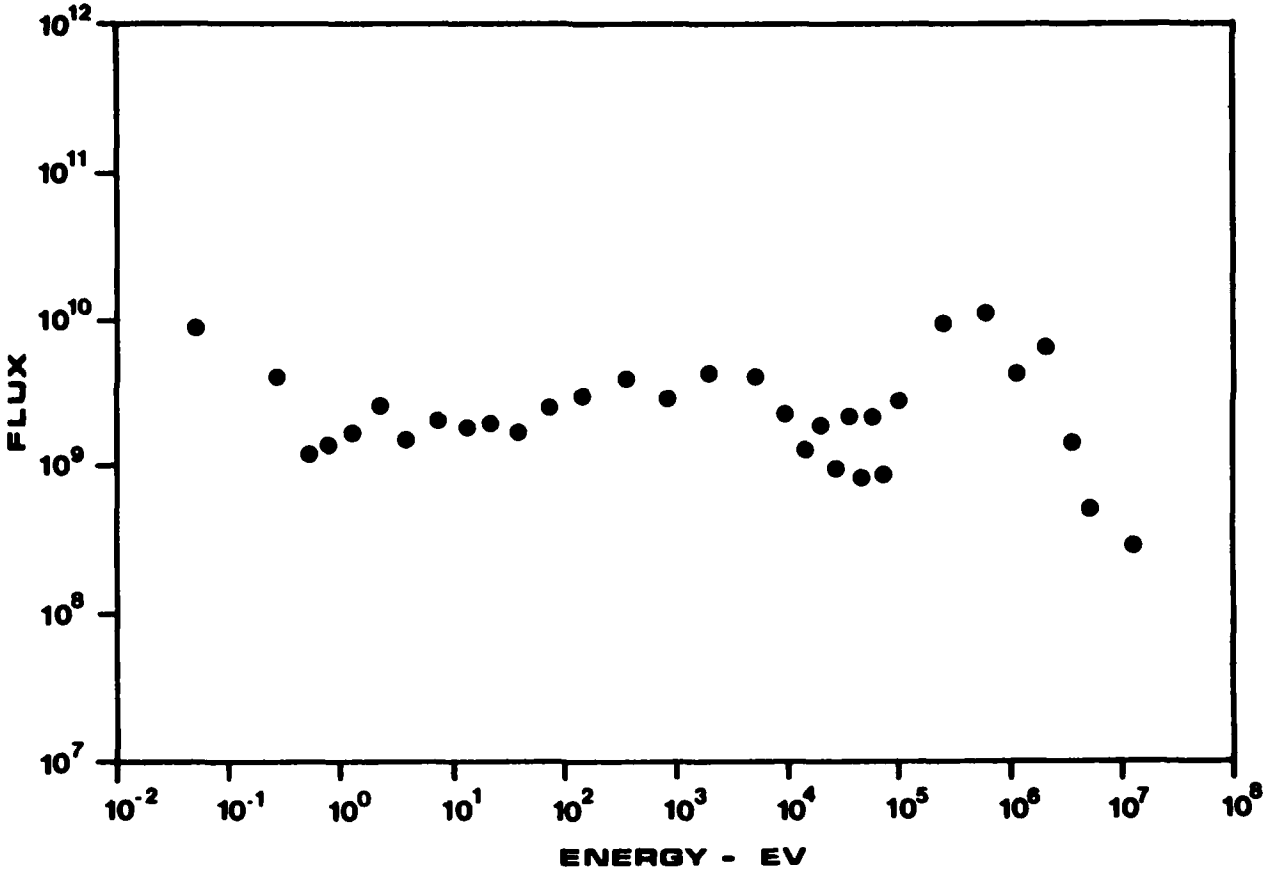
FLUX
10^{12}
10^{11}
10^{10}
10^{9}
10^{8}
10^{7}
10^{-2}
10^{-1}
10^{0}
10^{1}
10^{2}
10^{3}
10^{4}
10^{5}
10^{6}
10^{7}
10^{8}
ENERGY - EV

Figure 40

Bonner Multisphere Reference Spectrum for PuBe Source at 1 Meter. Spectrum Calculated from Data Taken at the Hazards Control Calibration Facility, Lawrence Livermore National Laboratory.

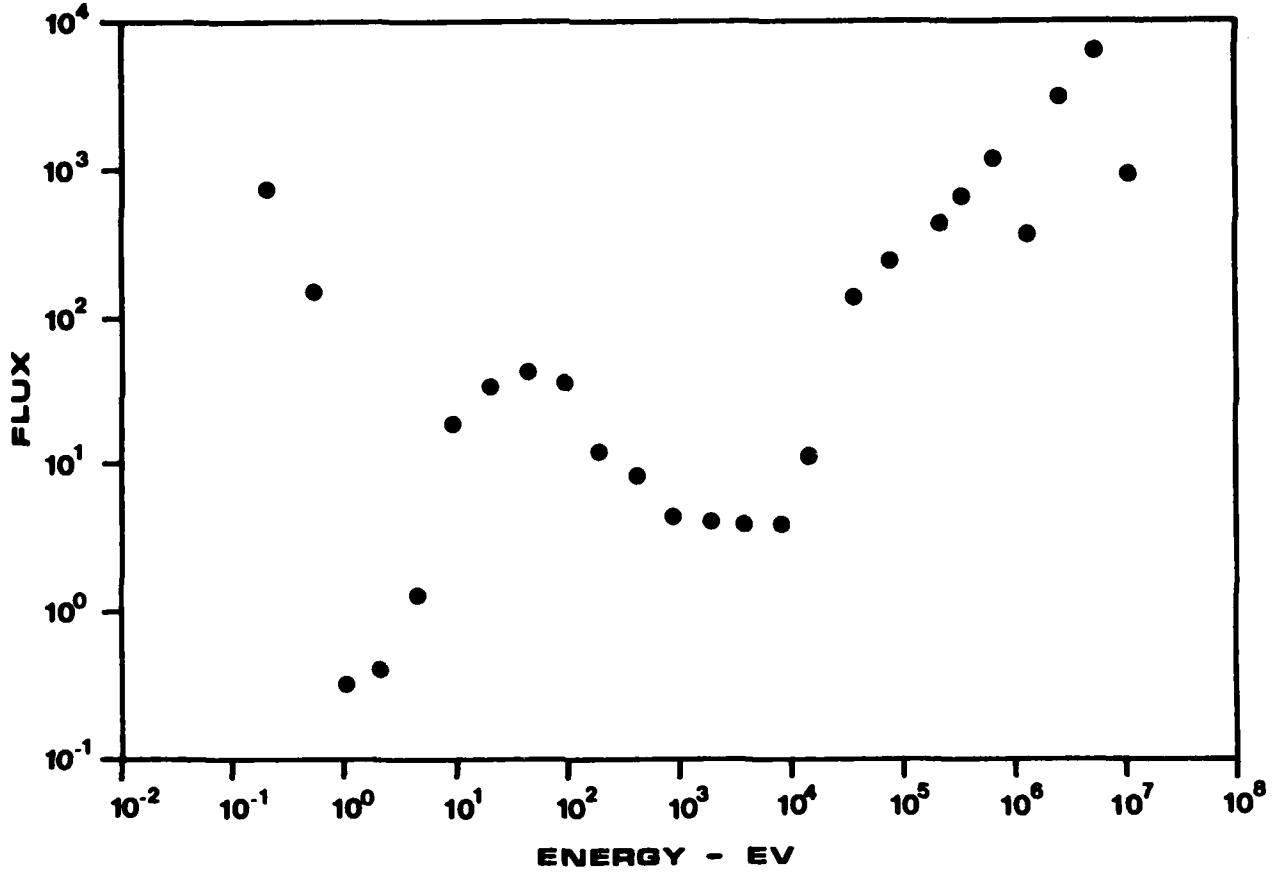
FLUX
10^4
10^3
10^2
10^1
10^0
10^{-1}
10^{-2}
10^{-1}
10^0
10^1
10^2
10^3
10^4
10^5
10^6
10^7
10^8
ENERGY - EV

Figure 41

Bonner Multisphere Reference Spectrum for Cf-252 Source at 1 Meter. Spectrum Calculated from Data Taken at the Hazards Control Calibration Facility, Lawrence Livermore National Laboratory.

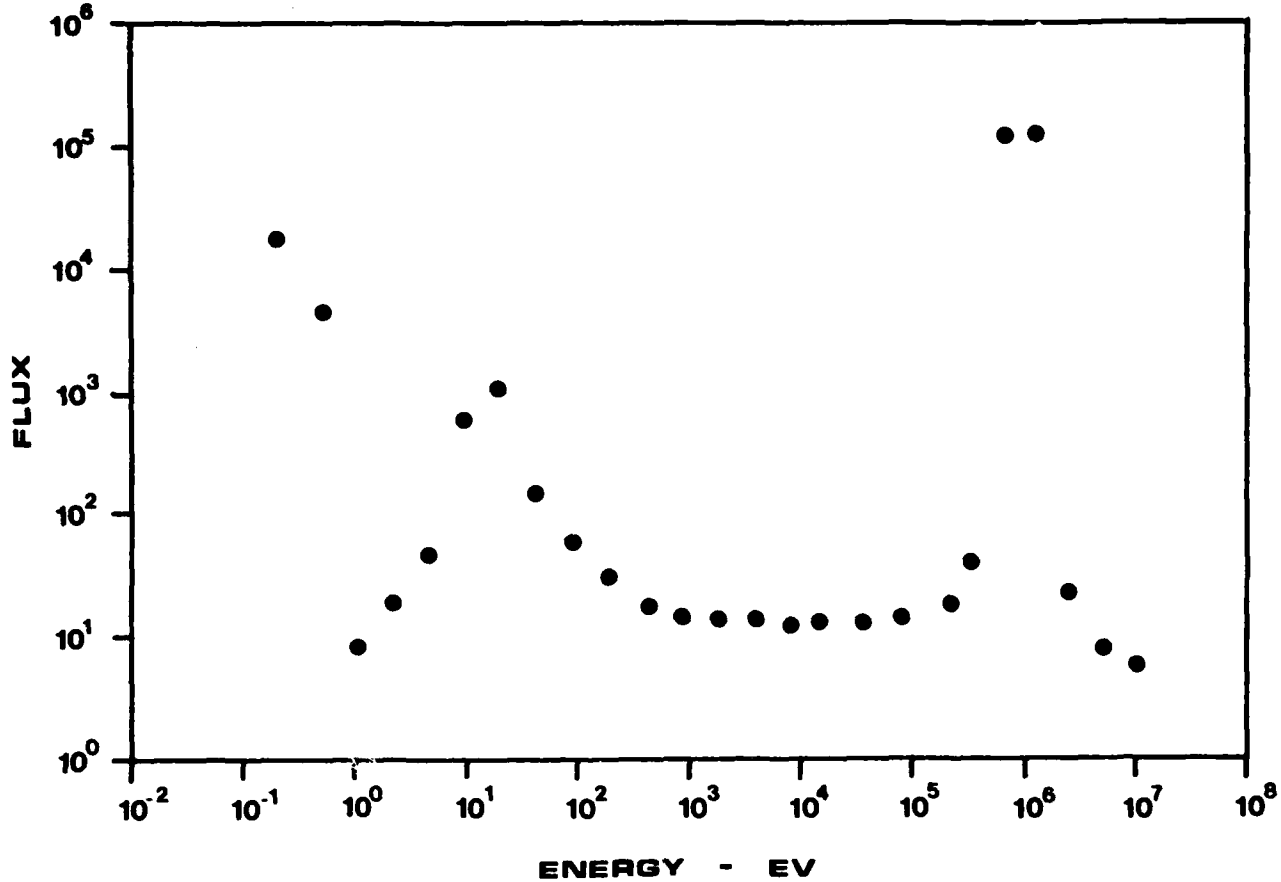
FLUX
10^6
10^5
10^4
10^3
10^2
10^1
10^0
10^{-2}
10^{-1}
10^0
10^1
10^2
10^3
10^4
10^5
10^6
10^7
10^8
ENERGY - EV

Figure 42

Bonner Multisphere Reference Spectrum for Cf-252 Source at 2 Meters. Spectrum Calculated from Data Taken at the Hazards Control Calibration Facility, Lawrence Livermore National Laboratory.

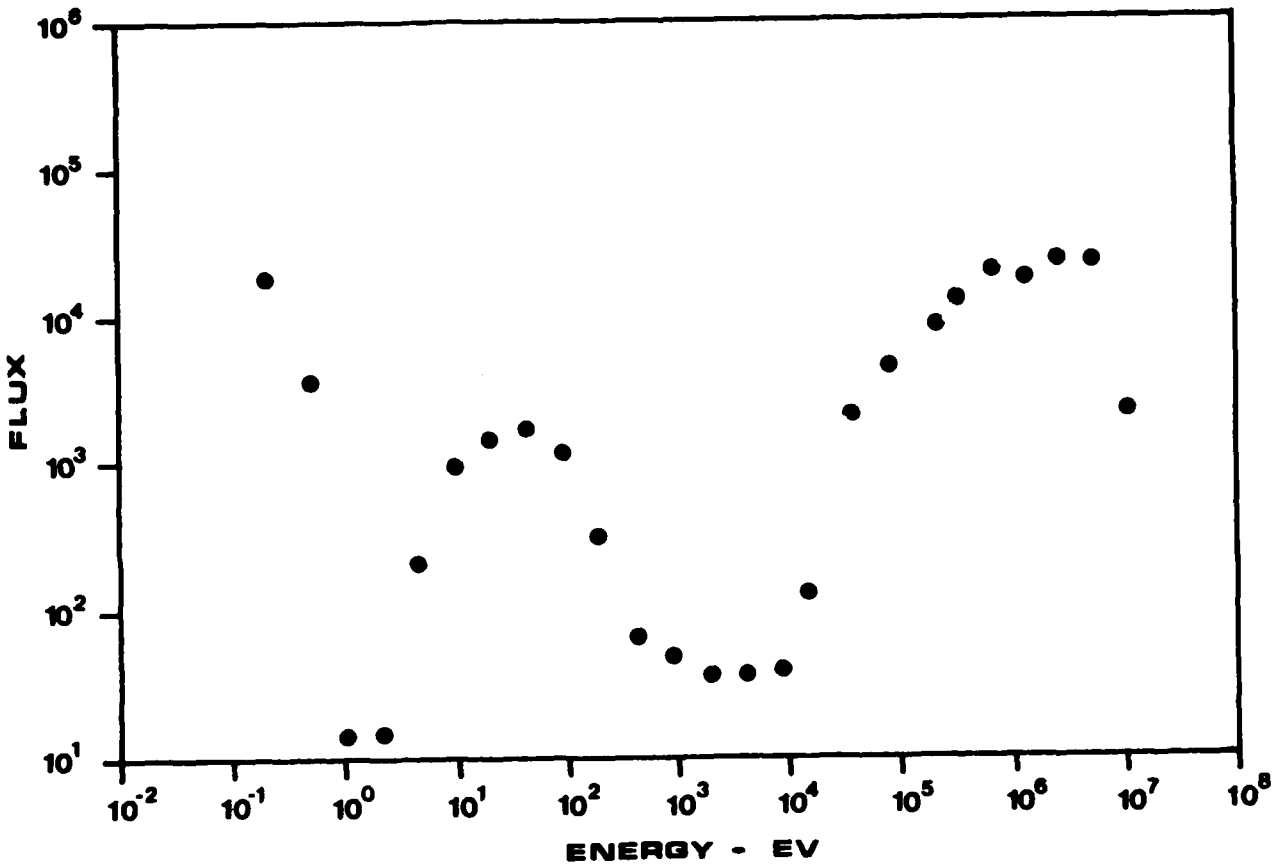
FLUX
10^6
10^5
10^4
10^3
10^2
10^1
10^{-2}
10^{-1}
10^0
10^1
10^2
10^3
10^4
10^5
10^6
10^7
10^8
ENERGY - EV

Figure 43

Bonner Multisphere Reference Spectrum for Cf-252 Source Moderated by 5 cm D_2O Filled Stainless Steel Sphere. Spectrum Calculated from Data Taken 1 Meter from Source Centerline at the Hazards Control Calibration Facility, Lawrence Livermore National Laboratory.

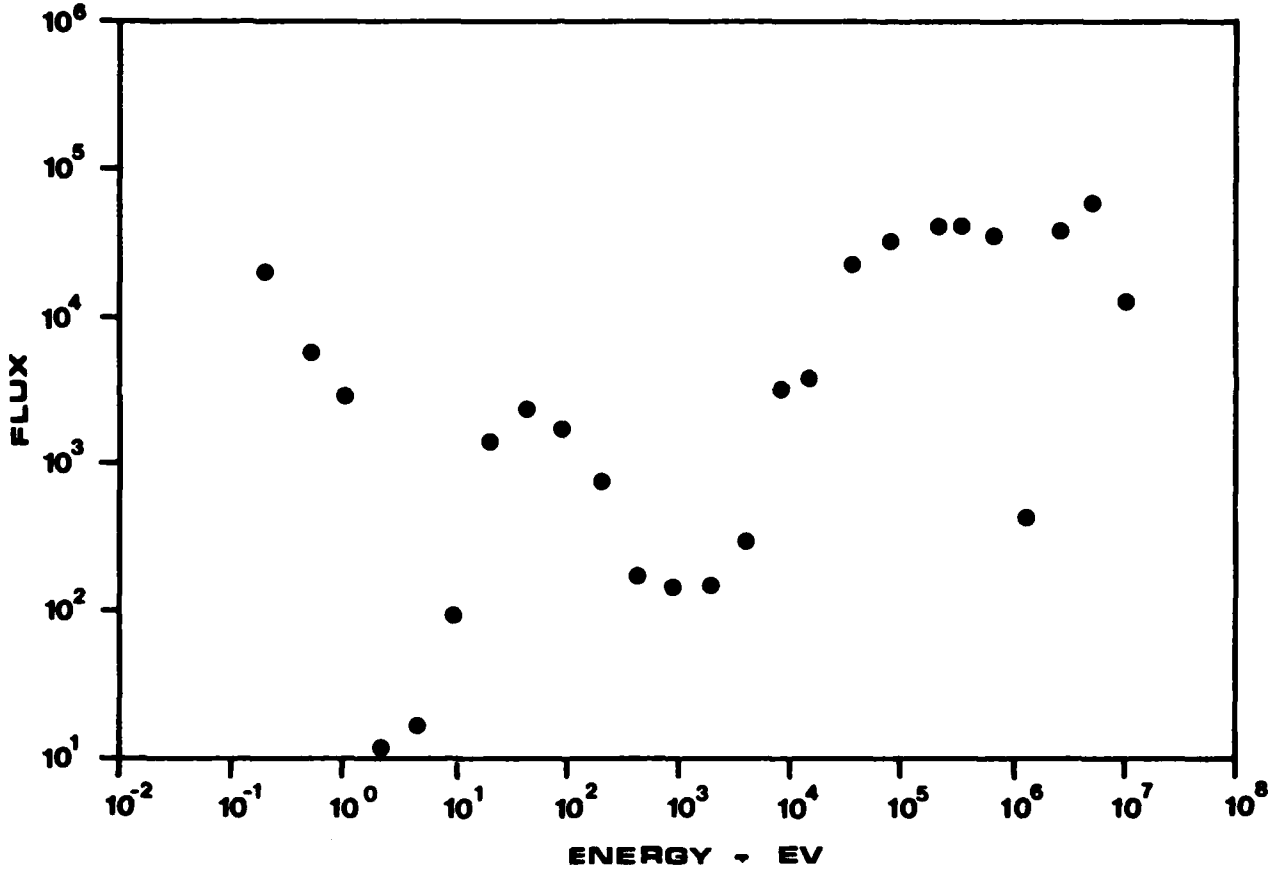
FLUX
10^6
10^5
10^4
10^3
10^2
10^1
10^{-2}
10^{-1}
10^0
10^1
10^2
10^3
10^4
10^5
10^6
10^7
10^8
ENERGY - EV

Figure 44

Bonner Multisphere Reference Spectrum for Cf-252 Source Moderated by 10 cm D_2O Filled Stainless Steel Sphere. Spectrum Calculated from Data Taken 1 Meter from Source Centerline at the Hazards Control Calibration Facility, Lawrence Livermore National Laboratory.

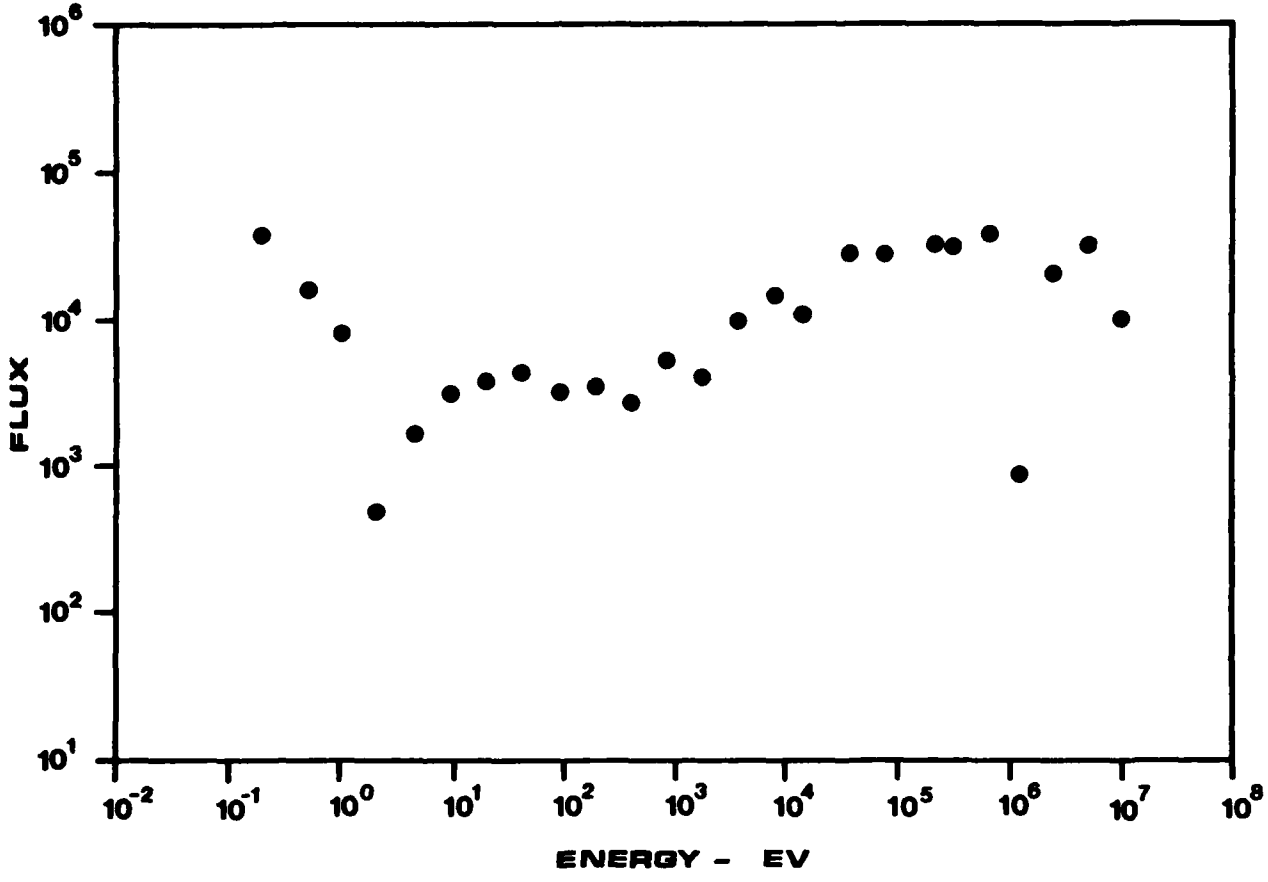
FLUX
10^6
10^5
10^4
10^3
10^2
10^1
10^{-2}
10^{-1}
10^0
10^1
10^2
10^3
10^4
10^5
10^6
10^7
10^8
ENERGY - EV

Figure 45

Bonner Multisphere Reference Spectrum for Cf-252 Source Moderated by 15 cm D_2O Filled Stainless Steel Sphere. Spectrum Calculated from Data Taken 1 Meter from Source Centerline at the Hazards Control Calibration Facility, Lawrence Livermore National Laboratory.

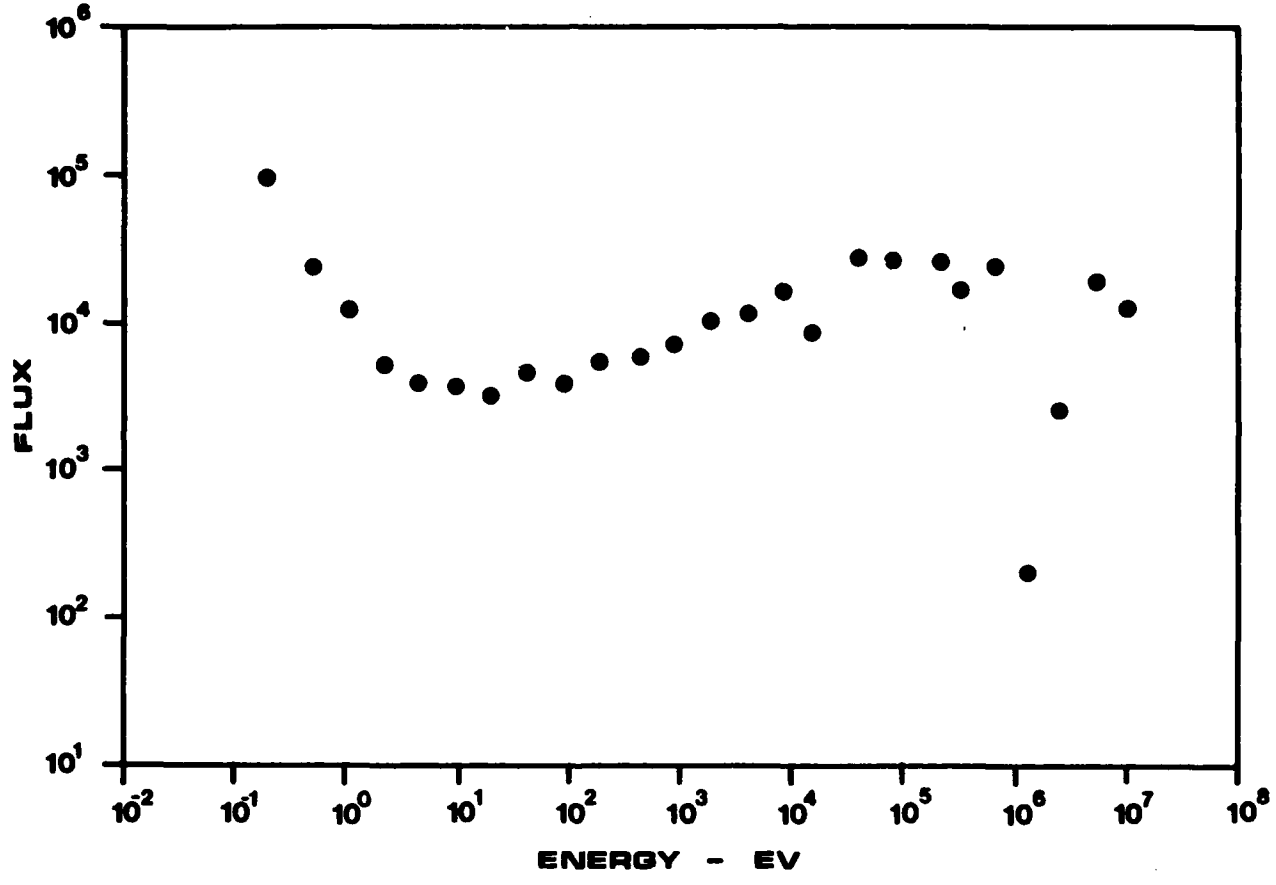
FLUX
10^6
10^5
10^4
10^3
10^2
10^1
10^{-2}
10^{-1}
10^0
10^1
10^2
10^3
10^4
10^5
10^6
10^7
10^8
ENERGY - EV

Figure 46

Bonner Multisphere Reference Spectrum for Cf-252 Source Moderated by 15 cm D_2O Filled Cadmium Covered Stainless Steel Sphere. Spectrum Calculated from Data Taken 1 Meter from Source Centerline at the Hazards Control Calibration Facility, Lawrence Livermore National Laboratory.

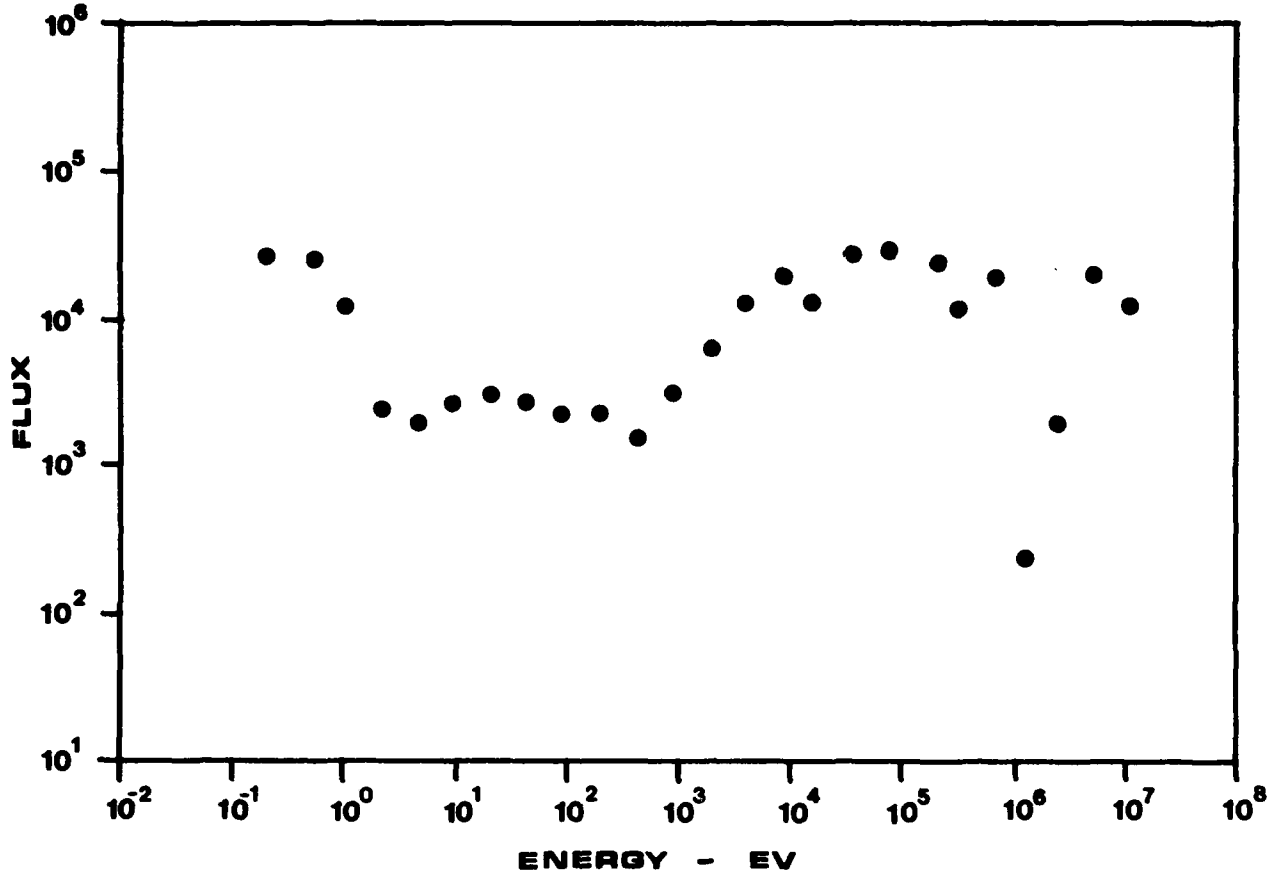
FLUX
10^6
10^5
10^4
10^3
10^2
10^1
10^{-2}
10^{-1}
10^0
10^1
10^2
10^3
10^4
10^5
10^6
10^7
10^8
ENERGY - EV

Figure 47

Bonner Multisphere Reference Spectrum for Cf-252 Source Moderated by 25 cm D_2O Filled Stainless Steel Sphere. Spectrum Calculated from Data Taken 1 Meter from Source Centerline at the Hazards Control Calibration Facility, Lawrence Livermore National Laboratory.

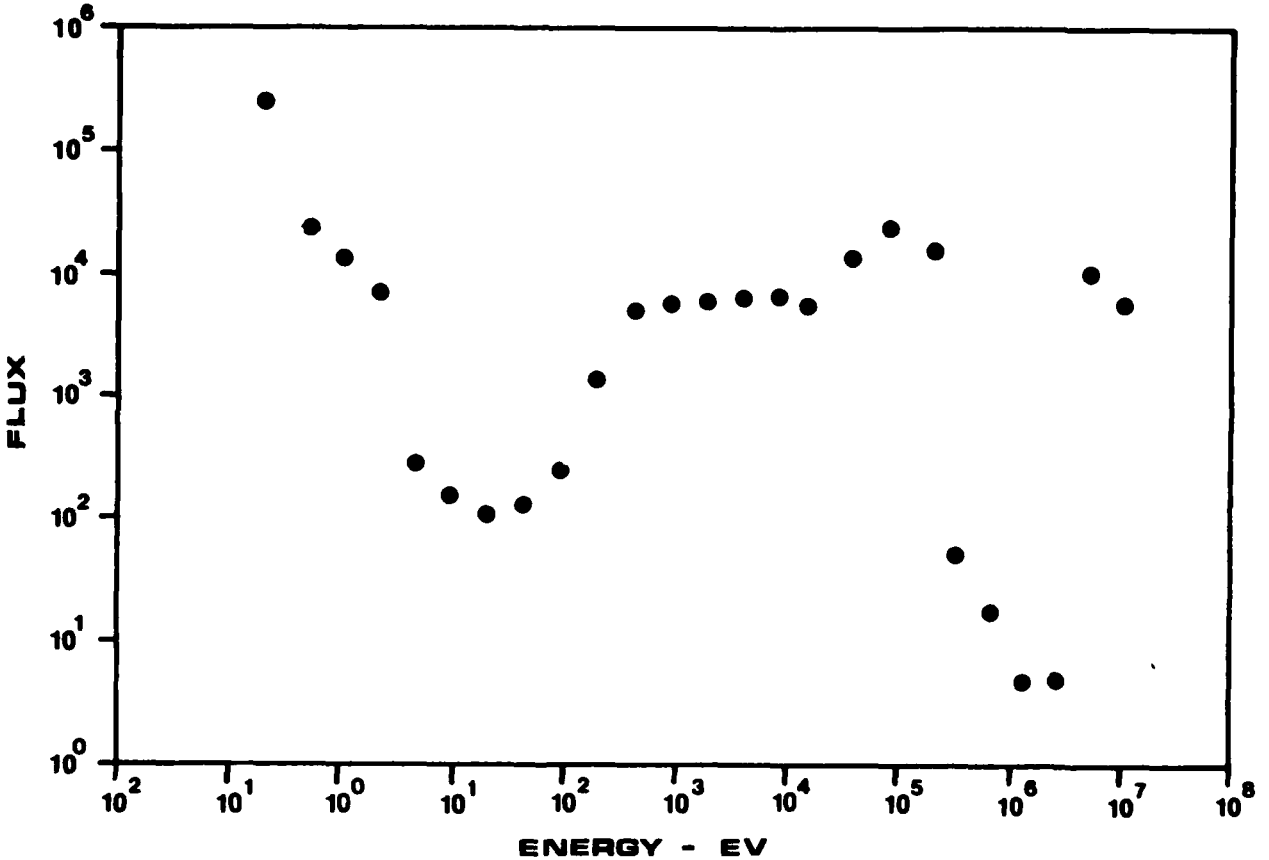
FLUX
10^6
10^5
10^4
10^3
10^2
10^1
10^0
10^2 10^1 10^0 10^1 10^2 10^3 10^4 10^5 10^6 10^7 10^8
ENERGY - EV

Figure 48

Bonner Multisphere Reference Spectrum for Cf-252 Source Moderated by 20 cm Solid Aluminum Sphere. Spectrum Calculated from Data Taken 1 Meter from Source Centerline at the Hazards Control Calibration Facility, Lawrence Livermore National Laboratory.

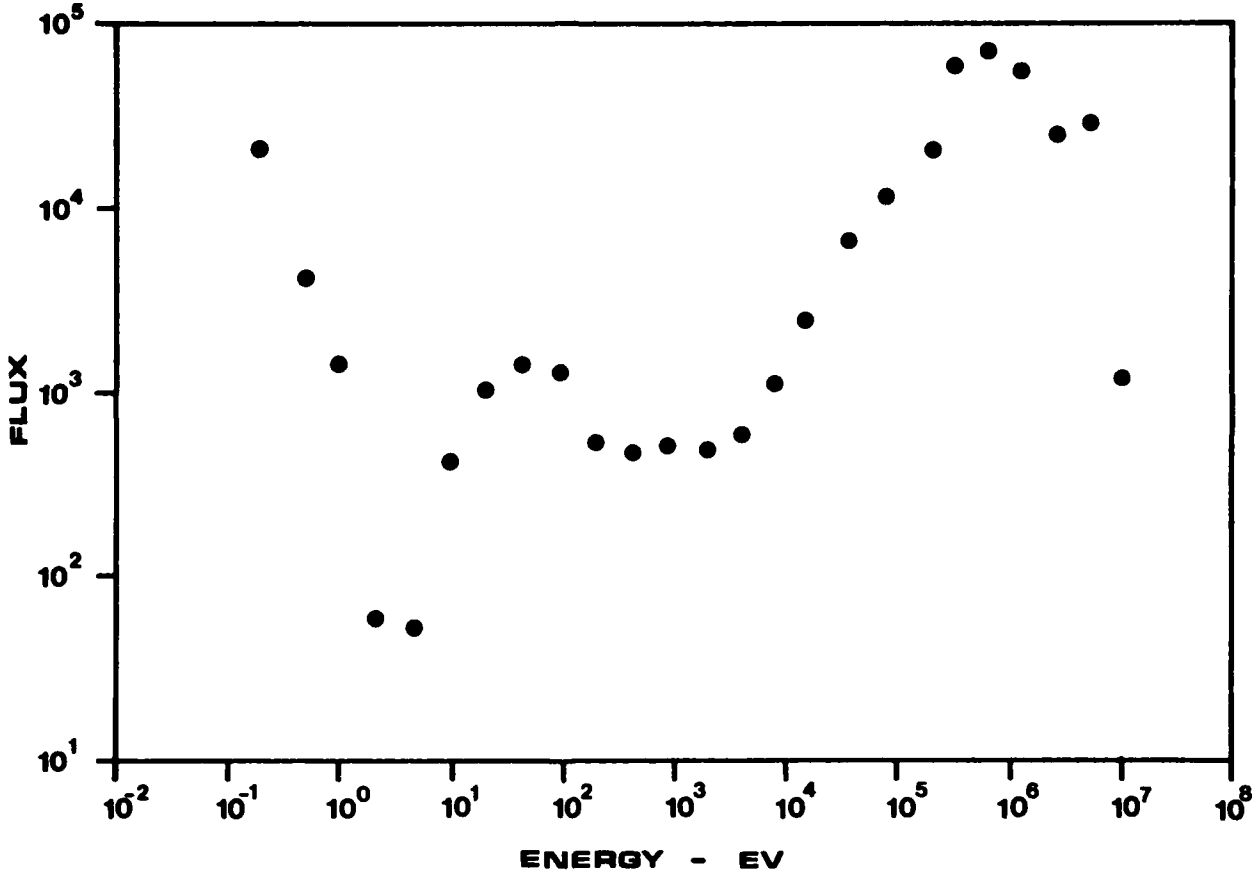
FLUX
10^5
10^4
10^3
10^2
10^1
10^{-2}
10^{-1}
10^0
10^1
10^2
10^3
10^4
10^5
10^6
10^7
10^8
ENERGY - EV

BIBLIOGRAPHY

A174 Alsmiller, J. R. Jr., and Barish, J., The Calculated Response of LiF Albedo Dosimeters to Neutrons with Energies less than or equal to 400 MeV, Health Physics 26(1), pp 13-28 (1874)

ANSI76 American National Standards Institute, Inc., American National Standard for Personnel Neutron Dosimeters (Neutron Energies Less than 20 MeV), ANSI N319 (1976)

ANSI82 American National Standards Institute, Inc., Criteria for Testing Personnel Dosimetry Performance, ANSI N13.11 (1982)

Ei81 Eisenhauer, C. and Schwartz, R., Difficulties in Calculating Spectrum-Averages Values of Neutron Dose Equivalent, Health Physics 41(5), pp 774-777 (1981)

Fa82 Faust, L. G., Battelle Pacific Northwest Laboratories, personal communication, June 1, 1982.

FR79 Federal Register, Vol 44, pp 53785, September 17, 1979.

FR81 Federal Register, Vol 46, pp 7836, January 23, 1981.

FR83 Federal Register, Vol 48, pp 34314, July 28, 1983.

Fu72 Furuta, Y., and Tanaka, S., Response of LiF and LiF Thermoluminescence Dosimeters to Fast Neutrons, Nuclear Instruments and Methods 104, pp 365-374 (1972)

G152 Glasstone, Samuel and Edlund, Milton C., The Elements of Nuclear Reactor Theory, D. Van Nostrand Company, Inc., (1952)

G183 Glickstein, S. S., Analytical Modeling of Thermoluminescen Albedo Detectors for Neutron Dosimetry, Health Physics 44(2), pp 103-114 (1983)

Gr78 Griffith, R. V., Slaughter, H. W., Patterson, H. W., Beach, J. L., Frank, E. G., Rueppel, D. W., and Fisher, J. C., Multi-Technique Characterization of Neutron Fields from Moderated Cf-252 and PuBe Sources, National and International Standardization of Radiation Dosimetry Vol. II, pp 167-188, IAEA-SM-222/14 (1978)

Gr79 Griffith, R. V. et al., Recent Developments in Personnel Neutron Dosimeters - A Review, Health Physics 36(3), pp 235-260 (1979)

Gr82 Greene, R. T. and Gilley, L. W., Measurements of the TLD-Albedo Ratio made at the Health Physics Research Reactor, Radiation Protection Dosimetry, 2(4),249-252 (1982)

Gr73 Griffith, R. V., The Use of B-loaded Plastic in Personnel Neutron Dosimetry, Neutron Monitoring for Radiation Protection Purposes, Vol. 1, p 237, Vienna: IAEA (1973)

Ha73 Hankins, D. E., A Small, Inexpensive Albedo-Neutron Dosimeter, Los Alamos Scientific Laboratory Report LA-5261 (1973)

Ha75 Hankins, D. E., Proceedings 9th Midyear Topical Symposium, Health Physics Society, Denver, Colorado, pp 861-868 (1975)

Ha77 Hankins, D. E., Lawrence Livermore National Laboratory, Personal Communication to H. W. Dickson, Oak Ridge National Laboratory (1977)

Ha79 Hankins, D. E., Cadmium-Capture Gamma-ray Exposure from Personnel Dosimeters, Health Physics 36(5), pp 644-647, (1979)

He78 Helwig, J. T., SAS Introductory Guide, SAS Institute Inc., Cary, North Carolina (1978)

He82 Henniger, J., Hubner, K,. and Pretzsch, G., Calculation of the Neutron Sensitivity of TL Detectors, Nuclear Instruments and Methods 192, pp 453-462 (1982)

Ho78 Horowitz, Y. S., and Freeman, S., Response of LiF and LiF Thermoluminescent Dosimeters to Neutrons Incorporatin the Thermoluminescent Linear Energy Transfer Dependency, Nuclear Instruments and Methods 157, pp 393-396 (1978)

Ho83 Hoots, S., Lawrence Livermore National Laboratory, personal communication, August 8, 1983.

ICRP63 Report of the RBE Committee, Health Physics 9, pp 357 (1963)

ICRP69 General Principles of Monitoring for Radiation Protection of Workers, ICRP Publication 12, International Commission on Radiological Protection, Pergamon Press, Oxford, (1969)

ICRP73 Data for Protection against Ionizing Radiation from External Sources: Supplement to ICRP Publication 15, ICRP Publication 21, International Commission on Radiological Protection, Pergamon Press, Oxford, (1973)

Lo80 Lowe, D., Recommendations for the Efficient Use of LiF Thermoluminescent Dosimeters in Mixed Neutron Gamma Fields Nuclear Instruments and Methods 177, pp 577-580 (1980)

NCRP54 NCRP Report 17, Permissible Dose from External Sources of Ionizing Radiation, National Bureau of Standards Handbook 59 (U.S. Government Printing Office, Washington) (1954)

NCRP71a NCRP Report 38, Protection Against Neutron Radiation, National Council on Radiation Protection and Measurements, Washington D. C. (1971)

NCRP71b NCRP Report 39, Basic Radiation Protection Criteria, National Council on Radiation Protection and Measurements, Washington D. C. (1971)

NCRP80 NCRP Statement on Dose Limits for Neutrons, National Council on Radiation Protection and Measurements, Washington D. C., February 21, 1980.

NRC77 U. S. Nuclear Regulatory Commission, Office of Standards Development, Personnel Neutron Dosimeters, Regulatory Guide 8.14, Revision 1 (1977)

P180 Plato, P. and Hudson, G., Performance Testing of Personnel Dosimetry Services: Supplementary Report on a Two-Year Pilot Study October 1977 through December 1979. Division of Technical Information and Document Control, U.S. Nuclear Regulatory Commission. NUREG/CR-130 (1980)

P182 Plato, P. and Miklos, J., Performance Testing of Personnel Dosimetry Services: Final Report for Test #3. Division of Technical Information and Document Control, U.S. Nuclear Regulatory Commission. NUREG/CR-2891 (1982)

Po72 Poston, J. W. and Haywood, F. F., 1972 Intercomparison of Nuclear Accident Dosimetry Systems at the Oak Ridge National Laboratory, Oak Ridge National Laboratory Report ORNL/TM-4387 (1972)

Sa73 Sanna, R. S., Thirty One Group Response Matrices for the Multisphere Neutron Spectrometer Over the Energy Range Thermal to 400 MeV, USDOE Report HASL-267 (1973)

Sc80 Schwartz, R. B. and Eisenhauer, C. M., The Design and Construction of D O-Moderated Cf-252 Source for Calibrating Neutron Personnel Dosimeters Used at Nuclear Power Reactors., Division of Technical Information and Document Control, U.S. Nuclear Regulatory Commission. NUREG/CR-1204 (1980)

Si81 Sims, C. S. and Killough, G. G., Reference Dosimetry for Various Health Physics Research Reactor Spectra, Oak Ridge National Laboratory Report ORNL/TM-7748 (1981)

Si83 Sims, C. S. and Killough, G. G., Neutron Fluence-to-Dose Equivalent Conversion Factors: A comparison of Data Sets and Interpolation Methods, Radiation Protection Dosimetry 5(1), pp 45-48 (1983)

Sn57 Snyder, W. S., NCRP Report No. 20 (1959)

So69 Sokal, R. R. and Rohlf, F. J., Biometry - The Principles and Practice of Statistics in Biological Research, W. H. Freeman and Company, San Francisco (1969)

Th77 Thompson, D. J., Characteristics of Sandia's Personnel Neutron Dosimeter, Sixth ERDA Workshop on Personnel Neutron Dosimetry, Oak Ridge, Tennessee, PNL-2449/UC-48, pp 19, (1977)

Ze79 Zeman, G. H. and Snyder, G. I., Neutron Dose Precision Using LiF TLD, Health Physics 36(1), pp 75-76 (1979)

END

FILMED

1-84

DTIC